BUAN

BOTSWANA UNIVERSITY OF AGRICULTURE AND NATURAL RESOURCES

Effects of Land Cover Land Use Change on Soil Organic Carbon Stocks in Greater Gaborone, Botswana.

By
SUH CELESTINE NEBA

Student ID: 202000799

M.Sc. Thesis (DRAFT)

Submitted to the Department of Agricultural and Bio-Systems Engineering in partial fulfilment of the requirements for the degree of Master of Science in Agricultural Engineering – Land Use Planning

Main Supervisor: Prof. Rejoice Tsheko

Co-Supervisors: Prof. Benedict Kayombo

Dr. Thebeetsile Scott Moroke

17th December 2022

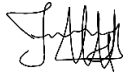## APPROVAL

_____ _____ _____
Main Supervisor   Signature   Date

_____ _____ _____
Co-Supervisor   Signature   Date

_____ _____ _____
Co-supervisor   Signature   Date

_____ _____ _____
External Supervisor   Signature   Date

DECLARATION

I, Suh Celestine Neba, hereby declare that this thesis entitled "**Effects of Land Cover Land Use Change on Soil Organic Carbon Stocks in Greater Gaborone, Botswana**" is my work and has not been published or submitted elsewhere for the requirement of a degree program. Also, all sources and quotes used have been indicated and acknowledged by means of complete references.

Suh Celestine Neba

ACKNOWLEDGEMENTS

DEDICATION

This work is dedicated to GOD Almighty and my entire family.

TABLE OF CONTENT

LIST OF TABLES

LIST OF FIGURES

LIST OF EQUATIONS

ACRONYMS

ANN   Artificial Neural Networks

ANOVA	Analysis of variance
APA	American Psychological Association
BSI	Bare Soil Index
C	Carbon
CA	Cellular Automata
CLUE	Conversion of Land Use and its Effects
CO_2	Carbon dioxide
CVA	Change Vector Analysis
FAO	Food and Agricultural Organization of the United Nations
GIS	Geographic Information Systems
km^2	Square kilometer
LCLU	Land cover and land use change
LR	Logistic Regression
m	meter
MCE	Multi Criteria Evaluation
ml	milliliter
mm	millimeter
MOLUSCE	Modules for Land Use Change Evaluation
MtC	Megatonne of Carbon
MTL	Metadata file
NDVI	Normalized Difference Vegetation Index
Pg	Pentagram
RS	Remote Sensing
SOC	Soil Organic Carbon
tC	tonnes of Carbon
Tg	Tera-grams
UNDP	United Nations Development Program
UNFCCC	United Nations Framework Convention on Climate Change
UTM	Universal Transverse Mercator
WoE	Weights of Evidence

ABSTRACT

Changes in Land cover land use (LCLU) have long been considered to be among the many factors responsible for the physical and chemical degradation of the soil. Soils are potentially a viable sink for atmospheric carbon and could contribute to mitigating global climate change. Soil Organic Carbon (SOC) content exhibits considerable spatial variability both horizontally according to land use and vertically within the soil profile. Land cover land (LCLU) use is one of the most important determinants of SOC stock. The focus of this study was to investigate the effects of LCLU change on SOC stock in the Greater Gaborone region of Botswana between 1988 and 2022. The study employed Remote Sensing and GIS tools for analyzing LCLU change in the study area between 1988 and 2022. Landsat images of 1988 and 2002 and Sentinel-2A images of 2022 were used to study the changes in the LCLU of the study area. Image classification was performed using a Supervised classification approach based on a Maximum Likelihood classifier. Six major LCLU types (water body, tree cover, cropland, shrubland, bare land, and built-up) were identified in the study area. Post Classification Comparison (PCC) approach was used to detect LCLU change and also quantify the magnitude of the change. Shrubland class was found to be the dominant LCLU type in the study area during the study period. In the study period, a significant LCLU gain was observed in the built-up class (75.12 km^2 (310.16%)), while significant losses were observed in shrub land (24.16 km^2 (5.67%)) and tree cover (33.32 km^2 (25.69%)) classes.

The Walkley and Black method (1934), core method (Blake and Hartge, 1986), Bouyoucos hydrometric methods (van Reeuwijk, 2002; Petrenko & Berezhnyak, 2008), and pH meter (Okalebo et al., 2002) were used to determine SOC content, bulk density, soil texture, and pH, respectively. The current SOC stock in the study area was estimated to be 4.36 MtC, with tree cover accounting for 1.13 MtC (25.87%), shrubland 2.83 MtC (64.86%), cropland 0.14 MtC (3.24%), built-up 0.22 MtC (5.11%), and bare land 0.04 MtC (0.92%). The higher SOC in the build-up compared to bare land was due to its higher clay and silt content. This study found that LCLU changes were responsible for variations in SOC content, soil bulk density, pH, and texture in the study area. Also, it was found that soil under tree cover stored more SOC compared to the other LCLU types due to its low bulk density, low pH, and high silt and clay contents. Furthermore, soil bulk density, pH, and sand fraction negatively correlated with SOC content, while silt and clay showed a positive correlation. In addition, the study found that converting from tree cover to

shrubland or from shrubland to either cropland, built-up or bare land resulted in the loss of SOC from the study area.

Analysis of future LCLU changes between 2022 and 2040, modelled using the CA-ANN model in MOLUSCE, showed that the tree cover will lose 17.4 km^2 of its area coverage by 2040, implying more SOC will be lost from the study area. SOC loss is detrimental to the environment as it increases the concentrations of greenhouse gas CO_2 in the atmosphere, which contributes to climate change. Therefore, appropriate land management interventions that increase SOC stock and reduce carbon emissions should be designed and implemented in the study area.

Keywords

LCLU change, image classification, soil organic carbon, Module for Land Use Change Evaluation, Greater Gaborone

CHAPTER 1: INTRODUCTION

1.1. Study Background

Land cover land use change (LCLU) is one of the driving forces of environmental change and is increasingly becoming a global concern due to its impact on the local, regional, and global environment (Matlhodi et al., 2021; Permatasari et al., 2021). LCLU change refers to the modification of the earth's terrestrial surface due to complex interactions between humans and the physical environment (Liping et al., 2018). These changes have historically been linked to variations in biophysical factors, whereas more recent changes are primarily attributed to anthropogenic factors such as population growth, agriculture, economic and industrial development, and others (Matlhodi et al., 2019; Hossain & Moniruzzaman, 2021).

Over the past decades, humans have increasingly taken a large role in the modification of the environment (Pandian et al., 2014; Andualem et al., 2018). Studies from Sub-Saharan Africa (SSA) and other developing countries have shown that agriculture expansion, population growth, poverty, and the unsustainable use of natural resources are responsible for LCLU changes, especially in local communities surrounding the natural resource base (Haller et al., 2008). In Botswana, LCLU changes are primarily due to human and livestock population pressures, rapid urbanization, and general development activities such as increased demand for arable land, tourism, water, and others (Vanderpost et al., 1998). Some examples of LCLU changes that have been reported in Botswana, specifically in the South East District, include:

- Vegetation changes in the vicinity of settlements (Ringrose et al., 1996);
- A significant decrease in dense woody vegetation covers and a significant decline in the area of high-quality rangeland in the Notwane catchment area (Ringrose et al., 1996);
- Bush encroachment, precisely in the area covering the Gaborone dam catchment (Moleele et al., 2002);
- Increased croplands and built-up areas around the Gaborone dam catchment (Matlhodi et al., 2019).

These changes were attributed to anthropogenic and natural factors, with the anthropogenic factors being the most significant drivers (Matlhodi et al., 2019).

Land-use patterns, influenced by a variety of social processes, often result in changes in land cover that affect biodiversity, water and radiation budgets, greenhouse gas (GHG) emissions, and other factors that, when combined, affect the global climate and the biosphere. Changes in LCLU have emerged as a key issue within the scientific community concerned with global environmental changes (Dhakal et al., 2010). Land use is one of the most important determinants of soil organic carbon (SOC) stock status, as it governs long-term vegetation patterns and the amount of organic matter (OM) returned to the soil (Dhakal et al., 2010). Carbon is stored in the living biomass of plants by the process of photosynthesis, and it builds up in soils when dead and decaying biomass is detached from the parent plant. Long-term carbon sequestration in soils benefits both the environment and agriculture. Changes from one LCLU type to another are responsible for large carbon fluxes in the terrestrial ecosystem (Dhakal et al., 2010). Changes in LCLU contribute approximately 26% of global GHG emissions (natural forest conversion contributes 13.8%), compared to 14.3% from transportation and 19% from industry (Wainkwa Chia et al., 2017). Tree savannah and shrubland are important ecosystems in semi-arid areas and are regarded as carbon sinks, and the conversion of these systems into other uses ultimately reduces soil carbon due to soil erosion, decreased plant residue, organic matter input, or soil tillage (Murty et al., 2002; Wainkwa Chia et al., 2017).

Soil is the foundation of terrestrial ecosystems, providing most ecosystem services that benefit mankind (Stockmann et al., 2013; Edmondson et al., 2014; Yang et al., 2018). It contains about 2344 Pg (1 petagram = 10^{15} grams) of organic carbon and plays an important role in the global carbon cycle (Stockmann et al., 2013). Organic carbon stored in the soil is regarded as one of the most important soil properties, exhibiting both temporal and significant spatial variability, both horizontally across different LCLUs and vertically within the soil depth (Yao et al., 2020). It improves many soil-related functions and services, such as the water holding capacity, structural stabilization, and retention and release of plant nutrients (Lal et al., 2018; Lefèvre et al., 2017; Szatmári et al., 2019; Senwo, 2021). Also, it contributes significantly to overall soil health, agriculture, climate change, and food security solutions (Yang et al., 2018). Excessive depletion of SOC can degrade soil fertility, reduce biomass productivity, adversely affect water quality and food security, and contribute to global climate change (Yang et al., 2018; Senwo, 2021). Reducing

SOC loss is therefore an effective strategy for food security enhancement and climate change mitigation, thereby achieving Sustainable Development Goals (SDGs) 2 and 13, respectively.

1.2. Problem Statement

Greater Gaborone has experienced significant population growth between 1981 and 2022, primarily driven by rural to urban migration. It had a population of 72,127 in 1981 and 429,293 in 2022 (Figure 1). According to Cavrić & Keiner (2006), most of the rural-urban migration that takes place in the country is directed to Gaborone and its neighbouring settlements due to more available job opportunities, better infrastructure, social amenities, and public services. The growing population, combined with the unprecedented economic and industrial development (for example, housing, road construction, and other anthropogenic activities) in and around the city of Gaborone over the past decades, has resulted in an increasing proportion of land being converted into a built-up area (replacing croplands and shrublands). These have also promoted the expansion of peri-urban satellite settlements, resulting in areas previously occupied by agricultural lands and natural vegetation being converted into built-up areas (such as Phakalane) (Sebego & Gwebu, 2013).
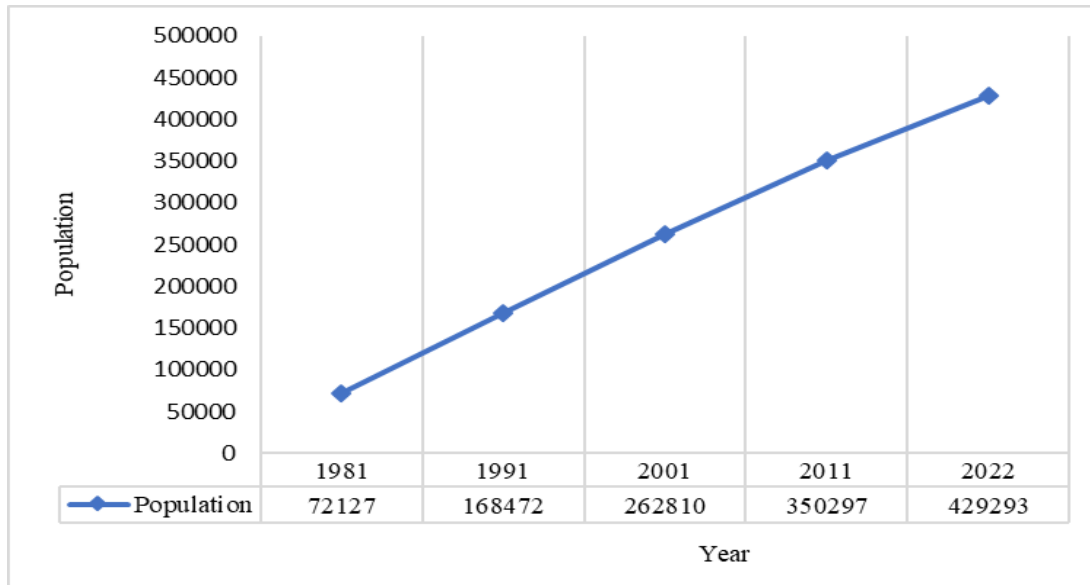
Figure 1. Population growth in Greater Gaborone Botswana (Sebego, 2014; Statistics Botswana, 2014; Statistics Botswana, 2022)

Even though several studies on LCLU change detection have been conducted in Greater Gaborone over the past years, a study on the effects of the LCLU change on SOC stock has not been done, limiting our understanding of how LCLU change affects SOC stock in the area. Therefore, information about the nature of the LCLU change, where it occurs, and the rate at which it occurs is requisite. Furthermore, very little effort has been made to estimate the SOC stock under the different LCLU types in the greater Gaborone area, thereby, justifying the importance of this study.

1.3. Objectives of the study

The main objective of this study was to identify LCLU changes in the Greater Gaborone region of Botswana between 1988 and 2022 and to examine the effect of these changes on SOC stock.

The specific objectives were as follows:

1. To document the existing LCLU types in the area
2. To detect and analyze current and future LCLU changes in the area
3. To estimate the soil organic carbon stock where LCLU change has occurred
4. To examine the effect of the LCLU change on SOC stock in the area

1.4. Research questions

The following questions were developed as a roadmap for achieving the specific objectives:

1. What are the different LCLU types in the area?
2. Where has the LCLU change occurred in the area?
3. How much SOC is stored where an LCLU change has occurred, and how much SOC is stored where no LCLU change has occurred?
4. Has the change in LCLU impacted SOC stock in the area?

1.5. Research hypothesis

1. Different LCLUs have different concentrations of SOC in the study area.
2. Changes in LCLUs bring changes in SOC stock in the study area.

1.6. Significance of the study

The findings of this study provide a better understanding of how LCLU changes affect SOC stock in the Greater Gaborone region of Botswana. Understanding the effect is vital for policy formulation and implementation of appropriate land management interventions that increase SOC

storage and reduce carbon emissions, as recommended by the United Nations Framework Convention on Climate Change (UNFCCC, 2004). The findings of this study will also serve as a scientific database for land managers and policymakers.

1.7. Structure of the Thesis

This research thesis consists of six chapters, as described below:

Chapter 1 provides an overview of the research. It also sets out the research problem, which leads to the formulation of research objectives and questions, as well as presents the importance of this study.

Chapter 2 provides a brief review of the literature on LCLU changes, soil organic carbon stock, and key concepts used in the field of study. The chapter also highlights key trends and findings from international and regional studies where Geographic Information System (GIS) and remote sensing (RS) techniques were used to assess LCLU change, as well as stimulate future change. Some techniques or methods for detecting and forecasting future LCLU changes have been explored. Furthermore, the effects of LCLU change on soil organic carbon stock were explored, as well as different methods for determining soil organic carbon content.

Chapter 3 provides a brief description of the study area. It also focuses on the application of remote sensing and GIS for detecting LCLU changes for the 1988, 2002 and 2022, as well as modelling future LCLUs for 2040. Furthermore, it focuses on the laboratory analysis of soil samples collected in and around Greater Gaborone for the determination of SOC and other soil-related properties that influence SOC accumulation in an ecosystem.

Chapter 4 discusses the results obtained in Chapter 3.

Chapter 5 concludes by summarizing the key findings of the research. It also provides recommendations and suggestions for further studies.

Chapter 6 provides a list of references used in the study.

CHAPTER 2: LITERATURE REVIEW

2.1. Land Cover Land Use Change: Concepts and Definitions

Land cover and land use are closely related terms that are often used interchangeably, although they describe different aspects of the landscape (Munthali, 2020). However, there are differences of opinion regarding the distinction between these two terms. Several researchers have defined land cover as the observed physical or biophysical features covering the earth's surface, which includes vegetation, bare land, hard surfaces, water bodies, and artificial structures (Jansen & Gregorio, 2000; Brown & Duh, 2004; Chingombe et al., 2021). Natural scientists define the "term land use" by emphasizing the various useful aspects of human activities on land, such as farming, forestry, and man-made constructions. Turner et al. (1995) defined land use as "the manner in which biological attributes of land are manipulated." The term "land use," according to Jansen and Gregorio (2000), refers to how humans intend to use or exploit land cover for activities such as forestry, settlement, grazing, and agriculture while altering processes such as biogeochemical, hydrological, and biodiversity on the land's surface. Similarly, Chingombe et al. (2021) defined land use as "human modification of the earth's terrestrial surface for socioeconomic purposes such as construction, forestry, agriculture, and others." Therefore, LCLU change refers to qualitative changes or shifts in the structure and function of a given type of land cover or use, as well as quantitative changes in the area extent of that land cover or use (Seto et al., 2002). According to Lambin et al. (2003), LCLU change can be broadly classified into two types: conversion and modification. Conversion refers to a change from one LCLU category to another, whereas modification refers to the changes that affect the structure or function of the LCLU type (Mukete et al., 2017).

Over the past decades, humans have increasingly taken a large role in the modification of the environment (Andualem et al., 2018). With the increasing number of developing technologies, man has emerged as a major and most powerful instrument of environmental change (Pandian et al., 2014). The induced changes in the environment result from complex interactions between human activities and the biophysical environment. Anthropogenic factors such as increasing population, urbanization, economic and industrial development, agricultural expansion, deforestation, and improper land use are largely known to contribute significantly to LCLU changes (Benzer, 2010).

2.2. Drivers of LCLU change

Changes in LCLUs are mostly driven by a combination of socioeconomic, political, biophysical, and technological factors (also known as land use drivers), which drive and influence the development of any landscape at different spatial and temporal scales (Briassoulis, 2003; Dietzel et al., 2005; Kalaba, 2014). Land is static, and how it is used changes constantly in response to the drivers (Munthali, 2020).

Drivers of LCLU change vary over time and so are their impacts as the local landscape changes (Lambin et al., 2003). The drivers of LCLU change are broadly divided into two categories: proximate and underlying drivers. Proximate (or direct) causes are related to the immediate actions taken by humans to meet their needs through land use, such as agricultural expansion, wood extraction, infrastructural expansion, and so on, that alter the physical state of land cover (Geist & Lambin 2002). The underlying (indirect or root) drivers, on the other hand, are related to fundamental socio-economic and political processes that push proximate causes into immediate action (Geist & Lambin, 2002). At the proximate level, change in LCLU could be explained by multiple factors rather than a single variable (Geist & Lambin, 2002). Proximate causes operate at the local level (individual farms, householders, or communities), whereas the sources of underlying causes are at regional and national levels such as districts, provinces, or countries (Lambin et al., 2003). Understanding the proximate and underlying drivers is critical for analyzing LCLU change, as well as developing realistic models for simulating future LCLUs and changes (Munthali, 2020).

Studies from Sub-Saharan Africa (SSA) and other developing countries have shown that agriculture expansion, population growth, poverty, and the unsustainable use of natural resources are responsible for LCLU changes, especially in local communities surrounding the natural resource base (Haller et al., 2008). For instance, a study conducted by Brink and Eva (2009) revealed that floods, population growth, drought, globalization, climate change, economic development, and landslides are the prominent drivers of LCLU changes in the SSA. Chaturvedi (2004), in his study, identified the use of biomass as an energy source as an important variable contributing to LCLU changes in most developing countries. According to Feldmann & Marlis (2011), about 80 – 90% of the population in SSA uses firewood, charcoal, animal dung, and agricultural residues as fuel sources. In addition, high population growth rates coupled with

poverty and the lack of alternative economic opportunities lead to over-dependence and unsustainable use of natural resources base, resulting in natural resource degradation (Kangalawe & Lyimo, 2010; Ahmed et al., 2011). Furthermore, Brink & Eva (2009) reported that LCLU changes occurring in the SSA are due to globalization, droughts, population growth and floods.

Most of the LCLU changes experienced globally result from a lack of clear and logical planning and regard for the environment (Jabbar & Zhou, 2011). Unplanned changes in LCLU are currently the most prominent issue. Failure to monitor LCLU changes can result in severe environmental challenges such as land fragmentation, which is most likely to cause climate change, biodiversity loss, and pollution, among others. Changes in LCLU can induce climate change because greenhouse gases are released into the atmosphere once vegetation is cleared, causing global warming and, eventually, climate change (Chingombe et al., 2021). Vegetation acts as a carbon sink as it absorbs CO_2 produced by both natural and anthropogenic activities.

Climate change is detrimental to both terrestrial and aquatic ecosystems. Most species become extinct or migrate to other areas once their habitats are lost. Furthermore, seasonal changes caused by climate change lead to poverty intensification, severely affecting the economy as more funds are channelled towards poverty alleviation at the expense of other developmental projects (Chingombe et al., 2021). Knowledge of LCLU change can help in the formulation of policies that strike a balance between conservation, conflicting uses, and development pressures. Therefore, it is necessary to continuously monitor LCLU changes at a micro-level (village or district) to mitigate the effects of improper land-use practices and to ensure sustainable natural resource planning and management.

2.3. LCLU change detection

Change detection refers to determining and/or describing changes in land cover or land use by observing them at different times (Munthali, 2020). It is done by quantitatively identifying the differences between multi-temporal data sets using remote sensing or GIS applications to understand the dynamics of the phenomena of interest. The LCLU change detection procedure, according to Lu et al. (2004) and Jensen (2005), consists of six major steps: the nature of change detection problems, the selection of suitable remotely sensed data, image preprocessing, image processing, or classification, the choice of change detection algorithms, and the evaluation of

change detection results. The LCLU change detection procedures and the main contents for each step, as recommended by Munthali (2020), are depicted in Figure 2.
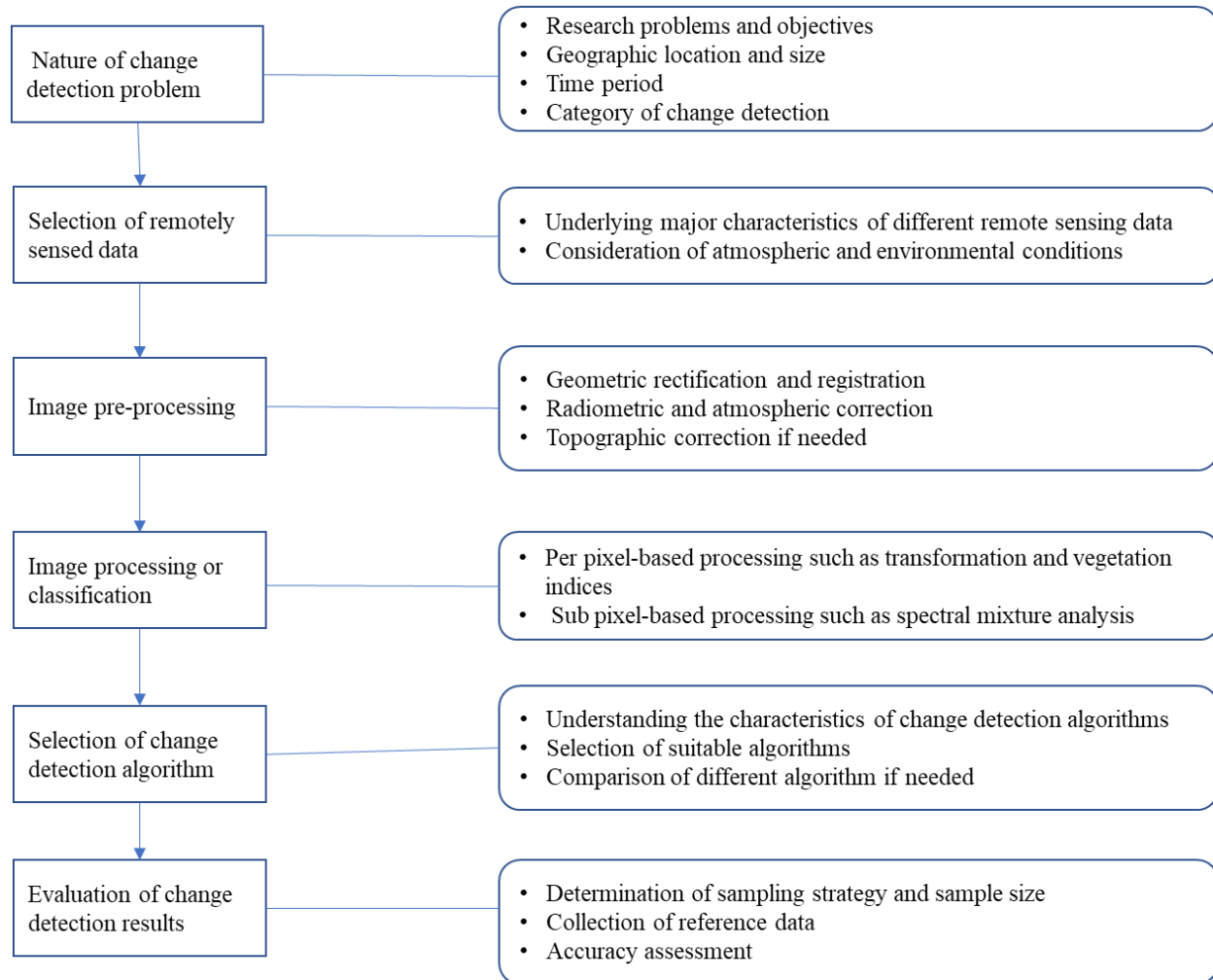
Figure 2. LCLU change detection procedure and corresponding main contents (Munthali, 2020).

Change detection aims to compare the spatial representation of two points in time by controlling all variances caused by differences in the variables of interest (Munthali, 2020). Accurate detection of changes in features on the earth's surface provides a foundation for a better understanding of the relationships between humans and natural phenomena to better manage and use natural resources (Munthali, 2020). Lu et al. (2004) suggested that a sound change detection study should provide the following indispensable information: the area of change and change rate, the spatial distribution of changed types, the change trajectories of land-cover types, and an accuracy assessment of the detection results.

The major source of data for change detection is geographic, and it is usually in digital formats, such as satellite imagery, analogue format (older aerial photos), and vector format (e.g. feature maps). Remotely sensed data such as traditionally Landsat, Satellite Probatoire d'Obsersation de la Terre (SPOT), radar, and Advanced Very High Resolution Radiometer (AVHRR) (Munthali, 2020), but recently, more high resolution satellite datasets have become available such as the Sentinel 2A. These are primary data sources for different LCLU change detection applications due to their repetitive data acquisition, synoptic view, and digital format for computer processing.

2.3.1. Image Pre-processing

Image pre-processing is the preparatory phase designed to improve the quality of image features or data for further processing or analysis (Munthali, 2020). Image pre-processing procedures include radiometric, atmospheric, geometric, and topographic corrections. Radiometric correction is performed to remove any unwanted disturbances or distortions in image data caused by satellite optical sensor limitations, changes in scene illumination, atmospheric conditions, and viewing geometry (Lu et al., 2004). Atmospheric correction removes the scattering and absorption effects of the atmosphere in order to obtain surface reflectance (Du et al., 2002). The atmospheric conditions at the different acquisition dates affect the spectral signatures of the same invariant objects (Vicente-Serrano et al., 2008; Chander et al., 2009). Therefore, a proper atmospheric correction method is required to convert raw data to surface reflectance.

2.3.2. Image Processing and Classification

Image classification is the process of categorizing pixels in an image into a smaller number of individual LCLU classes based on reflectance values (Jensen, 2005; Campbell & Wynne, 2011). Furthermore, it entails extracting different LCLU categories from raw remotely sensed digital satellite data (Weng, 2002). In a classification process, a classifier identifies and maps the patterns associated with each pixel in the image.

Image classification consists of two stages or steps (Mather, 2004). First, the user decides on the number and type of categories that will be used to describe the land cover. The LCLU class can be forest, water, pasture, or bare land. Secondly, numerical labels are assigned to pixels based on their properties using a decision-making procedure known as a classification rule or a decision rule. The images are classified using a sample set generated from training samples. These training samples

are representative of the desired LCLU classes and are determined based on ground truthing, the researcher's personal experience, and prior knowledge of the study area (Magidi, 2010). Classification can be carried out using either a group of pixels (spatial or neighborhood classifiers) or a single pixel (spectral or point classification) (Campbell & Wynne, 2011; Lillesand et al., 2008). The most commonly used method for image classification is the per-pixel-based approach (Blaschke et al., 2000). Per-pixel-based approaches are less costly and easier to program than spatial classifiers (Campbell, 2002).

The classification process for each pixel can be either supervised or unsupervised (Foody, 2002; Munthali, 2020). In supervised classification, the analyst identifies and assigns various land cover or land use types to predetermined classes. Unsupervised classification, on the contrary, entails using a computer algorithm to identify and group areas with similar spectral characteristics (Munthali, 2020). Unlike unsupervised classification, supervised classification requires the analyst to have prior knowledge of the object or features in the study area (Jensen, 2005). The most commonly used supervised classification algorithms are Parallel-piped, Maximum Likelihood, and Minimum Distance to Means (Campbell & Wynne, 2011; Eastman, 2009; Lillesand et al., 2008).

Parallel-piped classification uses a set of signature files to classify remotely sensed data. It is based on a set of lower and upper reflectance threshold values determined for each band. In this method, the pixel must have reflectance within this range for each band considered before it can be assigned to a specific class. This approach is less accurate and least precise (Eastman, 2009).

Maximum Likelihood Classification is based on a probability density function associated with specific training sites. Pixels are assigned to the most likely class based on their likelihood of belonging to each of the signatures under consideration. The Maximum Likelihood Classifier is also known as a Bayesian classifier because it can incorporate prior knowledge using Bayes' Theorem (Eastman, 2009). Prior knowledge is expressed as the probability that each class exists. It can be specified as a single value that applies to all pixels.

The Minimum Distance to Means classifier uses information from a set of signature files to classify remotely sensed data. In this approach, a signature is classified based on the mean reflectance of each band, and pixels are assigned to the class with the mean that is closest to the pixel's value (Eastman, 2009). This method is slower than parallel-piped classification and is often used when

the number of pixels used to define signatures is small or when training sites are poorly defined (Eastman, 2009). Nowadays, there is a concerted effort to use machine learning image classification techniques such as Artificial Neural Networks and Random Forest Classifiers (Munthali, 2020).

2.4. Change Detection Techniques

Over the past decades, the availability of large archived data sets has resulted in the development and evaluation of numerous digital change detection techniques and methods for analyzing and detecting LCLU changes (Munthali, 2020). These techniques and methods have been extensively reviewed and provided with excellent descriptions and comprehensive summaries (Williams et al., 2006; Haque & Basak, 2017). Different change detection methods generate different change detection maps depending on the method used (Bekalo, 2009). Therefore, the selection of an appropriate method for change detection is essential for producing accurate results because digital change detection is heavily influenced by the temporal, spatial, spectral, and thematic resolutions of remotely sensed data (Lu et al., 2004).

Change detection methods are grouped into seven (7) categories: algebra, transformation, classification, advanced models, GIS approach, visual analysis, and other approaches. The most common change detection techniques or approaches, along with examples, are summarized in Table 1.

Studies have shown that combining two change detection techniques like Image Differencing and Principal Component Analysis (PCA), Vegetation Index Differencing (VDI) and PCA, or PCA and Change Vector Analysis (CVA), improves the results of the change detection (Munthali, 2020). Image differencing, image rationing, PCA, CVA, and Post Classification Comparison (PCC) are the most commonly used change detection methods (Shaoqing & Lu, 2008; Bekalo, 2009). Pre-classification techniques such as Image differencing, PCC, PCA, and CVA are the most accurate change techniques because they are straightforward, effective for identifying and locating change, and simple to implement (Munthali, 2020).

Table 1. LCLU Change detection techniques.

Technique/ Approach	Examples of method
Algebra	▪ Image differencing ▪ Image regression ▪ Image rationing ▪ Vegetation Index Differencing ▪ Change Vector Analysis
Transformation	▪ Principal Component Analysis (PCA) ▪ Tasselled Cap (KT) ▪ Gramm-Schmidt (GS) ▪ Chi-square
Classification	▪ Post-Classification Comparison ▪ Spectral-Temporal Combined Analysis ▪ Expectation-maximization (EM) detection ▪ Unsupervised Change Detection ▪ Hybrid Change Detection ▪ Artificial Neural Networks (ANN)
Advanced models	▪ Li-Strahler Reflectance Model Spectral Mixture Model ▪ Biophysical Parameter Method
Visual analysis	▪ Visual interpretation
Other change detection techniques	▪ Measures of spatial dependence ▪ Knowledge-based vision system ▪ Area production method ▪ Combination of three indicators: vegetation indices, land surface temperature, and spatial structure ▪ Change curves ▪ Generalized linear models ▪ Curve-theorem-based approach ▪ Structure-based approach ▪ Spatial statistics-based method

Source: (Munthali, 2020)

2.4.1. Image Differencing

Image differencing change detection technique is the process of obtaining LCLU change results by subtracting the digital number (DN) of a pixel in the first-date image from the second-date image (Lu et al., 2004; Theau, 2012; Alqurashi & Kumar, 2013), as shown in equation **(1).**

$$DX_{ij}^k = X_{ij}^k(t_2) - X_{ij}^k(t_1) \tag{1}$$

Where DX_{ij}^k is the difference between pixel value x located in row i and column j for band k between acquisition date 1 (t_1) and date 2 (t_2).

In this technique, unchanged areas have a pixel value of 0, whereas areas that have changed significantly have positive or negative pixel values (Lu et al., 2004). Image differencing is a widely used change detection technique because it is straightforward and the results are

easily interpreted (Lu et al., 2004; Podeh et al., 2009). The major constraint with this technique is figuring out the threshold values for the changed and no-changed areas (Shaoqing & Lu, 2008; Munthali, 2020). Another challenge is that the two images being compared should be normalized to neutralize any changes that are superficial, such as atmospheric artefacts. The technique provides adequate information about the change itself.

2.4.2. Image Rationing

Change detection by Image Rationing is accomplished by calculating the ratio of the DN values (as shown in equation **2**) of corresponding pixels in two images taken at different times with the same number of bands (Hafez 2011).

$$DX_{ij}^k = \frac{X_{ij}^k(t_1)}{X_{ij}^k(t_2)} \hspace{3cm} (2)$$

Where DX_{ij}^k is the ratio between pixel value x located at row i and column j for band k between acquisition date 1 (t_1) and date 2 (t_2).

In this method, pixels with no change values have the same value of 1 for both dates, and changes are represented by pixels with values less than or greater than 1 (Theau, 2012; Alqurashi & Kumar, 2013). The effects of radiance change, shadows, image noise, and the angle of the sun are reduced when image rationing is used (Lu et al., 2004). Some researchers, however, argue that because it is difficult to select threshold values, this method cannot be used to analyze LCLU change. Chi et al. (2009) used image rationing and post-classification comparison (PCC) to assess urban dynamic changes in Southeastern China and found that the post-classification comparison (PCC) method produced better results than image rationing.

2.4.3. Change Vector Analysis

Change vector analysis (CVA) is a multivariate change detection technique that processes the image data in all dimensions (spectral and temporal) and represents both the magnitude and direction of the change (Munthali, 2020). The direction provides information about the nature of change, and the magnitude provides information about the level of change. The total magnitude per pixel is calculated by determining the Euclidean distance between endpoints in n-dimensional change space, as shown in equation **(3)**.

$$CM_{pixel} = \sum_{i=1}^{n}(X_2 - X_1)^2 \hspace{3cm} (3)$$

where X_1 and X_2 are date 1 and date 2 of the pixel value in i band

Change vector analysis is difficult to implement, but it can provide information about changes in all data layers rather than just selected bands (Theau, 2012; Alqurashi & Kumar, 2013).

2.4.4. Principal Component Analysis

Principal component analysis (PCA) is a technique that transforms a correlated dataset into a simpler dataset for easy interpretation (Alqurashi & Kumar, 2013). It converts the data into variables representing the essential information from the original dataset (Jensen, 2005). The PCA is done in two ways. The first step entails combining the datasets of each image into a single file and analyzing the image components separately. Second, the second image dataset is subtracted from the first image dataset. (Lu et al., 2004). After performing PCA, the no-change areas are mapped in the first component, and the changed areas are mapped in the last component (Theau, 2012). The variance-covariance matrix (C) of the multi-band images is calculated as:

$$C = \frac{\sum_{i=1}^{n}(X_j - M)(X_j - M)^T}{n - 1} \qquad (4)$$

Where M and X are multi-band image mean and individual pixel value vectors, respectively, and n is the number of pixels.

PCA reduces data redundancy and dimensionality in remote sensing datasets by assuming that change areas are not highly correlated (Lillesand et al., 2008). However, the method necessitates the selection of thresholds for detecting the change. Furthermore, PCA results are challenging to interpret and label, and they do not provide a complete matrix of change class (Lu et al., 2004).

2.4.5. Post Classification Comparison

Post Classification Comparison (PCC), an approach used in this study, is the most common, useful, and adaptable detection method for extracting LCLU change information from images with varying spatial and spectral resolutions acquired by different sensors (Alphan et al., 2009; Aguirre-Gutiérrez et al., 2012; Kindu et al., 2013). The technique entails detecting changes in the land cover type and creating maps showing the complete change matrix by coding the spectral classification results for time one and time two using a pixel-by-pixel or segment-by-segment comparison (Munthali, 2020). In this method, the analyst defines the land cover classes. The PCC technique employs both Supervised and Unsupervised classification algorithms. In PCC, the classification of individual pixels reduces atmospheric, radiometric, geometric, and sensor differences between the two dates (Alqurashi & Kumar, 2013; Munthali, 2020). However, time

and expertise are required to perform the PCC, and the quality of the classified image for each date influences the final accuracy.

2.5. Accuracy Assessment of Classified Images

The level of agreement between image classification and ground reference data is referred to as classification accuracy (Campbell & Wynne, 2011). Classification accuracy allows us to understand classification errors or classification results better. A classified error occurs when there is a mismatch between the classified data on the map and the actual class on the validation data in the field or ground reference data (Foody, 2008). Classification accuracy is done using an Error matrix, also known as the Confusion matrix (Campbell & Wynne, 2011). The Error matrix compares the relationship between known referenced data and the corresponding automated classification results on a category-by-category basis. The Error matrix calculates the overall accuracy, user's accuracy (Commission error), producer's accuracy (Omission error) and the Kappa coefficient.

The overall accuracy (OA) describes how well the classified map represents the features on the ground (Foody, 2002). It is computed by dividing the total number of correctly classified pixels (the sum of the major diagonal) by the total number of assessment points (Tempfli et al., 2009). Producer accuracy (PA) describes how well the map producer identified all the LCLU types on the maps using remotely sensed data. The user's accuracy (UA) describes how well a person using the map will locate the different LCLU classes on the ground. Kappa coefficient (KC) measures the difference between the actual and chance (random) agreement between the map and validation data on the ground (Congalton, 2001).

Kappa coefficients are measured on a scale of 0 to 1, and a value greater than 0.80 (80%) represents strong agreement and good accuracy; between 0.40 and 0.80 (40 - 80%) represents moderate agreement; and less than 0.40 represents poor agreement (Molla et al., 2018). The higher the classification accuracy, the more useful the classified map is for land administrators and land-use planners. Below are equations for computing OA, UA, PA, and KC:

$$OA = \frac{Sum\ of\ diagnal\ (correctly\ classified)}{Total\ number\ of\ sample} \times 100 \qquad (5)$$

$$UA = \frac{Samples\ correctly\ identified\ in\ the\ row}{Row\ total} \times 100 \qquad (6)$$

$$PA = \frac{Samples\ correctly\ identified\ in\ the\ Column}{Column\ total} \times 100 \qquad (7)$$

$$KC = \frac{Observed\ accuracy\ (Po) - Chance\ agreement\ (Pe)}{1 - Chance\ agreement\ (Pe)} \times 100 \qquad (8)$$

2.6. Modelling of LCLU Changes

The process of land cover and land use modelling entails simulating LCLU change using sample datasets to establish probabilistic transition rules that control how landscapes change over time (Bone & Dragicevic, 2009). In the 1960s, studies on LCLU modelling were conducted from a disciplined approach. Due to advancements in earth observation techniques such as GIS and RS, these local, regional, and global studies have taken on a multidisciplinary perspective (Parker et al., 2003; Chaikaew, 2019). Models for predicting LCLU patterns and changes have been developed and used depending on the goals (conversion, intensification, management) or the discipline (geography, natural science, economics, urban planning, regional science, and geographic information science) (Schaldach et al., 2011; Grinblat et al., 2015). According to Verburg et al. (2004), there is a growing interest in LCLU change modelling given that LCLU affects livelihoods, biodiversity and global climate. Therefore, different LCLU change models have been developed to meet specific needs and address when, where and why LCLU occurs (Bhattacharjee & Ghosh, 2015).

Based on Bhattacharjee and Ghosh's (2015) findings, LCLU models can be used:

- To provide decision support in a variety of decisions, including the development and implementation of effective policies and management strategies for sustainable natural resource management, use, and conservation, which necessitates knowledge and understanding of future LCLU patterns and changes;
- To describe the spatial and temporal relationships between the drivers and resulting patterns of LCLU changes;

- To predict or forecast future configurations of LCLU patterns under different scenarios of biophysical change, such as climatic and socio-economic change;
- As an instrument to assess the impact of past or future activities in the environmental and socio-economic spheres;
- To prescribe "optimum" patterns of LCLU for sustainable use of land resources and development;
- To evaluate a set of land use alternatives that have to be evaluated based on specific criteria.

According to Parker et al. (2003), understanding the drivers of LCLU changes requires linking landscape observations at spatial and temporal scales to empirical simulation models.

Over the past decades, a diverse range of LCLU models from different disciplines and backgrounds have been developed. Examples of some of these models include the Markov Chain Model, Cellular Automata (CA), Cellular Automata–Markov model (CA–Markov), Artificial Neural Network (ANN), Logistic Regression (LR), Conversion of Land Use and its Effects (CLUE), and Modules for Land Use Change Evaluation (MOLUSCE) (Hossain & Moniruzzaman, 2021; Kamaraj et al., 2022).

According to Verburg et al. (2008), no single model is capable of considering all the processes of LCLU changes at different scales; thus, integrated land-use models that combine one or two models are most often preferred for simulating and predicting LCLUs. Among these models, the MOLUSCE was used in this study for simulating and predicting future LCLUs because of its ability to estimate a pixel's current condition based on its initial state, surrounding neighborhood effects, and changeover laws (Kamaraj et al., 2022). Furthermore, it is user-friendly and capable of accurately depicting non-linear spatial stochastic LCLU change processes (Saputra & Lee, 2019).

2.7. Soil Organic Carbon Stock

2.7.1. Soil Organic Carbon Content

Soil is the largest carbon pool in the terrestrial biosphere, containing approximately 2344 Pg of organic carbon globally (Stockmann et al., 2013). It is one of the most important components of the biosphere, providing essential ecosystem services and processes that benefit humans (Ogle et al., 2005). Soil plays a vital role in mitigating climate change and regulating the global carbon

cycle (Muktar et al., 2018). It acts as a net source or net sink of atmospheric CO_2 (Lal et al., 2012; Anokye et al., 2021). Organic carbon stored in the soil represents 62% of the global carbon pool (Senwo, 2021), and minor changes in SOC storage can influence atmospheric CO_2 concentrations (Stockmann et al., 2013; Gebrehiwot, 2021). In addition, SOC is one of the most important properties of the soil that shows not only temporal but spatial variability, both horizontally across different LCLUs and vertically within the soil profile (Yao et al., 2020). This can be observed on the Global Soil Map (Figure 3), which depicts the amount of SOC stock in the 30 cm soil profile across different regions of the globe (Hiederer, 2011).
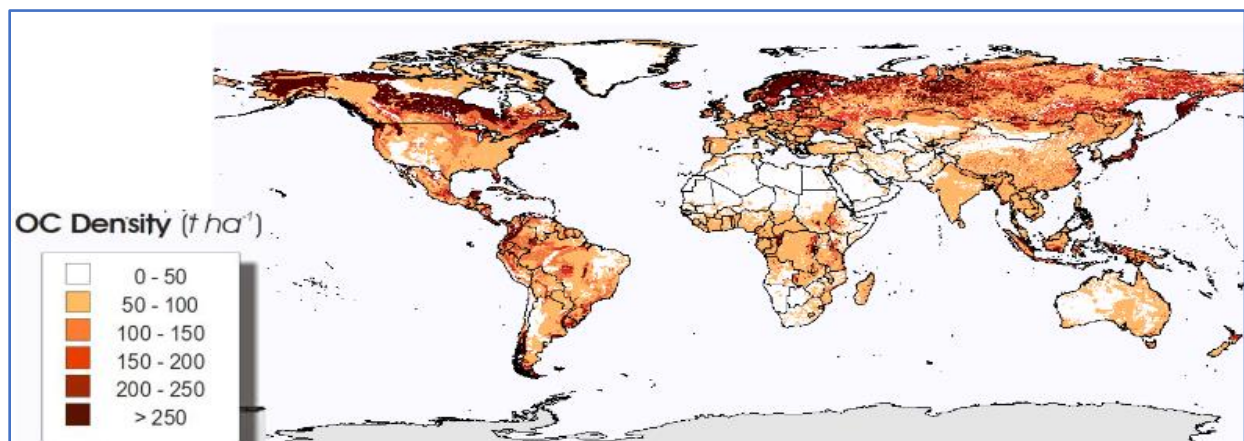
Figure 3. Global Soil Organic Carbon stock (t ha^{-1}) for combined topsoil and subsoil layer (Hiederer and Köchy, 2011).

The soils of Botswana, located in the Southern Hemisphere, are characterized by a low concentration of organic carbon content, ranging from 0 – 50 t/ha, as indicated on the SOC map (Figure 3). This is consistent with the results obtained by the Food and Agricultural Organization of the United Nations (FAO), the United Nations Development Program (UNDP), and the Government of Botswana during the Botswana Soil Mapping and Advisory Service project in 1990 (GoB, 1990). The results also revealed spatial variation in SOC content across districts in Botswana. In the South East District, for instance, the amount of SOC content within the 30 cm soil profile varies substantially across different geographical locations (Table 2). The sampled points are depicted in Figure 4. The variation in SOC across different geographical locations can be attributed to the vegetation cover type, soil types, soil pH and soil texture in the area. The soil pH in the area ranges from 5.5 to 7.9, while the SOC content ranges from 0.1 to 0.8 % (Huesken et al., 1989).

Table 2. Variation of SOC content in different locations in the South East District in 1989

ID	Latitude	Longitude	Carbon (weight %)	pH
R-0011	*-24.8912*	*25.784*	*0.4*	*6.8*
L-0053	*-25.1431*	*25.636*	*0.5*	*7.9*
R-0004	*-24.8186*	*25.838*	*0.2*	*7.9*
*R-0007	*-24.7703*	*25.837*	*0.1*	*6.0*
R-0015	*-24.9514*	*25.696*	*0.8*	*7.6*
R-0020	*-24.8028*	*25.743*	*0.1*	*4.9*
*G-0518	*-24.6694*	*26.156*	*0.3*	*5.9*
L-0902	*-25.2444*	*25.696*	*0.6*	*5.9*
L-0008	*-25.0847*	*25.779*	*0.4*	*5.5*
L-0091	*-25.4236*	*25.574*	*0.6*	*6.0*
R-0024	*-24.8139*	*25.785*	*0.2*	*5.3*
*G-0901	*-24.5611*	*25.944*	*0.2*	*5.9*
L-0004	*-25.0425*	*25.761*	*0.5*	*5.5*

Source: Botswana Soil Mapping and Advisory Service project (FAO/BOT/85/011) (Huesken et al., 1989)
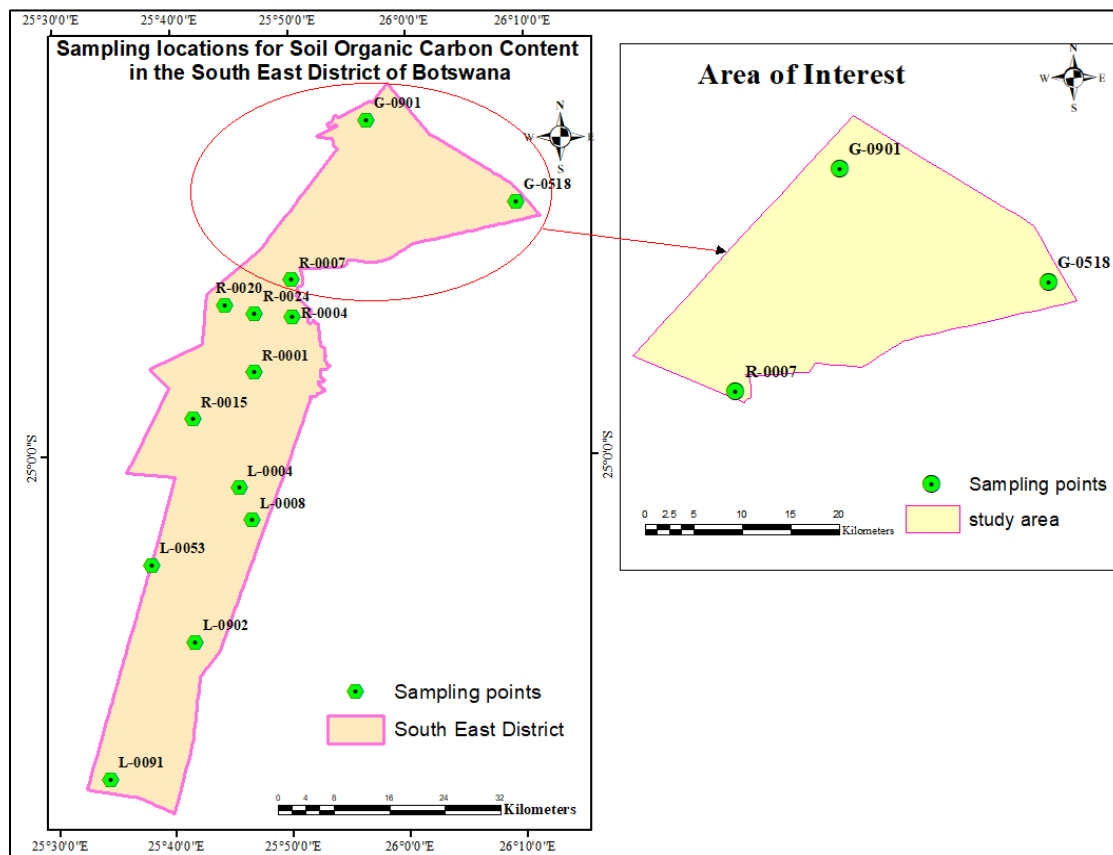
Figure 4. Sampling locations for SOC content in the South East District of Botswana in 1989 (Huesken et al., 1989)

2.7.2. Soil Organic Carbon Sequestration in Different LCLU Types

Carbon sequestration is the process of capturing and storing atmospheric CO_2 in a stabilized form. It is one of the techniques for reducing CO_2 levels in the atmosphere with the goal of mitigating climate change. The CO_2 is captured through the process of photosynthesis and stored in the soil through the decomposition of plant residues and organic matter (Izaurralde et al., 2000). According to the IPCC (2007), forests can save 5,380 Mt CO_2 per year, and forest soils can absorb about 70% of atmospheric CO_2, depending on the site's history and the LCLU pattern (Wolde et al., 2014). Agricultural land stores a small amount of SOC compared to other land uses (Phuntsho, 2016). They, however, have the potential to sequester more CO_2 from the atmosphere through improved land management practices (Phuntsho, 2016). The quantity and quality of organic matter input, decomposition rate, and land management strategies all play a vital role in determining the carbon sequestration capacity of agricultural lands (Bayer et al., 2006; Cochran et al., 2007). This is because proper agricultural land management (such as the use of farmyard manure) can largely increase soil carbon storage (Mosier et al., 2003). Proper land management practices, such as planting trees along the edges of agricultural fields, can increase carbon storage under agricultural land (Wani et al., 2012). Tilled soil under agricultural land has low SOC stock due to increased carbon emissions, contributing to increasing levels of atmospheric CO_2 and climate change. A study conducted by Schlesinger (1999) on carbon sequestration potential in agricultural lands, for example, revealed a significant SOC stock variation in tilled (1,250 g C m/2) and untilled soil (1,740 g C/m2).

Badgery et al. (2014) reported that temporal changes in SOC stock in different LCLU types occur in the topsoil. According to Batjes (1996), the top 1m soil profile stores approximately 1,500 Gt of SOC and about half of it is present in the top 30 cm. This is because it is the most biologically active layer of the soil (Drayton & Chandler, 2016). This also explains why the concentration of SOC decreased exponentially with depth, as reported by several studies (Soussana & Lemaire, 2014; Orgill et al., 2014). Also, it is the depth recommended by the IPCC (2003) for SOC stock assessment for national or global carbon accounting. Changes in SOC stock in deeper soil layers often appear several years (typically more than ten years) following land use/management (Knops & Bradley, 2009; Stahl et al., 2016).

2.7.3. Factors Influencing SOC Stock in Different LCLU Types

The amount of SOC stock in any given terrestrial ecosystem is influenced by several factors, such as vegetation cover type, climatic conditions, soil texture, soil pH, and land management practices (Zimmermann, 2013; Phuntsho, 2016).

Vegetation cover impacts carbon dynamics by influencing soil respiration, carbon flux, and carbon fixation (Phuntsho, 2016). Vegetation cover type is regarded as one of the important factors influencing SOC variation because it is a major source of carbon (Dar & Sundarapandian, 2015). Furthermore, the amount of SOC stored is also influenced by the rate of leaf deposition, temperature, moisture, and soil microorganisms (Phuntsho, 2016).

Climate parameters such as temperature and precipitation also influence SOC accumulation. As temperature rises, the amount of SOC in the soil decreases. Shrestha et al. (2004) reported that temperature increase reduces SOC stock despite higher primary productivity potentials. This is because the decomposition rate increases with temperature rise, thereby lowering the SOC storage (Phuntsho, 2016).

High soil moisture content highly favours SOC accumulation (Phuntsho, 2016). However, areas with frequently occurring anaerobic conditions due to high precipitation and waterlogging, such as wetlands and peatlands, tend to lower SOC decompositions due to the inhibition of microbial activity (Zimmermann, 2013).

Soil pH regulates microbial activity as well as turnover rates. Higher acidity generally inhibits microbial activity and reduces mineralization, resulting in higher accumulations of SOC (Kemmitt et al., 2006). Zhou et al. (2019) reported that low pH favours SOC accumulation because the bacteria or organisms most responsible for breaking down the organic matter experience a sharp drop in activity once the pH falls below 6.0.

Land use and soil management practices significantly impact SOC concentration and carbon flux (Ghimire et al., 2019). According to studies, the main factor governing SOC content is the land use type, which alters soil properties and the supply of soil nutrients (Dejun et al., 2012; Muktar et al., 2018; Yan et al., 2012). Several studies have found that converting natural ecosystems to managed systems results in a significant loss in SOC (Fan et al., 2016; Guillaume et al., 2015; IPCC, 2013; Yihenew & Getachew, 2013). Similarly, empirical studies have reported a loss in

SOC ranging from 2.3 to 8.0 t/ha in a year following land use conversion (Assefa et al., 2017; Kassa et al., 2017). However, several other studies have reported an increase in SOC stock due to switching from non-tree to agroforestry systems (Priano et al., 2018). Intensive use of mineral fertilizer in agricultural land tends to reduce SOC accumulation while increasing crop yield in the short run (Shrestha et al., 2004). Also, the use of no-tillage techniques improves SOC stock. Generally, sustainable land management practices improve SOC storage.

Soil texture influences SOC accumulation through its ability to stabilize soil organic matter (Baldock & Skjemstad, 2000). Fine-textured soil has more SOC content than coarse-textured soil due to its capacity to store water, retain more nutrients, and provide a better soil structure for plant growth (Dlamini et al., 2014). However, coarse-textured soils have low SOC content due to the absence of protection provided by clay particles (Chan et al., 2010).

2.7.4. Effects of LCLU Change on SOC Stock

The present global SOC stocks show a declining trend in all regions due to changes in LCLU practices (Gelaw et al., 2014; Yang et al., 2018). Several studies have reported that SOC stock either increases or decreases following an LCLU change. For example, in China, Luo et al. (2014) investigated soil carbon storage and water consumption patterns in an Oasis-desert ecotone facing land use change and found that cropland expansion led to a significant reduction in SOC stock. Also, Yang et al. (2018) investigated the effects of land use change on soil carbon storage in the Shi Yang river basin in China over the last 40 years and found that land use changes in the area resulted in a loss of 3.89Tg (Teragram) of soil carbon storage between 1973 and 2012. Furthermore, Sharma et al. (2019) assessed the effect of land use change on SOC stock in the semi-arid region of Rajasthan, India and found a net loss of 11.05 MtC between 1993 and 2014.

Soil carbon pools may become "sources" of atmospheric CO_2 if LCLU changes continue. For instance, it was estimated that the release of carbon to the atmosphere due to these reasons from the world's soils is at 40–50 Pg C per year, and over the last 150 years, the reduction in SOC has contributed 6–8% of the rise in atmospheric CO_2 (Yang et al., 2018). Rising levels of atmospheric CO_2 contribute to climate change (Anokye et al., 2021). Climate change effects are easily noticed in changing soil carbon storage, net primary productivity, and soil respiration (Yang et al., 2018). Other noticeable impacts of climate change include fluctuations in temperatures and precipitation

regimes, glacier retreat, sea-level rise, and low crop yields (Pattarawan, 2016). SOC storage is related to soil quality and continued carbon loss from soil reduces land productivity on a local scale while exacerbating the greenhouse effect on a global scale. Therefore, appropriate land management practices that increase SOC storage need to be implemented to reduce SOC stock losses.

2.7.5. Methods for Estimating SOC Stock

Several methods for determining SOC content have been developed and used over the past decades. The most widely used methods include the Walkley and Black Method (Walkley & Black, 1934), Loss-on-ignition (Santisteban et al., 2004), geospatial method (Kumar et al., 2016), geostatistical method (Baggaley et al., 2016), visible near infrared (Vis-NIR) (Peng et al., 2015), and Isotopic analysis (Nordt et al., 1998), spectroscopic technique (FOA, 2019).

In the determination of SOC content using dry combustion or the elementary method, 20 g of soil is pre-treated with phosphoric acid (H_3PO_4) for 12 hours to remove any carbonates that may be present (FAO, 2019). A fraction of the sample is then combusted at 900 °C, and the SOC concentration is determined based on the amount of CO_2 released from the sample (Phuntsho, 2016). Compared to other methods, the dry combustion method is relatively more accurate and is widely used for determining SOC concentration.

The loss on ignition (LOI) method requires a muffle furnace to measure SOC content. The method is based on the differential thermal effects on the soil samples. LOI measures the weight loss of the soil sample after drying it at 550 °C (Santisteban et al., 2004) for a couple of hours.

The Walkley-Black method (the method used in this study) is a wet chemistry method (Donovan, 2013). This method is as accurate as the Elementary method except for soils with low Organic Carbon. In contrast to the other methods, this method is more accurate, less expensive and simpler (Phuntsho, 2016), explaining why it was adopted in this study.

The spectroscopic technique involves the use of electromagnetic radiation to characterize the physical and biochemical composition of a soil sample. It is the fastest method to determine SOC content. In this method, light is shone on a soil sample, and the properties of the reflected light

(visible-near-infrared, near-infrared, or mid-infrared) are representatives of molecular vibrations that respond to the mineral and organic composition of soils (FAO, 2019).

The geospatial method estimates soil organic carbon content using the bare soil index (BSI) or normalized difference vegetation index (NDVI) derived from remote sensing data (Kumar et al., 2016). The use of spectral indices derived from remote sensing data for SOC stock quantification came from the use of wavelengths in Vis-NIR spectroscopy. To estimate SOC stock using the NDVI approach, an NDVI map is generated using the near-infrared and red bands of the remotely sensed data as follows:

$$NDVI = \frac{(NIR - Red)}{(NIR + Red)} \qquad (9)$$

Where NIR and Red belong to the Near-Infrared and red bands of the satellite image, respectively.

NDVI value ranges from -1 to 1. Areas with high NDVI values indicate healthy vegetation, while those with low NDVI values represent bare land or water bodies (Kumar et al., 2016). Since SOC influences biomass productivity, it suggests that areas with healthy vegetation have higher SOC contents than areas with no vegetation cover.

However, to determine SOC content using the BSI approach, the following equation **(10)** is used to generate the BSI map for the study area (Kumar et al., 2016). The BSI value also ranges from -1 to 1. High BSI values indicate the area has more open or bare soil, whereas low BSI values are associated with soil covered with vegetation (Kumar et al., 2016).

$$BSI = \frac{[(B5 + B3) - (B4 + B1)]}{[(B5 + B3) + (B4 + B1)]} \qquad (10)$$

Where BSI is the bare soil index, B1 is the Blue band, B3 is the Green band, B4 is the Red band, and B5 is the Near-infrared band.

Using satellite imagery is a less costly approach but requires previous studies on soil properties (Peng et al., 2015). The geospatial method was one of the possible methods to be adopted in this study, but due to limited data and the challenges in distinguishing different LCLU types in the generated NDVI or BSI map of the study area due to spectral ambiguity, the geospatial approach

was not adopted. Even though the geospatial and geostatistical methods are used to map large areas, the traditional method, which involves laboratory analysis, continues to serve as a source of reference (Tsao, 2017), an approach used in this study.

CHAPTER 3: MATERIALS AND METHODS

3.1. Description of the Study Area

Greater Gaborone lies between the Longitudes 25^0 45' 17.76" E and 26^0 11' 01.04" E and Latitudes 24^0 41' 15.44" S and 24^0 42' 45.96" S. It covers a surface area of 669 km^2 and has an average elevation of approximately 1000 m above mean sea level. To the east, the area includes the tribal villages of Tlokweng, Oodi, and Modipane; to the west, it includes Mogoditshane and Gabane; to the south, it includes Mokolodi; and to the north, Gaborone is bordered by the Bakgatla tribal land (Figure 5). These peri-urban villages have grown with the influence of the city and have attained the status of its suburbs, even though their land tenure remains tribal (Sebego, 2014). Historically, significantly large areas of present-day Gaborone used to be freehold farmland. For example, the area west of the railway line (now known as Gaborone – West) and Broadhurst did not exist until the early 1980s, when the government bought freehold farms in those areas to make way for development (Sebego, 2014). Private landholders have also contributed to the expansion of the city. Some farms have been developed into huge townships like Pakalane Estates, Gaborone North, and Mokolodi. These areas are now fully developed suburbs, well established with all the social amenities that go along with modern residential development. The population of the villages had grown rapidly between 1988 and 2022 (Table 3). The development of such peri-urban villages means that land is constantly being converted from its natural state to urban status.

Table 3. Population figures for Gaborone and surrounding villages

Location	1981	1991	2001	2011	2022
Gaborone	59 657	133 468	186 007	231 592	246 325
Tlokweng	6 657	12 501	21 133	36 323	55 508
Oodi	-	2 282	3 440	5 687	10 257
Modipane	-	-	2 508	3,197	7 945
Mokolodi	-	-	507	624	1 242
Mogoditshane	3 125	14 246	38 816	57 637	88 006
Gabane	2 688	5 975	10 399	15 237	20 010
Total population	**72 127**	**168 472**	**262 810**	**350 297**	**429 293**

Source: (Sebego, 2014; Statistics Botswana, 2014, 2022)

The climate of the study area is semi-arid, characterized by a hot, wet season (November–April), a long, dry season (May–October), and a winter season (May–August). The average temperature of the area is 20.6 °C, with average minimum and maximum monthly temperatures of 12.8 and

28.6 °C, respectively (Dikinya et al., 2016). The annual average rainfall brought by winds from the Indian Ocean averages 500 mm (Tsheko, 2021). Prolonged dry spells during rainy seasons are common, and rainfall is erratic, highly variable, and spatially localized (Madisa et al., 2017).
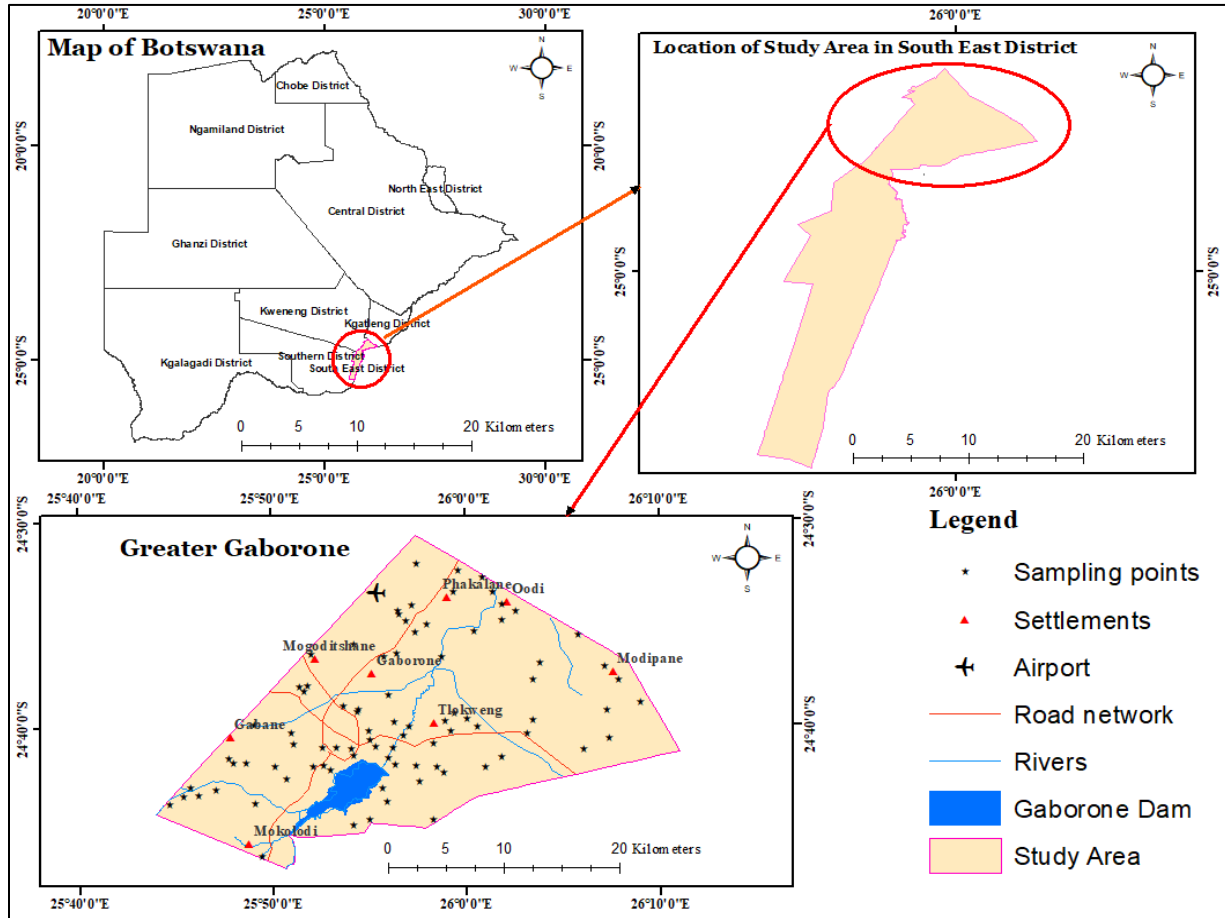
Figure 5. Map of the study area

Agricultural practices include irrigated agriculture, rainfed agriculture and livestock production. Permanent water bodies found in the area include the Gaborone Dam and the Sewage treatment ponds. The vegetation cover consists mainly of Acacia shrubs and tree savanna. The most common tree species in this study area are *Acacia tortilis* and *Acacia erubescence* (Sebego, 2014).

The soil types in the area consist of Vertisols, Haplic Lixisol, and Eutric regosols (FAO, 2006). Vertisols are a group of heavy textured soils characterized by high values of clay content (30%), soil pH (7.5 – 8.5), organic matter content and water-holding capacity with variable bulk densities due to the swelling and shrinking nature of the soil as moisture content changes (Virmani et al.,

1982). Lixisols are heavily weathered soils with limited nutrient availability and reserves, low water holding capacity, low cation exchange capacity, and high pH (Ebelhar et al., 2008). Regosols are characterized by medium to fine-textured soil, which may be alluvial in origin and lack significant soil horizon (layer) formation. They have low values of water-holding capacity and organic matter content and are prone to soil erosion (Virmani et al., 1982).

3.2. Software Packages

The following packages were used in this study for data collection, processing, and presentation:

- ArcGIS—for data creation, dataset preparation, image classification, change detection, and accuracy assessment;
- QGIS—for future LCLU prediction; this was chosen because a plugin is readily available.
- Google Earth Pro (high resolution imagery)—for identifying LCLU classes and accuracy assessment;
- Microsoft Office—for documentation and presentations.
- R program—for statistical analysis of soil properties.

3.3. Detection of LCLU Change

Figure 6 represents a methodology flow chart that was used to analyze LCLU changes between 1988 and 2022, as well as to predict 2040 LCLU in the study area.
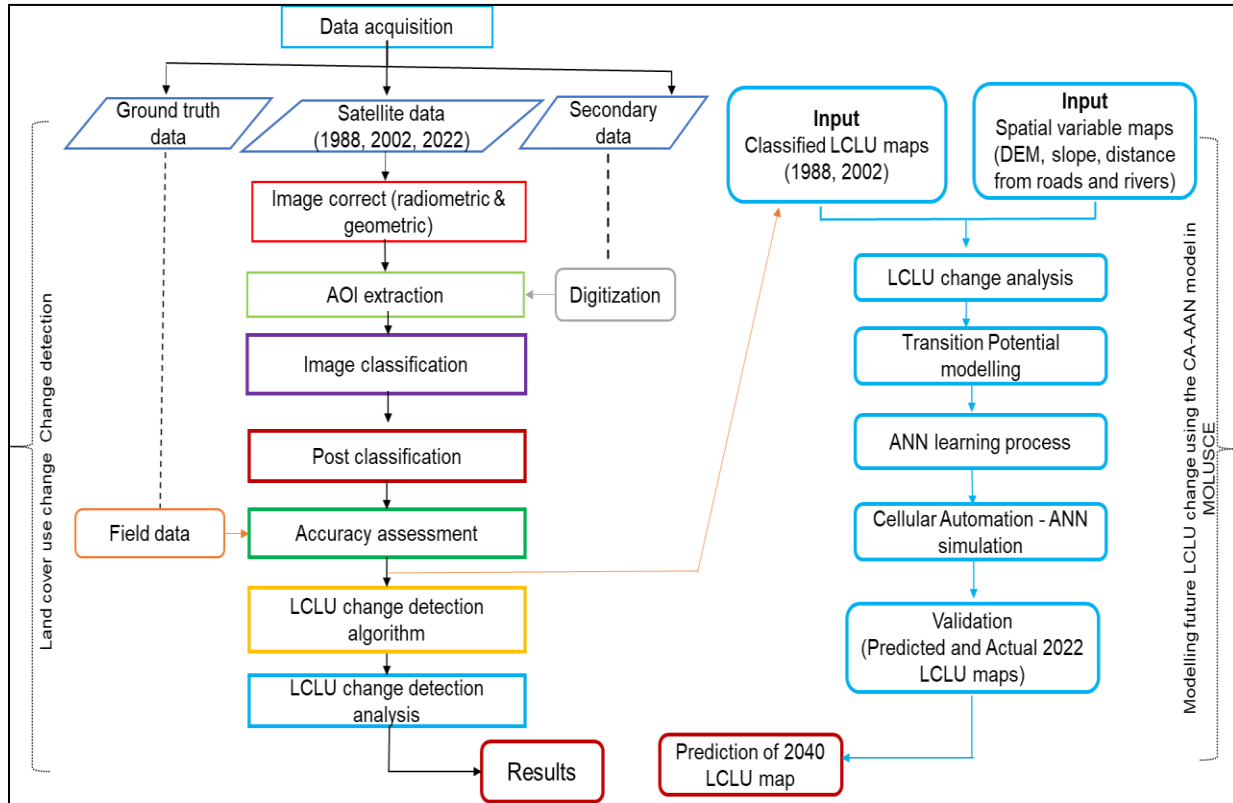
Figure 6. Methodology flow chart.

3.3.1. Data Acquisition

This study explored Landsat 5 (Thematic Mapper) for 1988 satellite imagery, Landsat 7 (Enhanced Thematic Mapper Plus) for a 2002 satellite imagery, and Sentinel-2A Multi-Spectral Instrument (MSI) for a 2022 satellite imagery from the United States Geological Survey (USGS) Earth Explorer (www.usgs.gov), using path 172 and row 77 for Landsat images and T35JLN/MN for Sentinal-2A (Table 4). The selected images had a cloud cover of less than 10% (for easy interpretation) and were acquired in March for temporal consistency that minimizes seasonal and sun varying position effects. The area of interest (AOI) was digitized in Google Earth Pro, exported as a KML file and later converted to a shapefile in ArcGIS using the Conversion tool in ArcGIS 10.7. Ground control points (GCP) were collected using a Geographical Positioning System (GPS).

Table 4. Images used for LCLU classification and analysis

Year	Satellite/Sensor	Path/Row	Acquisition date	Resolution (m)	Bands used	Source
1988	Landsat 5 (TM)	172/077	March 19	30*30	1,2,3,4,5,6,7	USGS
2002	Landsat 7 (ETM+)	172/077	March 6	30*30	1,2,3,4,5,6,7	USGS
2022	Sentinel-2 (MSI)	T35JMN	March 30	10*10	2,3,4,8	USGS
2022	Sentinel-2 (MSI)	T35JLN	March 30	10*10	2,3,4,8	USGS

3.3.2. Image Pre-processing

Landsat images used for LCLU classification are often affected by atmospheric and topographic/geometric errors, thus requiring correction (Phiri et al., 2018). Radiometric correction is an essential step in the pre-processing of satellite imagery because image classification is done based on radiometric values. The process of radiometric correction includes atmospheric correction, sun elevation correction, and earth-sun distance correction, as well as simpler processes such as radiometric normalization and histogram equalization (Gašparović, 2020). Radiometric correction is essential, especially when measurements are taken from multiple sensing platforms, such as the combination of Landsat-5, 7, 8, and Sentinel-2 (Gašparović, 2020). In this study, radiometric correction was done by converting digital numbers to radiance. The image pixel values after correction represent an estimate of the surface reflectance or Bottom of Atmosphere (BOA) reflectance level (Pinto et al., 2020), thus having better image quality for easy interpretation.

Furthermore, because of the possibility of geometric distortion in satellite imagery which may result from ground curvature or topographic influence, it is essential to perform geometric correction, especially when carrying out spatiotemporal analysis (Gašparović, 2020). This correction was made possible by orthorectifying the images after projecting them to a common geographic reference system defined by the Universal Transverse Mercator (UTM), specifically, UTM zone 35S coordinate on WGS 1984. The orthorectification process eliminates the effect of terrain on the satellite image and converts the raw image to an orthorectified image, having a perfect alignment with ground features (Gašparović, 2020).

For image composition, the MTL metadata files of the Landsat images were loaded into ArcGIS to create a colour composite of the images. However, for the Sentinel-2A images, image composition was done by selecting bands 2, 3, 4, and 8 because each has a spatial resolution of 10m. The bands were combined in ArcGIS 10.7 using the band composite tool under the Data

Management tool. The study area is covered by one Landsat and two Sentinel-2 image tiles. The two Sentinel image tiles were mosaicked in ArcGIS 10.7 to create a new raster image using the Mosaic to New Raster tool under the Data Management tool before extracting the area of interest (AOI) for classification.

3.3.3. Image Classification

Image classification is the process of creating thematic maps from satellite data by classifying all pixels into LCLU classes based on their spectral properties (Chingombe et al., 2021). There are two methods for image classification: Supervised and Unsupervised methods. The Supervised classification method uses sample points or polygons (ground truth points) from known LCLU types to classify images and these ground truth points are used to train a classifier (Andualem & Guadie, 2018). The Unsupervised classification approach, on the other hand, is a form of image classification in which the user has no idea about the LCLU types present in the area of study and it is purely based on the spectral histogram of all available pixels in an image (Andualem & Guadie, 2018). The classification process in Supervised classification is managed by using the signature editor to create, manage, evaluate, and change signatures (Andualem & Guadie, 2018). Signatures are specific areas to which the names of the LCLU classes are assigned. Signatures are used to break the different LCLU classes into as many subclasses as per the classification requirement. The Supervised classification method, according to Chingombe et al. (2021), produces more accurate classification than the Unsupervised method because the algorithm is trained based on user knowledge.

In this study, a supervised classification method based on a Maximum Likelihood classifier was adopted because of the ease of implementation to extract the LCLU classes. This classifies pixels based on the highest probability that a pixel belongs to a given class. In addition, Maximum Likelihood classification allows the validation of classified images through ground truthing (Chingombe et al., 2021). Furthermore, this method assumes that the spectral values of the training pixels are normally distributed and computes the probability that the given pixel belongs to a specific class (Tendaupenyu et al., 2017).

A band combination of Red, Green and Blue was used to display the raw images. Training classes were selected through visual interpretation of high-resolution satellite images in Google Earth Pro

maps. The training areas of each LCLU class were selected throughout the study area to obtain good representatives (Tendaupenyu et al., 2017). The centre of large patches of LCLU features that were unlikely to contain mixed classes were selected in order to improve the accuracy of the classified image. Using a rule-of-thumb approach, at least 500 pixels per class were selected to enable a meaningful calculation of statistics (Mather & Tso, 2009). Based on the characteristics of Landsat and Sentinel-2A satellite images from 1988, 2002, and 2022, six major LCLU types were identified in the study area: water bodies, tree cover, cropland, shrubland, bare land and built-up (Table 5).

Table 5. Description of LCLU classes in the study area

	LCLU type	**Description**
1	Waterbody	This includes streams, rivers, dams or reservoirs and ponds.
2	Tree cover	Woody plants that are taller than 5 meters and have a distinct crown.
3	Cropland	This includes forage, orchards, nurseries, horticultural land, and cultivated land.
4	Shrubland	This includes woody plants less than 5 m tall with no defined crown and a mix of trees and grasses.
5	Bare land	This includes exposed soils, sand, bare rocks, and areas with less than 10% vegetation cover.
6	Built-up	This includes residential, commercial, industrial, transportation and urban areas.

Source: *Matlhodi et al., 2019)*

3.3.4. Post Classification Refinement

A classified image often contains noise caused by the isolated pixels of some classes within another dominant class, which can form large patches (Erasu, 2017). It is important to presume that these isolated pixels are more likely to belong to this dominant class than to the classes to which they were initially assigned as a result of classification errors. An appropriate smoothing process applied to a classification image will not only 'clean up' the image but also make it visually less noisy and improve the accuracy of classification (Erasu, 2017). However, Post Classification refinement may degrade classification results due to class overestimation because some pixels are replaced by values from the majority of their neighbours (Nhamo et al., 2018). This is common,

especially when using the Nibble tool in ArcGIS. Post-classification smoothing with a majority filter is essential to reduce unnecessary errors and may further improve classification accuracy (Erasu, 2017). Filtering entails conveying isolated pixels to the leading class within which they lie. In this study, tools such as the Majority filter and Boundary clean tools integrated within the ArcGIS software were used to smoothen or refine the classified images to improve classification accuracy.

3.3.5. Accuracy Assessment

Accuracy assessment for image classification is essential as it measures the number of ground truth pixels that have been classified correctly – producer's accuracy (Chingombe et al., 2021) and the expected accuracy when using the created map – user's accuracy. In this study, a classification accuracy assessment was performed based on points that were identified on the images and selected to represent the different LCLU classes in the study area. A stratified random sampling method was used to collect a total of 232, 274, and 296 reference data from the classified LCLU maps of 1988, 2002, and 2022, respectively, to ensure that all six (6) LCLU classes were adequately represented based on the proportional area of each class. The data was imported into Google Earth Pro maps to assess the classification accuracy. The ground truth data and the classification data were compared and statistically analyzed using an error matrix to determine if the pixels were grouped to the correct feature class. The Error matrix was then used to compute the overall accuracy (OA), user's accuracy (UA), producer's accuracy (PA) and Kappa statistic (KC). The overall accuracy, user accuracy and producer accuracy, respectively, indicate the accuracy of the entire classification, the likelihood that a classified pixel represents the class on the ground or in reference data, and how well the trained pixels of the given cover type are classified (Matlhodi et al., 2019). In this study, equations **(5)**, **(6)**, and **(7)** were used to compute the OA, UA, and PA, respectively.

The KC represents the measure of reproducibility and assesses the probability of chance agreement between the reference and the image datasets (Turner, 2005). In this study, the Kappa coefficient was calculated using equation **(11)** derived by Jensen & Cowen (1999). In Kappa analysis, a KC value of 0.8 and above indicates a very strong agreement, while a KC value between 0.4 and 0.8 indicates a good agreement, and a value below 0.4 indicates a poor agreement (Molla et al., 2018).

$$KC = \frac{N \sum_{i=1}^{r} X_{ii} - \sum_{i=1}^{r}(X_{i+} * X_{+i})}{N^2 - \sum_{i=1}^{r}(X_{i+} * X_{+i})} \qquad (11)$$

Where Kc is the Kappa coefficient, N is the total number of observations included in the matrix, r is the number of rows in the error matrix, X_{ii} is the number of observations in row i and column i (on the major diagonal), X_{i+} is the total number of observations in row i (shown as marginal total to the right of the matrix), and X_{+i} is the total number of observations in column i (shown as marginal total at bottom of the matrix).

3.3.6. Change Detection Analysis

Change detection is the process of detecting changes in the state of LCLU classes by observing them at different times (Andualem et al., 2018). Change detection quantifies the changes in the landscape associated with LCLU changes using remotely sensed images acquired in the same geographical area at different acquisition dates (Ramachandra & Kumar, 2004). It is useful in many applications, such as LCLU changes, habitat fragmentation, sprawl, and other changes that may occur within the environment (Noor et al., 2013). Several techniques with varying degrees of outlay, accuracy, and proficiency have been developed and widely used to assess changes that occur in the environment (Hassan et al., 2018). The Normalized Difference Vegetation Index (NDVI), Artificial Neural Networks (ANN), Change Vector Analysis (CVA), Post Classification, and Image Differencing are among the most commonly used methods for detecting changes in the environment (Peters et al., 2002; Alqurashi & Kumar, 2013; Hossain & Moniruzzaman, 2021).

Among these techniques, the Post Classification Comparison (PCC) approach was employed in this study to detect the LCLU changes that had happened in the study area. PCC uses pixel-based comparison to generate change information on a pixel-by-pixel basis and thus interpret the changes more efficiently by taking advantage of "from-to" information (Matlhodi et al., 2019). In addition, this approach provides detailed information on the initial and final LCLU types in a complete matrix of direction change (Chingombe et al., 2021). The use of the PCC technique resulted in a cross-tabulation matrix (LCLU change transition matrix), which was computed using the overlay functions in ArcGIS. The computed LCLU change transition matrix consisted of rows (displaying LCLU type for time 1, T_1) and columns (displaying LCLU type for time 2, T_2), as shown in Table 6.

Table 6. General LCLU change transition matrix for comparing two maps between observation times.

	LCLU type	LCLU 1	LCLU 2	LCLU 3	LCLU 4	LCLU 5	LCLU 6	Total T1	Loss
					Time 2 (T_2)				
Time 1 (T_1)	LCLU 1	A_{11}	A_{12}	A_{13}	A_{14}	A_{15}	A_{16}	A_{1+}	$A_{1+} - A_{11}$
	LCLU 2	A_{21}	A_{22}	A_{23}	A_{24}	A_{25}	A_{26}	A_{2+}	$A_{2+} - A_{22}$
	LCLU 3	A_{31}	A_{32}	A_{33}	A_{34}	A_{35}	A_{36}	A_{3+}	$A_{3+} - A_{33}$
	LCLU 4	A_{41}	A_{42}	A_{43}	A_{44}	A_{45}	A_{46}	A_{4+}	$A_{4+} - A_{44}$
	LCLU 5	A_{51}	A_{52}	A_{53}	A_{54}	A_{55}	A_{56}	A_{5+}	$A_{5+} - A_{55}$
	LCLU 6	A_{61}	A_{62}	A_{63}	A_{64}	A_{65}	A_{66}	A_{6+}	$A_{6+} - A_{66}$
	Total T2	A_{+1}	A_{+2}	A_{+3}	A_{+4}	A_{+5}	A_{+6}	1	
	Gain	$A_{+1} - A_{11}$	$A_{+2} - A_{22}$	$A_{+3} - A_{33}$	$A_{+4} - A_{44}$	$A_{+5} - A_{55}$	$A_{+6} - A_{66}$		

Where A_{ij} is the land area that experiences a transition from LCLU type i to LCLU type j, A_{ii} are the diagonal elements indicating the land area that shows the persistence of LCLU type i while the entries of the diagonal indicate a transition from LCLU type i to a different type j, A_{i+} (total columns) is the land area of LCLU type i in time 1 (T_1) which is the sum of all j of A_{ij}, A_{+j} (total rows) is the land area of LCLU type in time 2 (T_2) which is the sum of overall of i of A_{ij}, Losses ($A_{1+} - A_{ii}$) is the proportion of landscape that experiences gross loss of LCLU type i between time 1 and 2, and Gains ($A_{+1} – A_{ii}$) is the proportion of landscape that experiences gross gain of LCLU type j between time 1 and 2.

The gains and losses in each LULC type between 1988 and 2022 were categorized into three (3) time periods being: (a) 1988–2002, b) 2002–2022, and c) 1988–2022). The following four aspects recommended by Macleod & Congalton (1998) were examined after the change detection was performed:

- Assessing the changes that have occurred;
- Identifying the nature of change;
- Calculating the areal extent of change; and
- Assessing the spatial pattern of the change.

3.4. Annual Rate of LCLU Change

For each time period, the pattern of change for each LCLU class was calculated, and the magnitude of change in LCLU types within and between time periods was compared. The rate of change was measured in square kilometres (km^2) per year, and the percentage (%) share of each LCLU type was, respectively, calculated to demonstrate the magnitude of the changes experienced between the periods using equations **(12)** and **(13)** (Hassen & Assen, 2017; Matlhodi et al., 2019):

$$CA = \frac{A_2 - A_1}{A_1} * 100 \tag{12}$$

$$D = \frac{A_2 - A_1}{A_1(T_2 - T_1)} * 100 \tag{13}$$

Where CA is the percentage change in the area of LCLU class between initial time T_1 and final time T_2, D is the annual average rate of change (%), A_1 is the area of the LCLU class at time 1 (T_1), and A_2 is the area of the LCLU class at time 2 (T_2).

3.5. Modelling Future LCLU Change

With knowledge of the annual change rate in the LCLU classes in the study area over the past three decades (1988 – 2022), the study sought to gain insight into the future LCLUs. Knowledge of future LCLUs and changes will enable natural resource managers to make better decisions about future land use policies and strategies within the context of sustainable land use planning. An insight into future LCLUs and changes can be gained through a modelling approach. Modeling LCLU change has recently been regarded as one of the most valuable tools for ensuring that the current natural resource base guarantees the future and continuous supply of natural resources (Munthali, 2020). Several models for LCLU simulation and prediction have been developed in recent years. Some of the most widely used models/approaches include the Markov Chain Model, Cellular Automata (CA), Cellular Automata–Markov model (CA–Markov), Artificial Neural Network (ANN), Logistic Regression (LR), Conversion of Land Use and its Effects (CLUE), Modules of Land Use Change Evaluation (MOLUSCE), among others (Hossain & Moniruzzaman, 2021; Kamaraj et al., 2022).

Among these models, the Cellular Automata (CA) is a powerful approach for understanding land-use systems and their integral dynamics, especially when integrated with other tools such as

Artificial Neural Networks (ANNs) (Mnyali & Materu, 2021). According to Verburg et al. (2008), no single model is capable of considering all the processes of LCLU changes at different scales; thus, integrated land-use models that combine one or two models are most often preferred for simulating and predicting LCLUs. Therefore, this study deployed the use of the MOLUSCE, a QGIS-based tool, for predicting future LCLUs and changes. The plugin incorporates algorithms such as utility modules, cross-tabulation techniques, and algorithmic modules such as artificial neural networks (ANNs), multi-criteria evaluation (MCE), weights of evidence (WoE), logistic regression (LR), and cellular automata (CA) models (Kamaraj et al., 2022). It was developed by Asia Air Survey to analyze, model, and simulate LCLU changes (Asia Air Survey, 2012). Its user interface provides an easy-to-use interface with specific modules and functions. Several researchers have used this approach in different landscapes over the last few years to model, monitor, predict, and simulate LCLU changes, and the technique produced accurate and reliable results (Saputra & Lee, 2019; Kamaraj et al., 2022; Muhammad et al., 2022).

The CA-ANN model in MOLUSCE is considered one of the most reliable tools for simulating and predicting future LCLUs because of its ability to estimate a pixel's current condition based on its initial state, surrounding neighbourhood effects, and changeover laws (Kamaraj et al., 2022). Furthermore, it is able to generate complex patterns and accurately depict non-linear spatial stochastic LCLU change processes (Saputra & Lee, 2019). The CA represents the state and dynamics of the environment. A significant challenge in the development of CA models is the determination of rules that govern system behaviour and incorporating heterogeneity and dynamism into these rules.

The graphical user interface (GUI) of the MOLUSCE plugin consists of 6 main components: Inputs, Evaluation Correlation, Area Changes, Transition Potential Modelling, Cellular Automata Simulation and Validation.

3.5.1. Inputs

The initial (time1) and final (time2) LCLU maps, as well as spatial variables such as elevation (DEM), slope, distance from roads, and distance from rivers and streams, are loaded in this panel. The LCLU change information and the spatial variables are used for modelling and simulating LCLU changes. A "Check geometry" function is also included in the "Inputs" tab to ensure that all

datasets have the same spatial geometry (i.e., extent and spatial resolution). The input datasets for this study were the classified LCLU maps of 1988 and 2002, as well as spatial variable factors such as the digital elevation model (DEM), slope, and distance from major roads and rivers. The properties of the maps and the spatial variable factors were extracted in the same raster format, same projection (UTM 35S on WGS 1984), and same spatial resolution (10 m) before they were loaded into the module. The spatial variables were used as independent variables, while the classified LCLU images were used as dependent variables to predict the LCLU of 2040 (i.e. 18 years prediction).

3.5.2. Evaluation of Correlation

This tab contains three methods for determining correlation among spatial variables: Pearson's correlation, Crammer's coefficient, and Joint Information Uncertainty (Gismondi et al., 2014). In this study, the Person's correlation method was used to examine the correlation among spatial variable factors because it provides information about the magnitude of the association as well as the direction of the relationship between spatial variables (Mnyali & Materu, 2021).

3.5.3. Area Change

In this component, LCLU area, changes and transition probabilities were computed. This section also generated an LCLU change map. The transition probability matrix generated in this section showed the proportion of pixels that changed from one LCLU category to another (Kamaraj et al., 2022). The area change map depicts the change in LCLUs that occured between 1988 and 2002.

3.5.4. Transition Potential Modelling

In this component, many methods for computing transition potential maps are available such as artificial neural networks (ANN), weights of evidence (WoE), logistic regression (LR), and Multi-Criteria Evaluation (MCE). Each method uses information from the LCLU maps and spatial variables as inputs to calibrate and model LCLU changes (Gismondi et al., 2014). The ANN (Multilayer Perception) technique was selected due to its simplicity and reliability (Saputra & Lee., 2019).

3.5.5. Cellular Automata Simulation

Transition potential maps, as well as simulated LCLU maps, are generated under this component (Gismondi et al., 2014). In this component, data from the LCLU maps (1988 and 2002), spatial variables and transition probability matrix were used to train the ANN classifier. The trained classifier was then used to simulate the 2022 LCLU map. The following model parameters were set for the ANN learning process to simulate an accurate LCLU map for 2022 (to test the trained classifier using the training data): 1000 iterations; a neighbourhood value of 1 X 1 pixel; a learning rate of 0.1; 12 hidden layers, and 0.05 momentum.

3.5.6. Validation

The validation component computed the Kappa statistic for the simulated LCLU map. The accuracy of the model was then assessed by comparing the Kappa coefficients of the actual and simulated LCLU maps. An overall Kappa coefficient of 0.87 was obtained for the simulated LCLU of 2022. This Kappa value is acceptable for the validation of the model to predict future LCLU maps for the study. Finally, the trained model was then used to predict the LCLU in 2040.

3.6. SOC Stock Determination

Once the LCLUs of the study area had been determined and assessed, the concentration of SOC content in different LCLUs in the study area was investigated to determine how LCLU change influenced SOC content.

3.6.1. Sampling design

The SOC content in areas with LCLU changes was determined through stratified random sampling of the LCLU map. The LCLU types with significant changes were considered potential sampling sites for SOC estimation. Tree cover, shrubland, cropland, built-up land, and bare land were the LCLU types explored because significant LCLU changes were observed in these classes. Since the goal of this study is to determine how LCLU change affects SOC, water bodies were excluded. To ensure the sampled data truly represents the SOC stock where LCLU conversion has occurred, Arp & Krause (1984) suggested collecting 15 samples per stratum or class to achieve a 95 % confidence interval (CI) with a 5% error margin. Accordingly, 15 sampling points were randomly generated within each LCLU class.

The effect of LCLU change on SOC stock was examined by comparing the amount of SOC content in areas with and without LCLU change. It was assumed that the SOC in areas with no LCLU change has remained constant over time. To determine the amount of SOC content in areas with no LCLU change, soil samples were randomly collected from 5 points in each of the LCLU classes that did not change during the study period. The SOC in these areas served as a baseline for comparing the SOC in areas that had undergone LCLU change.

In total, 86 sample points were used in this study for soil sample collection. The random points and their geographical coordinates were generated in ArcGIS 10.7 using the Segmentation and Classification tool under Special Analyst tools. The selected points were located in the field using Google Maps. At the sampling points, soil samples were collected from a depth of 30 cm for SOC content, pH, and soil texture determination. Studies have shown that SOC is higher in the topsoil and decreases exponentially with depth (Soussana & Lemaire, 2014; Orgill et al., 2014; Husein et al., 2019). In addition, the 30 cm soil depth is considered the most relevant soil depth for SOC estimation because it is the most biologically active layer of the soil (Drayton Chandler, 2016) and is most affected by land management practices, particularly in the agricultural system (ploughing) (Vågen & Winowiecki, 2013). Equally, soil samples were collected from a depth of 15 cm using a core sampler with a known volume (144.32 cm^3) for bulk density determination. This depth was chosen because the bulk density at this depth is not significantly different from that at 15-30 cm. The samples were packed in labelled sealed plastic bags for easy identification and preservation, as recommended by Pule-Meulenberg et al. (2005). Finally, the samples were transported to the Botswana University of Agriculture and Natural Resources (BUAN) Department of Crop and Soil Sciences laboratory for analysis.

3.7. Laboratory Analysis

Soil samples (except those for bulk density) were prepared for laboratory analysis by air-drying, crushing, thoroughly mixing, and sieving with a 2.00 mm sieve (FAO, 2019). The parameters determined include SOC content, bulk density, pH and texture.

For bulk density determination, the soil samples collected with the core sampler were oven-dried at a temperature of 105ºC for 48 hours (Blake and Hartge, 1986). The weight of the oven-dried samples was divided by the core volume to obtain the bulk density, as shown in equation **(14)**.

$$Bulk\ density\ (g/Cm^3) = \frac{Oven\ dried\ weight\ of\ sample\ (g)}{Core\ volume\ (cm^3)} \qquad (14)$$

Soil Organic Carbon Content was determined using the Walkley and Black method (1934). In this method, 2g of the sieved soil sample was weighed into a 250 ml conical flask, followed by the addition of 10 ml of Potassium dichromate (0.2 M $K_2Cr_2O_7$) and 20 ml of 98% concentrated Sulphuric acid (H_2SO_4). The mixture was gently swirled and allowed to digest under a fume hood for an hour. Finally, a supper flock solution (200 ml) was added to the mixture and allowed to react for two hours under the fume hood. The concentration of organic carbon (%) in the solution was measured using a UV-Vis Spectrophotometer (Genesys 10S). The carbon in the solution was measured at 620nm wavelength and 2cm path length.

The SOC stock (kgC/m^2) for each sampled depth (30 cm) in the different LCLU types was calculated using equation **(15)** (Solomon et al., 2002; Chia et al., 2020).

$$SOC\ stock\ (kg/Cm^2) = (OC \times BD \times D) \times 10 \qquad (15)$$

Where C is the SOC stock (g/m^2) of a sampled depth, D is the depth at which the soil sample was collected (cm), BD is the bulk density (g/cm^3) of soil at a sampled depth, and OC is the SOC content (%) of a sampled depth.

Soil pH was determined by mixing 10 g of soil with 20 ml of distilled water (ratio, 1:2) to form a supernatant solution (Okalebo et al., 2002). The solution was placed in an electric mixer for 30 minutes to ensure thorough mixing. The pH of the solution was then determined using a pH meter (pH-Orion Star A111).

The soil texture was determined quantitatively using the Bouyoucos hydrometric method (van Reeuwijk, 2002; Petrenko & Berezhnyak, 2008). In this method, 50 g of the 2 mm sieved soil sample was mixed with 100 ml of distilled water, followed by the addition of 10 ml of sodium hexametaphosphate to disperse the particles. The solution was mixed in an electric mixer for 15 minutes to ensure that all of the soil particles were fully dispersed. The solution was then transferred to a 1000 ml measuring cylinder and filled to capacity with distilled water. A blank solution containing 10ml sodium hexametaphosphate and distilled water was also prepared in a

55

1000ml measuring cylinder. The temperature of both solutions was measured with a mercury-in-glass thermometer to be sure that both solutions were at the same temperature (but not exceeding 20 °C). The cylinder containing the sample was sealed with a rubber stopper and vigorously shaken to ensure that no sediment remained at the bottom of the cylinder. The time when mixing was stopped was noted, and the first hydrometric reading was taken with a hydrometer after 40 seconds (silt and clay fractions), and the second reading was taken after 2 hours (clay fraction). Equations **(16)**, **(17)** and **(18)** were used to calculate the percentages of clay, silt and sand (Dikinya et al., 2016).

$$\% \ Clay = \frac{Hydrometer \ reading \ after \ 2 \ hours}{Mass \ of \ sample \ (50g)} \times 100\% \tag{16}$$

$$\% \ Silt = \frac{Hydrometer \ reading \ after \ 2 \ hours}{Mass \ of \ sample \ (50g)} \times 100\% - (\% \ clay) \tag{17}$$

$$\% \ Sand = 100\% - (\% \ Silt + \% \ Clay) \tag{18}$$

Finally, the soil texture classes were determined using a Soil Textural Triangle developed by the United States Department of Agriculture (USDA) soil classification triangle.

3.8. Statistical Analysis

Statistical data analysis was carried out using R statistical software (version 4.21 for Windows) and Microsoft Excel. Statistically significant differences were accepted at $p < 0.05$. One–way ANOVA (analysis of variance) with Post-hoc least significant difference (LSD) was conducted to examine the differences in soil properties (SOC content, bulk density, pH and texture) with LCLU types. Also, the relationships between SOC and bulk density, pH, and texture were examined using Microsoft Excel.

3.9. Limitations of this study

There was a possibility that some errors might have occurred during image classification processes, particularly for the 1988 image, due to spectral resemblance for some classes with high spectral resemblance. This could have influenced both the derived LCLU classes and the estimated LCLU changes. This situation is common, especially when mapping LCLU for the past periods

for which it is impossible to obtain ground information (Enaruvbe & Pontius, 2015). Also, the study assumed that SOC content in areas where no LCLU change was observed was the same as it was in 1988. This was due to a lack of SOC content data for the various LCLU types in the study area in previous years. This may cause uncertainty in the change in SOC results obtained during the study period.

CHAPTER 4: RESULTS AND DISCUSSION

4.1. LCLU Types in 1988, 2002 and 2022

Landsat and Sentinel-2A images obtained from the USGS (www.usgs.gov) were analyzed using Supervised classification employing the Maximum Likelihood algorithm. These LCLU maps were developed to show the LCLU types identified in the study area in 1988, 2002, and 2022. The identified LCLU types in the study area were water bodies, tree cover, cropland, shrubland, bare land and built-up (Figure 7).
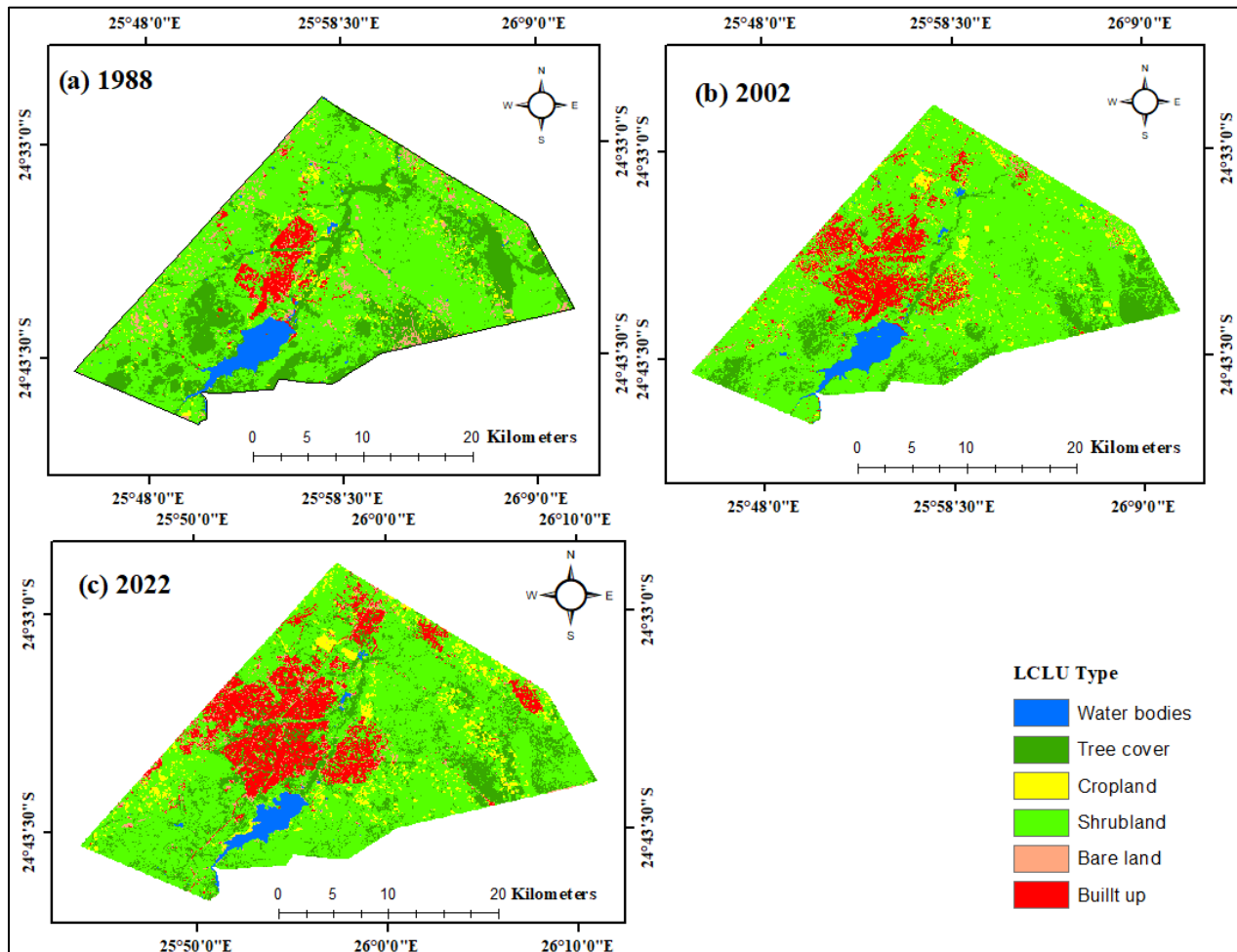
Figure 7. LCLU categories for (a) 1988, (b) 2002 and (c) 2022

The accuracy assessment for the three LCLU classifications was done by comparing the classification results with ground truth points. Error matrix was used to compute the OA, UA, PA,

and KC for the 1988, 2002 and 2022 LCLU maps and the results are presented in Tables 7, 8 and 9.

The OA for the 1988, 2002, and 2022 images were 85.8%, 86.1%, and 94.0%, respectively. These values are acceptable as OA statistics normally fall between 85% and 95%, according to Congalton (1996) and Mango (2010). The KC values for the 1988, 2002 and 2022 images were 0.83, 0.83, and 0.93, respectively. The KCs were greater than 0.8, indicating a high level of agreement between image data and ground truth data, as stated by Molla et al. (2018).

Table 7. Confusion matrix and classification accuracy of LCLU 1988 image

LCLU Type	Water	Tree cover	cropland	Shrubs	Bare land	Built up	Total User	UA (%)
Water	32	0	0	0	0	0	32	100.0
Tree cover	0	28	1	4	0	0	33	84.8
Cropland	0	1	39	1	0	0	41	95.1
Shrubland	0	6	1	36	2	0	45	80.0
Bare land	0	0	4	0	29	7	40	72.5
Built up	0	0	2	0	4	35	41	85.4
Total Producer	32	35	47	41	35	42	**232**	
PA (%)	100.0	80.0	83.0	87.8	82.9	83.3		
OA	85.8%							
Kc	0.83							

Table 8. Confusion matrix and classification accuracy of LCLU 2002 image

LCLU Type	Water	Tree cover	cropland	Shrubs	Bare land	Built up	Total User	UA (%)
Water	30	0	0	0	0	0	30	100.0
Tree cover	0	44	0	3	0	0	47	93.6
Cropland	0	0	34	2	2	4	42	81.0
Shrubland	0	3	4	57	0	0	64	89.1
Bare land	0	0	4	1	34	6	45	75.6
Built up	0	0	5	0	4	37	46	80.4
Total Producer	30	47	47	63	40	47	**274**	
PA (%)	100.0	93.6	72.3	90.5	85.0	78.7		
OA	86.1%							
Kc	0.83							

Table 9. Confusion matrix of 2022 and classification accuracy of LCLU 2022 image

LCLU Type	Water	Tree cover	Cropland	Shrubs	Bare land	Built up	Total User	UA (%)
Water	28	0	0	0	0	0	28	100.0
Tree cover	0	64	0	0	0	0	64	100.0
Cropland	0	0	34	2	0	1	37	91.9
Shrubland	0	2	5	63	0	0	70	90.0
Bare land	0	0	1	0	28	4	33	84.8
Built up	0	0	1	0	2	61	64	95.3
Producer	28	66	41	65	30	66	**296**	
PA (%)	100.0	97.0	82.9	96.9	93.3	92.4		
OA	94.0%							
Kc	0.93							

4.2. Area Statistics for LCLU types in 1988, 2002 and 2022 and trends (1988 – 2022)

The area statistics for the different LCLU types in 1988, 2002, and 2022 are presented in Table 10 and Figure 8. From Table 10 and Figure 8, the shrubland class was the most dominant LCLU type in the study area, covering an area of 426.47 km^2 (63.75%) in 1988, 438.35 km^2 (65.53%) in 2002 and 402.57 km^2 (60.18%) in 2022. The area coverage for this class decreased throughout the study period, which could be attributed to land clearing for built-up expansion and agricultural activities as a result of population growth.

The tree cover LCLU type occupied an area of 129.68 km^2 (19.39%) in 1988, 107.58 km^2 (16.08%) in 2002, and 96.42 km^2 (14.41%) in 2022. In 1988 and 2002, tree cover was the second most dominant class in the study area after the shrubland class. This class experienced a decline in coverage throughout the study period. This could be attributed to forest clearing for fuelwood and agriculture.

The built-up class occupied an area of 24.22 km^2 (3.62 %) in 1988, 73.59 km^2 (11%) in 2002, and 99.34 km^2 (14.86%) in 2022. In 2022, the built-up class was the second most dominant LCLU type after the shrubland class. Its trend increased throughout the study period. This result was consistent with the findings of Li et al. (2022), who found that built-up areas had expanded globally in recent decades despite a decrease in global population growth.

The bare land class occupied 26.65 km^2 (3.98%) of the total land area in 1988, 8.95 km^2 (1.34%) in 2002, and 21.62 km^2 (3.23%) in 2022. In 2002, bare land was the least dominant class. The area

coverage by this class decreased from 26.65 km^2 in 1988 to 8.95 km^2 in 2002 before expanding to 21.62 km^2 in 2022. The significant increase in bare land area coverage between 2002 and 2022 could be attributed to land clearing for development, fuelwood collection, agricultural activities, and livestock overgrazing (Tsheko, 2022).

The cropland class occupied 39.73 km^2 (5.94%) of the total land area in 1988, 20.93 km^2 (3.13%) in 2002, and 33.45 km^2 (5%) in 2022. The area coverage for this class decreased between 1988 and 2002. However, it experienced an increase in its area coverage between 2002 and 2022, which could be attributed to the presence of the Integrated Support Program for Arable Agricultural Development (ISPAAD) and other government support programs that provide appealing opportunities for subsistence farmers to increase their incomes (Kamwi et al., 2018).

The water body class covered an area of 22.19 km^2 (3.32%) in 1988, 19.54 km2 (2.92%) in 2002, and 15.42 km^2 (2.31%) in 2022. It was the least dominant class in 2022. Overall, its area coverage decreased throughout the study period.

Table 10. Area Statistics for the LCLU categories in 1988, 2002 and 2022

	LCLU 1988		**LCLU 2002**		**LCLU 2022**	
LCLU Type	*Area (km^2)*	*Area (%)*	*Area (km^2)*	*Area (%)*	*Area (km^2)*	*Area (%)*
Water bodies	22.19	3.32	19.54	2.92	15.43	2.31
Tree cover	129.68	19.39	107.58	16.08	96.42	14.41
Cropland	39.73	5.94	20.93	3.13	33.47	5
Shrubland	426.47	63.75	438.35	65.53	402.57	60.18
Bare land	26.65	3.98	8.95	1.34	21.63	3.23
Built up	24.22	3.62	73.59	11	99.41	14.86
Total	668.94	100	668.94	100	668.94	100
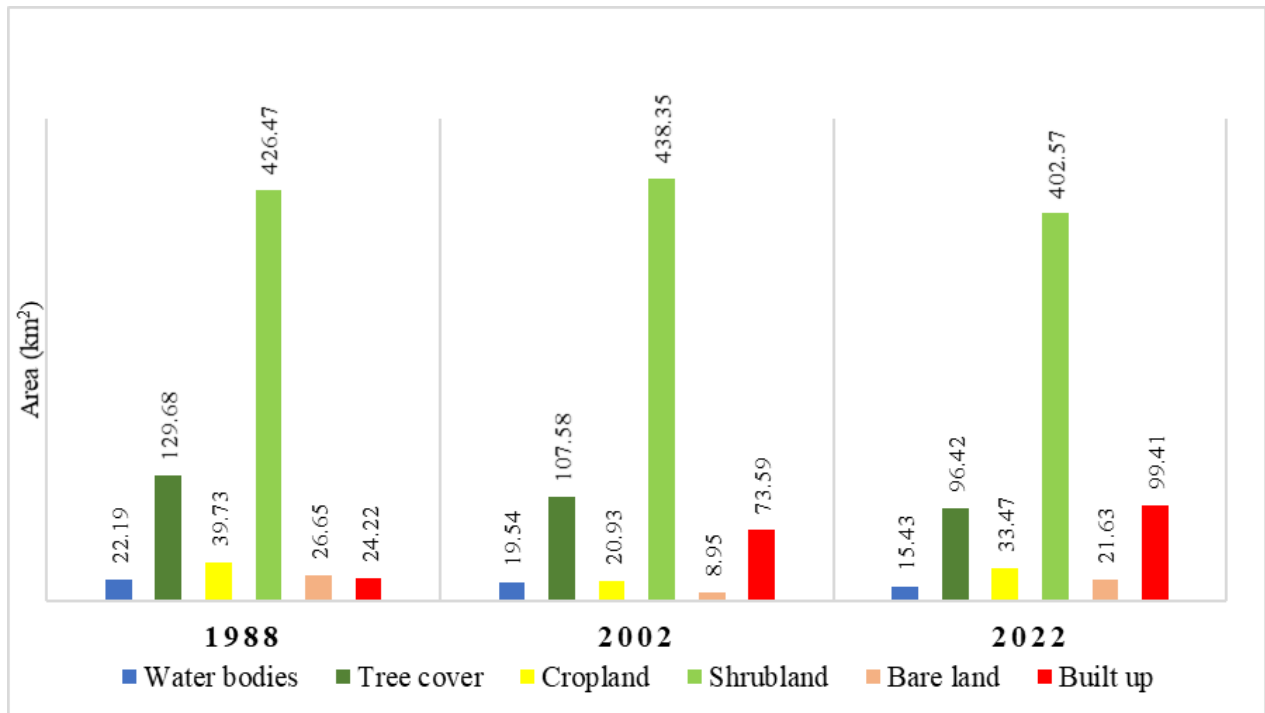
Figure 8. Area Statistics for the LCLU categories in 1998, 2002 and 2022

4.3. LCLU Change Detection Analysis (1988 – 2022)

4.3.1. Gains and Losses in LCLU Types

Throughout the study period, significant conversions of the LCLU types to others were observed (Figures 9 & 10). The spatial extent of an LCLU type shrinks once its portion is converted into another type. Gains and losses in the area coverage for the different LCLU types were assessed using the LCLU change matrix (Tables 11, 12, & 13).

The built-up LCLU type was gaining primarily from the shrubland throughout the study period. It gained 34.97 km^2 of shrubland between 1988 and 2002 (Table 11) and 49.21 km^2 between 2002 and 2022 (Table 12), thereby increasing its spatial extent. The built-up LCLU type gained 75.12 km^2 (310.16 %) from 1988 to 2022 (Table 16). The expansion in built-up areas could be attributed to population growth due to urban migration. This resulted in lands previously used for agricultural purposes or occupied by natural vegetation being converted into built-up areas to accommodate the growing population.
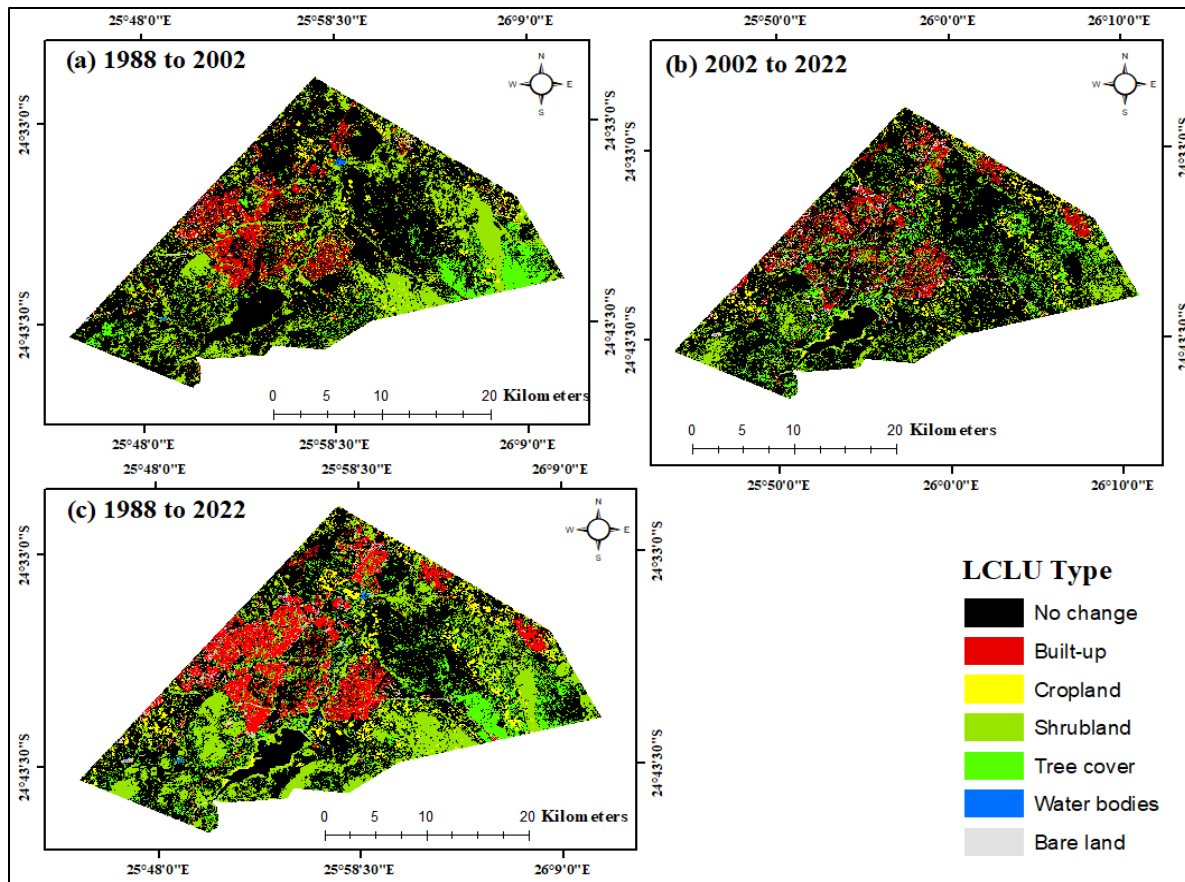
Figure 9. Changes in LCLU types from (a) 1988 to 2002; (b) 2002 to 2022 and (c) 1988 to 2022.
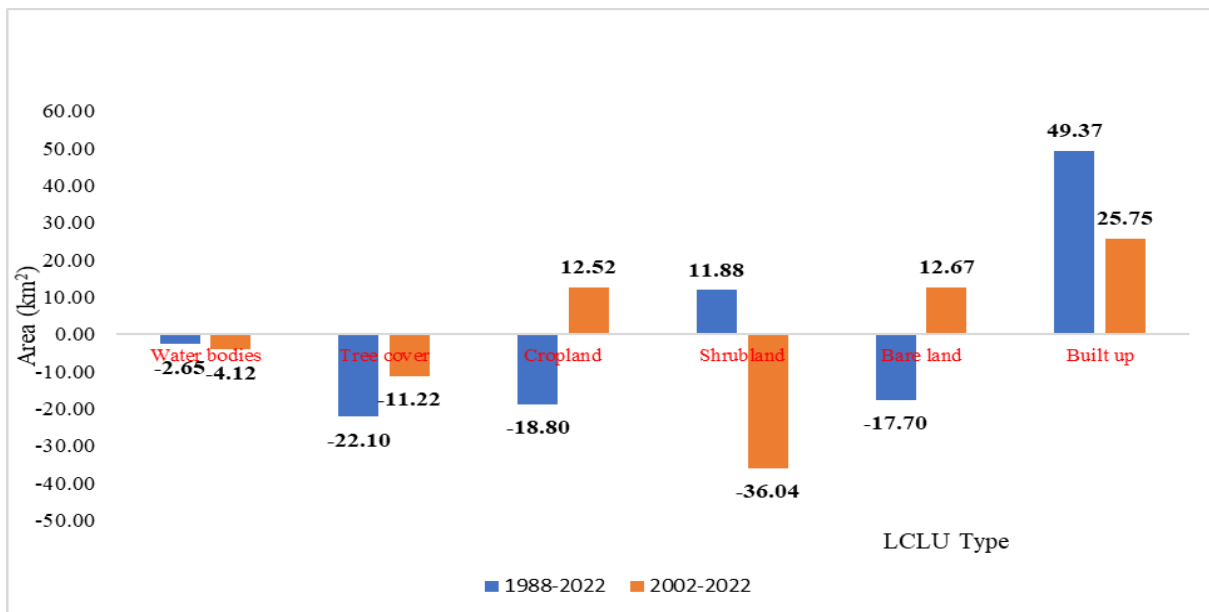
Figure 10. Gains and losses in LCLU classes from 1988 to 2022

Table 11. LCLU change matrix for 1988 – 2002 change period

	LCLU classes	2002							
		Water bodies	Tree cover	Cropland	Shrub land	Bare land	Built-up	Losses (km^2)	Losses (%)
1988	Water bodies	19.43	0.48	0.06	1.84	0.01	0.38	2.77	12.47
	Tree cover	0.51	34.44	2.01	107.34	0.65	3.37	113.88	76.78
	Cropland	0.03	0.51	3.24	20.98	0.28	1.61	23.41	87.83
	Shrubland	0.3	36.16	12.11	331.03	6.31	34.97	95.63	22.41
	Bare land	0.07	0.24	3.26	17.41	1.25	4.4	25.4	95.31
	Built-up	0.02	0.03	0.19	4.54	0.27	19.19	5.05	20.85
	Gains (km^2)	0.93	37.43	17.63	146.33	7.52	44.73	**266.14**	
	Gains (%)	4.55	52.08	87.83	30.65	85.76	69.98		

Table 12. LCLU change matrix for 2002 – 2022 change period

	LCLU classes	2022							
		Water bodies	Tree cover	Cropland	Shrub land	Bare land	Built-up	Losses (km^2)	Losses (%)
2002	Water bodies	15.07	0.25	0.98	3.18	0.87	0.01	5.28	25.96
	Tree cover	0.04	30.28	0.61	64.1	0.30	0.54	65.59	68.42
	Cropland	0.03	0.56	8.31	12.27	1.07	4.40	18.33	68.79
	Shrubland	0.19	36.23	22.67	337.58	14.1	42.17	139.43	29.23
	Bare land	0.00	0.29	0.26	4.12	0.71	3.38	8.05	91.85
	Built-up	0.12	4.21	0.52	5.66	4.19	49.21	14.69	22.99
	Gains (km^2)	0.38	41.54	25.04	89.33	20.52	50.5	**251.37**	
	Gains (%)	2.45	57.84	75.07	20.92	96.64	50.65		

The bare land LCLU type lost 17.41 km^2 of its coverage to the shrubland LCLU type between 1988 and 2002 (Table 10), which could be attributed to heavy rains received in the country after the prolonged drought period of 1993 – 1995 (Fox et al., 2017). A significant loss in bare land coverage was observed between 1988 and 2022. The bare land LCLU type was losing primarily to shrubland land.

Between 2002 and 2022, the bare land LCLU type gained 14.1 km^2 from the shrubland type (Table 11). This could be a result of prolonged drought periods caused by rainfall variability (Figure 11) (Akinyemi, 2017; Byakatonda et al., 2018). In addition, it could be attributed to the interaction of both climates (such as drought) and human activities (livestock grazing and land clearing for fuelwood and cultivation) that resulted in the loss of vegetal cover. The bare land LCLU type was

mainly gaining from the shrubland during this period. The gains in bare land were more significant around built-up areas (due to the expansion of built-up areas as a result of population growth) and croplands (bare fields after harvesting).

Table 13. LCLU change matrix for 1988 – 2022 change period

| | LCLU classes | 2022 | | | | | | | |
		Water bodies	Tree cover	Cropland	Shrub land	Bare land	Built-up	Losses (km^2)	% Losses
1988	Water bodies	14.59	0.76	1.09	4.69	0.97	0.08	7.60	34.24
	Tree cover	0.44	31.53	2.70	105.78	2.10	5.64	116.66	78.72
	Cropland	0.04	1.99	4.30	23.22	0.93	2.86	29.04	87.10
	Shrubland	0.31	58.3	9.11	265.58	14.97	65.62	160.78	37.71
	Bare land	0.07	1.37	3.55	14.65	1.24	5.74	25.38	95.35
	Built-up	0.00	1.93	0.12	1.39	1.03	19.77	4.46	18.42
	Gains (km^2)	0.85	64.34	16.57	137.26	20.00	79.94	**343.92**	
	% Gains	5.54	67.11	79.4	34.07	94.17	80.17		

Natural vegetation (shrubland and tree cover) demonstrated an overall decrease in coverage throughout the study period. Shrubland and tree cover lost 24.16 km^2 (5.67%) and 33.32 km^2 (25.69%) coverage, respectively, between 1988 and 2022 (Table 14). Tree cover losses were mainly to shrublands. The most common tree species found in the study area were *Acacia tortilis* and *Acacia erubescence*. Other tree species, such as *Combretum imberbe* and *Terminalia pruniouides*, were common in the 1980s but had been depleted because they were the most preferred species for fuelwood (Sebego, 2014). This result was consistent with the findings of Ringrose et al. (1996), who reported a decrease in dense woody vegetation covers in the Notwane catchment area between 1984 and 1994. Furthermore, Dougill et al. (2016) also reported a similar scenario in the Kalahari region of South Africa, where savanna landscapes had experienced extensive bush encroachment and changes in herbage.

Even though the shrubland LCLU type was generally losing its area coverage, a significant gain (11.88 km^2, 2.79 %) in its cover was observed between 1988 and 2002 (Table 14). Gain in shrubland during this period was mainly from tree cover (due to forest clearing for fuelwoods and other forest products) and bare land. The gain in shrubland from bare land indicated the ability of natural vegetation to regenerate even after extended periods of drought.

A significant loss in shrubland was observed between 2002 and 2022 (Figure 10). This result was consistent with the findings of Tsheko (2022), who reported a 1.6% loss in shrubland coverage between 2002 and 2020 in the Greater Gaborone area. Shrubland losses were mainly to croplands and built-up areas, resulting in the reduction of land reserved for forage as well as a reduction in the quality of forage. Furthermore, shrubland losses during this period could also be attributed to rainfall variability (Figure 11), as vegetation production in semi-arid regions is highly dependent on rainfall (Rutherford, 1980; le Houerou et al., 1988).
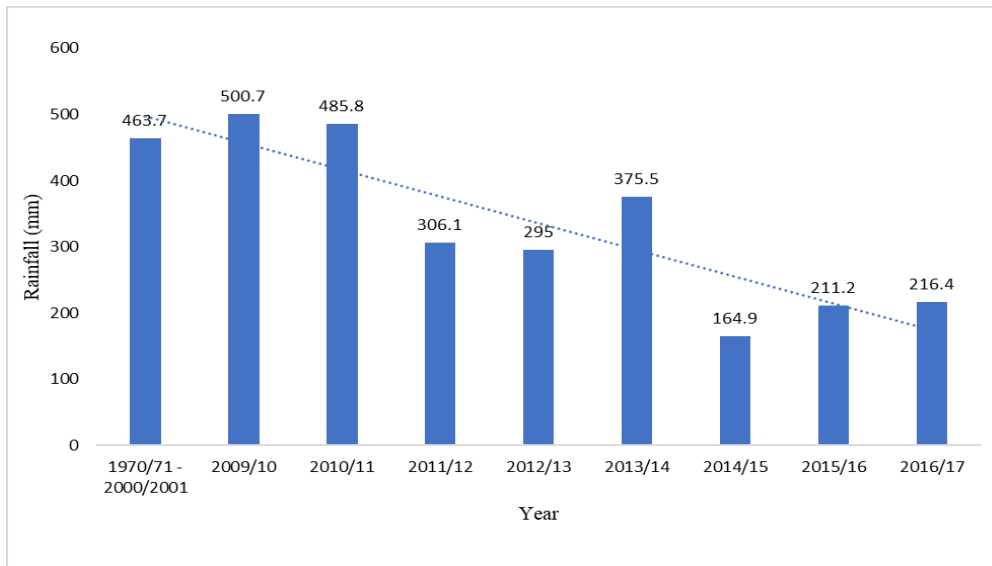
Figure 11. National Average Rainfall (mm) (long vs short terms) (Statistics Botswana, 2018).

There was a general loss in the area covered by the cropland LCLU type between 1988 and 2022. Despite the overall loss in cropland coverage, a significant gain in coverage was observed between 2002 and 2022 (Figure 10). The loss in cropland coverage observed between 1988 and 2002 can be attributed to field abandonment due to the failure of the agricultural support programs such as the Arable Land Development Program (ALDEP), the Arable Rain-Fed Agricultural Program (ARAP) (Seto et al., 2012). Abandonment of agricultural land has been reported to have increased globally and within Sub-Saharan Africa (Shackleton et al., 2013), despite the clear need for increased agricultural engagement and productivity. Cropland abandonment in Southern Africa has also been linked to a lack of draught power, variable rainfall, droughts and more modernized youths who are hesitant to live a marginal agrarian lifestyle (Blair et al., 2018).

The current study also found that most of the croplands were located in rural areas (for example, Oodi, Modipane, Gabane and Mokolodi) and were rainfed. The rural population, like in the rest of Botswana, relies on rain-fed subsistence farming combined with livestock raising (Matlhodi et al., 2019). This result indicated that agriculture remains the backbone of the rural economy, as evidenced by the observed gain in cropland between 2002 and 2022 (Figure 10). Bessah et al. (2019) noted that the expansion of agricultural land is a global trend, regardless of the economic status and location of a country. The gains in croplands observed during the 2002-2022 change period could be attributed to the need for more food production to meet the demand of the growing population. In addition, it could also be attributed to the presence of agricultural subsidy schemes such as ISPAAD and other government support programs. One of the objectives of ISPAAD was to provide farmers with 100% subsidy for ploughing and row planting (GoB, 2013), thereby encouraging more farmers to clear more land for cultivation. The expansion in croplands contributed to the reduction in shrubland. Cropland gain was also reported by Nkambwe & Totolo (2005) in Gaborone, where they found that arable lands were expanding into the woodlands and open grasslands, primarily used for communal grazing. In addition, cropland expansion was also observed in the Ameleke watershed in Ethiopia (Temesgen et al., 2014) and other developing countries where the loss of natural vegetation for crop production was crucial for cropland expansion (Lubowski et al., 2006).

Generally, water bodies shrank throughout the study period. A total of 6.77 km^2 (30.51%) of water coverage was lost during the study period (1988 – 2022). The water LCLU type was mainly losing to shrubland. The reduction in the spatial extent of the water body class indicates low rainfall and high evaporation in the study area. The water body LCLU type expansively lost its cover (4.12 km^2 or 21.08 %) between 2002–2022 (Table 15), which could be attributed to low rainfall experienced in the country over the past few years (Figure 11) and usage.

4.3.2. Annual Change Rate

The annual change rates for the different LCLU types between 1988 and 2002, 2002 and 2022, and 1988 and 2022 change periods are presented in Tables 14, 15, and 16. Spatially, the fastest annual change rates in the LCLU types were observed between 1988 and 2002 (Table 13). During this transition period, the bare land class shrank annually at a rate of 1.26 km^2/year (4.74%), making it the most reduced LCLU type in the period. The built-up category increased annually at

a rate of 3.53 km^2/year (14.56 %), making it the highest increased category in that period. This result agreed with the findings of López et al. (2001), who found that settlements in developing countries were growing five times faster than those in developed countries.

Table 14. Area Statistics for changes in the LCLU categories *from 1988 to 2002*

LCLU type	*LCLU 1988*		*LCLU 2002*		*Changes*		*Annual change rate*	
	Area (km²)	*Area (%)*	*Area (km²)*	*Area (%)*	*Area (km²)*	*Area (%)*	*Area (Km²/year)*	*Area (%/year)*
Water bodies	22.19	3.32	19.54	2.92	-2.65	-11.94	-0.19	-0.85
Tree cover	129.68	19.39	107.58	16.08	-22.1	-17.04	-1.58	-1.22
Cropland	39.73	5.94	20.93	3.13	-18.8	-47.32	-1.34	-3.38
Shrubland	426.47	63.75	438.35	65.53	11.88	2.79	0.85	0.20
Bare land	26.65	3.98	8.95	1.34	-17.7	-66.42	-1.26	-4.74
Built up	24.22	3.62	73.59	11.00	49.37	203.84	3.53	14.56
Total	**668.94**	**100**	**668.94**	**100**				

Between 2002 and 2022 (Table 15), the water body class decreased annually at a rate of 0.21 km^2/year. (1.05%), making it the most reduced category in the period. Conversely, the bare land class increased annually at a rate of 0.63 km^2/year (7.08%), making it the highest increased category in the period. From the results presented in Table 16, it can be concluded that tree cover and water bodies were the most reduced categories between 1988 and 2022, with annual change rates of 0.98 km^2/year (0.76%) and 0.2 km^2/year (0.9%), respectively. However, the built-up category recorded the highest increase, with an annual change rate of 2.21 km^2/year (9.12%) over the study period.

Table 15. Area Statistics for changes in the LCLU categories from 2002 to 2022

LCLU type	*LCLU 2002*		*LCLU 2022*		*Changes*		*Annual change rate*	
	Area (km²)	*Area (%)*	*Area (km²)*	*Area (%)*	*Area (km²)*	*Area (%)*	*Area (Km²/year)*	*Area (%/year)*
Water bodies	19.54	2.92	15.42	2.31	-4.12	-21.08	-0.21	-1.05
Tree cover	107.58	16.08	96.36	14.41	-11.22	-10.43	-0.56	-0.52
Cropland	20.93	3.13	33.45	5.00	12.52	59.82	0.63	2.99
Shrubland	438.35	65.53	402.31	60.18	-36.04	-8.22	-1.80	-0.41
Bare land	8.95	1.34	21.62	3.23	12.67	141.56	0.63	7.08
Built up	73.59	11.00	99.34	14.86	25.75	34.99	1.29	1.75
Total	**668.94**	**100**	**668.94**	**100**				

Table 16. Area Statistics for changes in the LCLU categories from 1988 to 2022

LCLU type	LCLU 1988		LCLU 2022		Changes		Annual change rate	
	Area (km²)	Area (%)	Area (km²)	Area (%)	Area (km²))	Area (%)	Area (Km²/year)	Area (%/year)
Water bodies	22.19	3.32	15.42	2.31	-6.77	-30.51	-0.20	-0.90
Tree cover	129.68	19.39	96.36	14.41	-33.32	-25.69	-0.98	-0.76
Cropland	39.73	5.94	33.45	5.00	-6.28	-15.81	-0.18	-0.46
Shrubland	426.47	63.75	402.31	60.18	-24.16	-5.67	-0.71	-0.17
Bare land	26.65	3.98	21.62	3.23	-5.03	-18.87	-0.15	-0.56
Built up	24.22	3.62	99.34	14.86	75.12	310.16	2.21	9.12
Total	**668.94**	**100**	**668.94**	**100**				

4.4. Prediction of LCLU in 2040

MOLUSCE was used to simulate future land uses based on existing LCLU patterns and dynamics. The model was calibrated using the spatial variables parameters such as the DEM, slope, distance from rivers and streams, and distance from major roads (Figure 12). These parameters were selected based on their relatively strong association with the LCLU categories (Muhammad et al., 2022). The CA-ANN approach was used for transition potential modelling (training the classifier using 2022 data) and the prediction of future LCLU for 2040.

The LCLU map for 2022 was simulated using the data from the spatial variables and the information from the LCLU maps of 1988 and 2002 (transition probabilities) as inputs. Before validating the model, the simulated and actual LCLU maps for 2022 (Figure 13) were compared using their Kappa coefficients. The overall Kappa coefficient for the simulated LCLU of 2022 was 0.87 (88.4% overall accuracy), while that for the actual LCLU map of 2022 was 0.93 (94.0% overall accuracy), hence, indicating a high level of agreement.
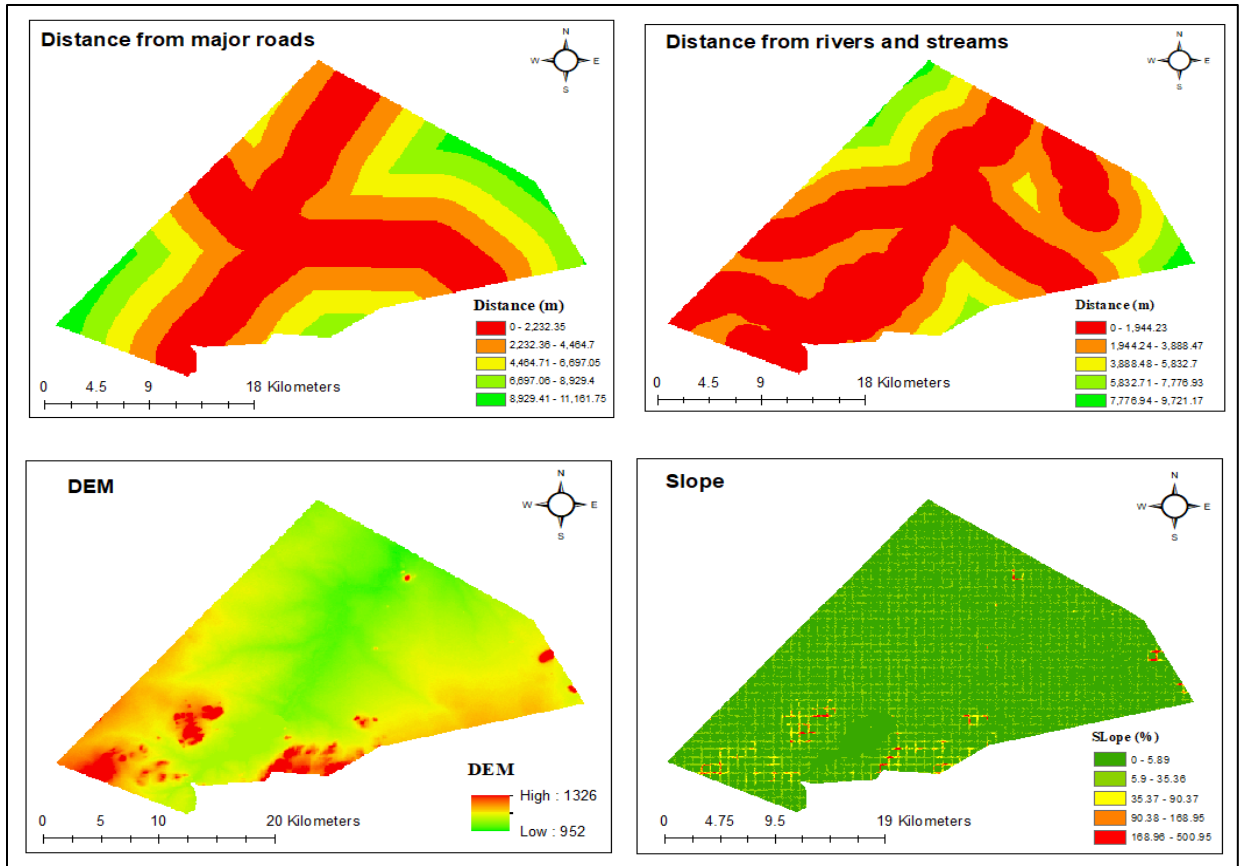
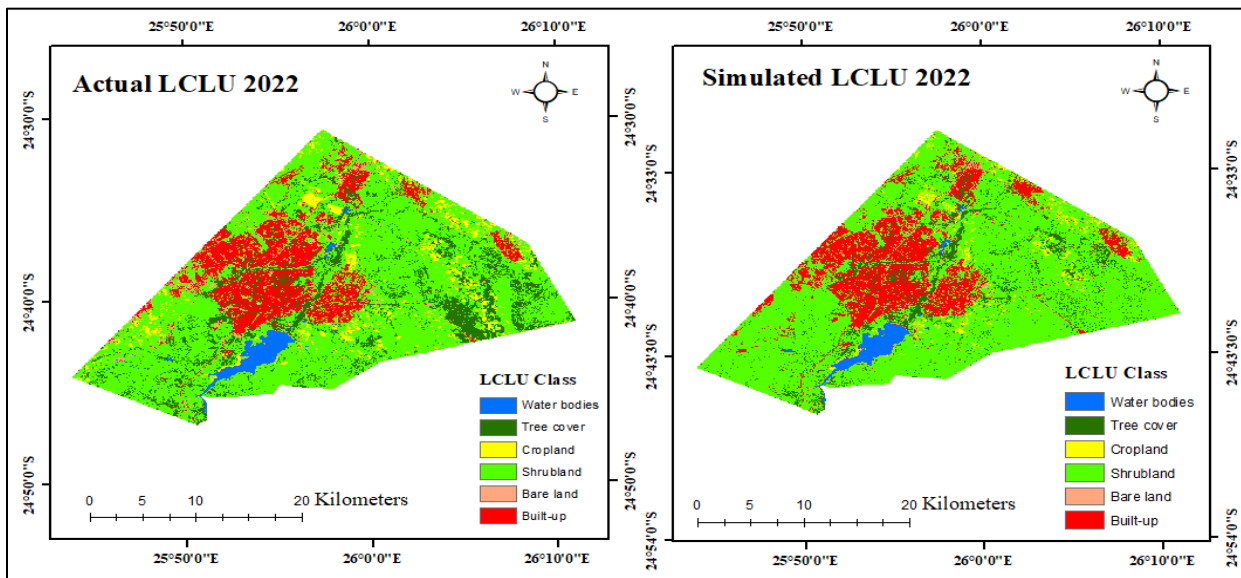*Figure 12. Spatial variables for the CA-ANN model*

Figure 13. Actual and simulated LCLU maps for 2022

The same information used to simulate the 2022 map was used to predict the 2040 map (Figure 14). From the data presented in Table 17, bare land occupied 21.62 km^2 (3.23%) of the total land area in 2022 and was expected to occupy 23.05 km^2 (3.44%) by 2040. Similarly, the built-up LCLU category occupied 99.34 km^2 (14.86%) in 2022 and was expected to expand to 111.40 km^2 (16.65%) by 2040. With the current high population growth rates of villages surrounding Gaborone city, such as Tlokweng (3.8%), Oodi (5.7%), Modipane (8.7%), and Gabane (2.6%) (Statistics Botswana, 2022), expansion in built-up areas was certain by 2040 to accommodate the growing population. However, tree cover and cropland occupied 96.36 km^2 and 33.45 km^2 in 2022, respectively, and were expected to occupy 78.56 km^2 and 20.16 km^2 by 2040 (Table 17). The water body was likely to be the most stable LCLU class by 2040.

Table 17. Area Statistics for the changes in LCLU categories from 2022 to 2040

| LCLU category	LCLU 2022		LCLU 2040		Change		Rate of change	
	Area (Km^2)	Area (%)	Area (Km^2)	Area (%)	Area (Km^2)	Area (%)	Area (Km^2/year)	Area (%/year)
Water bodies	15.42	2.31	15.41	2.30	-0.01	-0.06	0.00	0.00
Tree cover	96.36	14.41	78.56	11.74	-17.80	-18.47	-0.99	-1.03
Cropland	33.45	5.00	20.16	3.01	-13.29	-39.73	-0.74	-2.21
Shrubland	402.31	60.18	420.38	62.84	18.07	4.49	1.00	0.25
Bare land	21.62	3.23	23.03	3.44	1.41	6.52	0.08	0.36
Built up	99.34	14.86	111.40	16.65	12.06	12.14	0.67	0.67
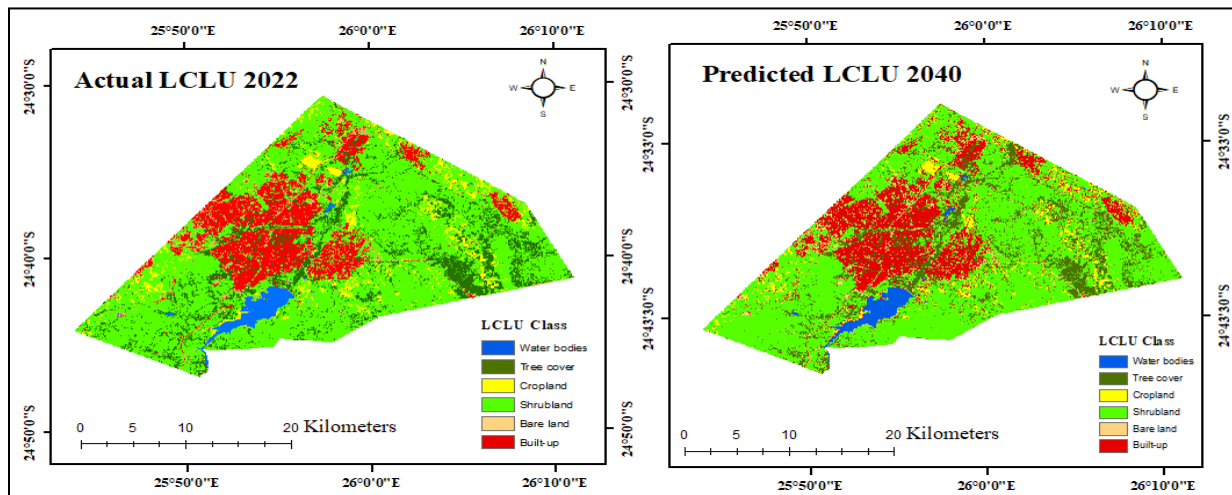
Figure 14. LCLU map for 2022 (Actual) and 2040 (Predicted)

4.4.1. Change detection between 2022 and 2040

Figure 15 depicts LCLU types in the study area following LCLU change over a period of 18 years. The black region represents areas that did not change. From the results presented in Table 18, it is expected that by 2040, 3.15 km^2 and 11.94 km^2 of shrubland will be converted to bare land and built-up areas, respectively. Also, the built-up LCLU type will gain a total of 11.46 km^2, while tree cover and cropland will lose 21.99 km^2 and 12.72 km^2 of coverage, respectively, to shrubland (Figure 16). Between 2022 and 2040, the net loss in tree cover and cropland will be 17.80 km^2 and 13.29 km^2, respectively, due to forest clearing and crop field abandonment (as a result of low crop yields caused by climate variability). The fastest rate of change will be observed in the tree cover LCLU type (0.99 km^2/year), which may be due to increased demand for forest products.

Table 18. LCLU change matrix for 2022 – 2040

	LCLU Category	LCLU 2040						losses (km^2)	losses (%)
		Water bodies	Tree cover	Cropland	Shrub land	Bare land	Built-up		
LCLU 2022	Water bodies	15.37	0.01	0.00	0.06	0.01	0.01	0.09	0.56
	Tree cover	0.00	71.82	0.00	21.99	0.54	1.55	24.08	25.11
	Cropland	0.00	0.27	19.81	12.72	0.05	0.53	13.56	40.65
	Shrubland	0.01	4.84	0.31	381.78	3.15	11.94	20.25	5.04
	Bare land	0.00	0.46	0.01	1.21	18.79	0.77	2.46	11.56
	Built up	0.00	1.01	0.00	1.87	0.45	96.41	3.33	3.34
	Gains (km^2)	0.01	6.60	0.32	37.85	4.19	14.79		
	Gains (%)	0.09	8.41	1.60	9.02	18.23	13.30		

From Figure 16, there will be food security issues in the built-up due to a reduction in cropland. However, food security issues in the urban area are evitable as food usually comes from outside the city limits. Therefore, proper infrastructure is needed to facilitate the supply of food to the city in order to achieve food security (SDG 2). Loss of tree cover will disrupt the carbon cycle and subject the area to a new climate.
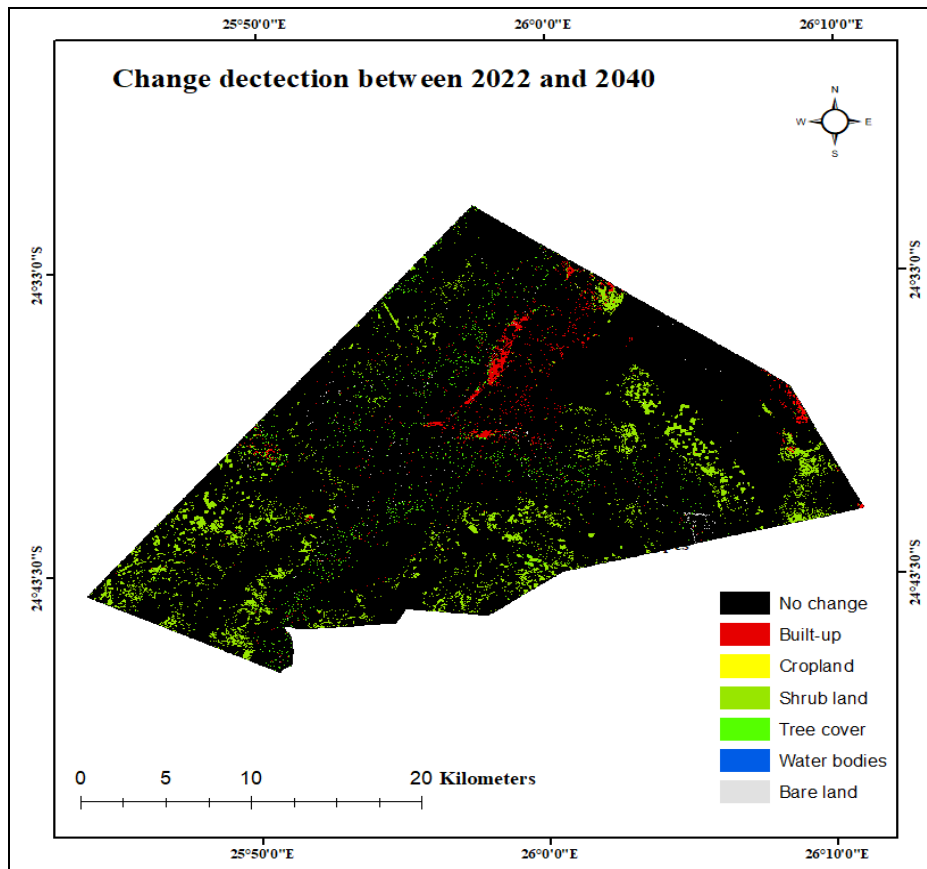
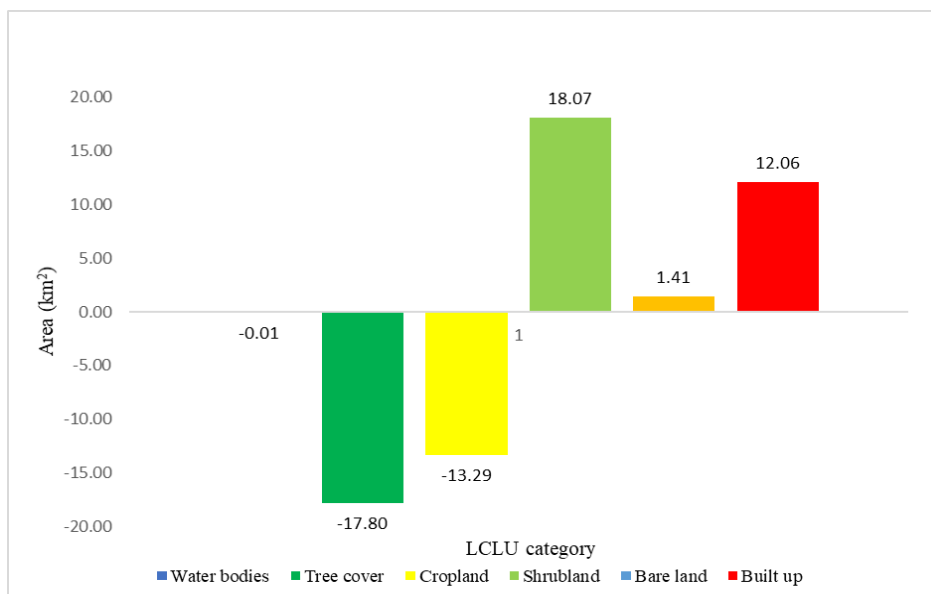*Figure 15. Changes in LCLU classes between 2022 and 2040*

Figure 16. Gains and losses in LCLU types between 2022 and 2040

4.5. Analysis of SOC Stock

4.5.1. Variation of Soil Parameters with LCLU Types

The mean values of soil parameters in the major LCLU types in the study area are presented in Table 19. The table also includes Post hoc LSD multiple comparison results, which test whether or not significant differences exist in values of soil parameters across different LCLU types.

Table 19. Variation of Bulk density, SOC content, pH and Texture in different LCLU types.

LCLU types	BD (g/cm³)	SOC (%)	pH	Sand (%)	Silt (%)	Clay (%)
Bare land	1.56 ± 0.14ᵃ	0.32 ± 0.26ᵈ	7.64 ± 0.90ᵃ	72.59± 11.85ᵃ	14.24 ± 5.87ᵃᵇ	13.18 ± 7.55ᵃ
Built-up	1.55 ± 0.11ᵃ	0.42 ± 0.19ᵈ	7.44 ± 0.98a	69.90 ± 6.14ᵃᵇ	14.75 ± 3.45ᵃᵇ	13.85 ± 4.90ᵃ
Cropland	1.50 ± 0.08ᵃᵇ	0.93 ± 1.04ᶜ	6.29 ± 0.59ᵇ	70.89 ± 15.46ᵃᵇ	12.67 ± 4.45ᵇ	16.84 ± 12.28ᵃ
Shrubland	1.44 ± 0.06ᵇ	1.40 ± 0.68ᵇ	5.82 ± 0.54ᵇᶜ	68.33 ± 12.49ᵃᵇ	14.00 ± 5.77ᵃᵇ	18.78 ± 8.55ᵃ
Tree cover	1.35 ± 0.11ᶜ	2.46 ± 1.00ᵃ	5.36 ± 0.13ᶜ	62.77 ± 18.24ᵇ	17.46±6.48ᵃ	20.25 ± 14.96ᵃ
p-value	**0.000*****	**0.000*****	**0.000*****	**0.319**	**0.162**	**0.441**
F $_{(4, 81)}$	**11.46**	**17.09**	**25.959**	**1.196**	**1.683**	**0.947**

Note: Values are shown as mean ± standard deviation. Means with the same letter in each column are not significantly different ($P < 0.05$). *** indicates that a significant difference exists at $p < 0.05$

From the data presented in Table 19, it can be deduced that significant differences existed in soil parameters within the 0 – 30 cm soil depth (except for the clay fraction) in the different LCLU classes in the study area. These results suggest that LCLU is a key determinant of soil parameters. We could not have found this difference if geology, climate, and soil type were significant factors for change in these parameters. A detailed analysis of each of the properties is given below.

4.5.1.1. Bulk Density

Soil bulk density varied across the different LCLUs (Figure 17). From the results presented in Table 19, the soil bulk density (BD) in bare land (1.55 ± 0.11g/cm³) was significantly higher than that in built-up, cropland, shrubland and tree cover LCLU type ($p < 0.001$), but not significantly different from that in built-up and cropland. Also, the soil bulk density in cropland was significantly higher than that of shrubland and tree cover but not significantly different from that in shrubland ($p < 0.001$). The higher bulk density in cropland compared to shrubland and tree cover could be attributed to increased soil organic matter decomposition rates due to agricultural activities such as tillage. Tillage without crop residue disrupts soil structure, resulting in the loss

of soil organic matter and compaction of the surface soil stratum (Gebrehiwot, 2021). Furthermore, the use of heavy machinery contributes to soil compaction, which increases soil density. The higher bulk density in shrubland than in tree cover may be due to soil compaction caused by animal trampling during grazing, since livestock grazing on communal pasture lands is legal. The lowest bulk density in tree cover compared to other LCLU types may be attributed to the high SOC content, which increases soil volume without affecting its weight. The findings were consistent with the findings of previous studies conducted globally (for example, Don et al., 2010; Shi et al., 2013; Yimer et al., 2007; Haile et al., 2014; Chia et al., 2020).
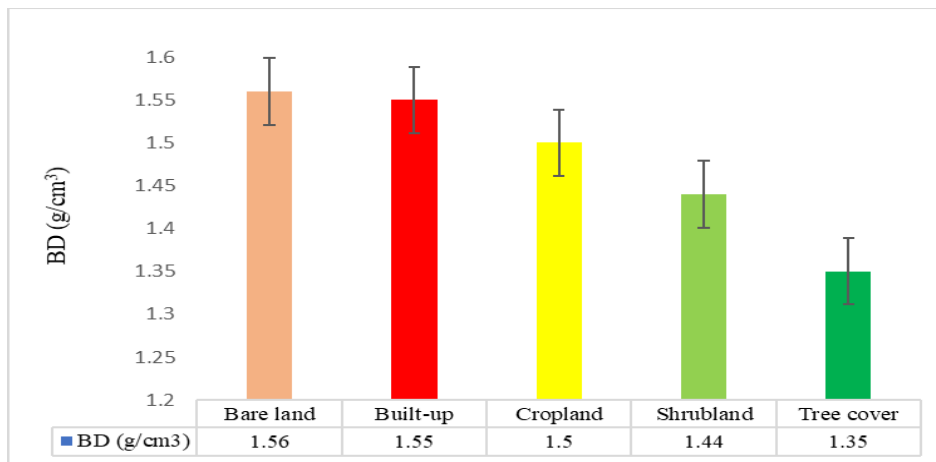
Figure 17. Variation of Bulk density in different LCLU types in the study area.

4.5.1.2. Soil pH

Analysis of variance (ANOVA) and LSD *Post hoc* results showed a significant difference ($p < 0.001$) in soil pH in different LCLU classes in the study area. The pH of soil under tree cover was found to be significantly lower than that of shrubland, cropland, built-up land, and bare land, but not significantly different from that of shrubland (Table 19 and Figure 18). The lower soil pH in tree cover and shrubland compared to cropland, built-up, and bare land soils could be attributed to the decomposition of more available organic matter (for example, leaf litter), resulting in the production of hydrogen ions (H^+) that lowered the soil pH (Ali et al., 2017). The soil pH results obtained in this study were similar to those obtained by Huesken et al. (1989) in the Botswana Soil Service and Advisory Project in the South East District in 1989 (Table 2).
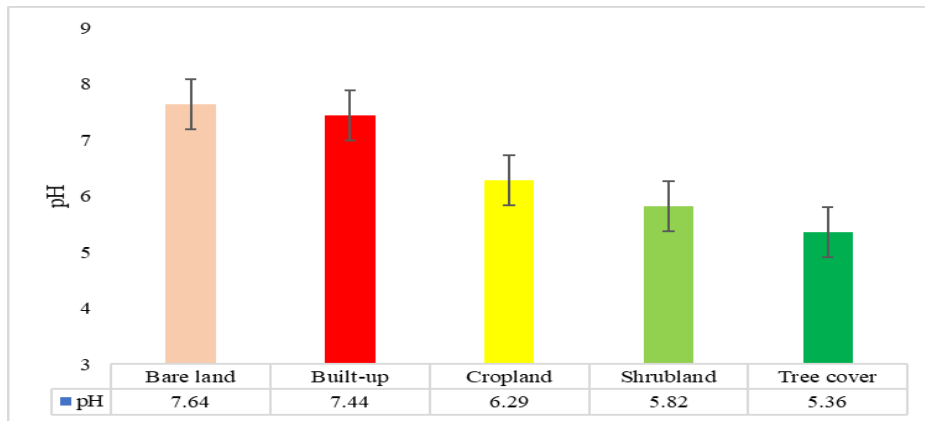
Figure 18. Variation of pH in different LCLU types in the study area.

4.5.1.3. Soil Texture

Soil particle size distribution for the various LCLU types in the study area was also examined (Figure 19). The sand fraction under tree cover was found to be lower than that in other LCLU types ($p > 0.05$) but was not significantly different from that in shrubland, cropland, and built-up (Table 19). Silt fraction was higher under tree cover and was significantly different from that in the other LCLU types. The clay fraction in tree cover was higher than in the other LCLU types but was not significantly different from that in shrubland and cropland. The high clay and silt content in tree cover could be attributed to the chemical weathering of the soil due to its high acidic content.

Figure 19. Variation of particle size in different LCLU types in the study area

Based on the USDA soil classification system, the findings of this study revealed that sandy loam soil dominates the study area (Figure 20).

Figure 20. Distribution of soil texture classes in Greater Gaborone

4.5.1.4. SOC Content

SOC content varies significantly across the different LCLUs (Figure 21). Analysis of variance (ANOVA) and *Post hoc* multiple comparisons showed that there was a significant difference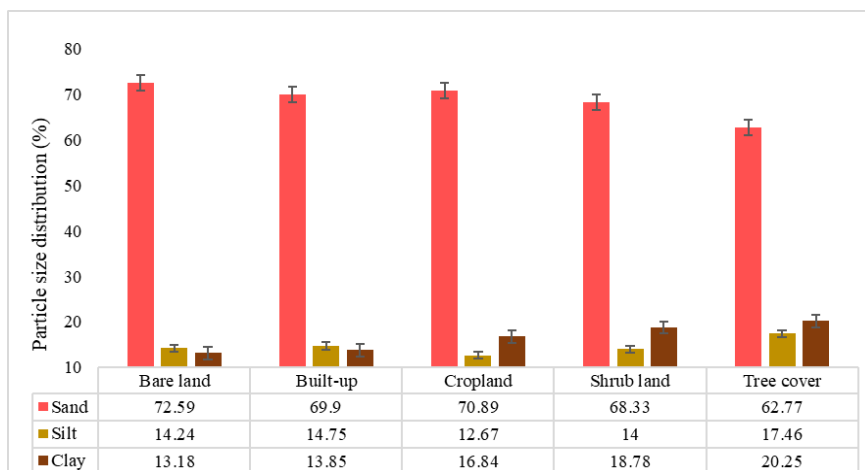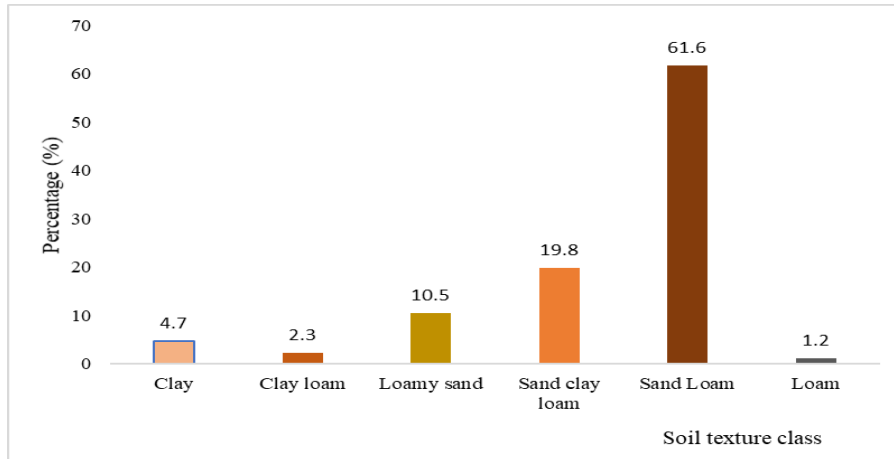 in SOC content in different LCLU types ($p < 0.001$). Differences in SOC content in different LCLUs supported the hypothesis that different LCLUs have different SOC content. The difference was very strong between bare land (0.32 ± 0.26 %) and tree cover ($2.46 \pm 1.00\%$). SOC content was significantly higher in soils under tree cover ($2.46 \pm 1.00\%$) and shrubland ($1.40 \pm 0.68\%$) compared to cropland ($0.93 \pm 1.04\%$), built-up ($1.95 \pm 0.88\%$) and bare land ($0.32 \pm 0.26\%$) (Table 19). Also, the SOC content in built-up was higher than in bare land but not significantly different.

The significantly higher SOC content in tree cover and shrubland compared to the other LULU classes indicated that there was more supply of litter or return of organic matter to the soil. However, frequent removal of biomass and crop residues from cropland during harvesting and continuous tillage could be the primary reasons for low SOC content in cropland compared to shrubland and tree cover. Furthermore, continuous tillage or ploughing exposes available SOC to moisture, aeration, and other decomposing agents, allowing for the rapid decomposition of available organic sources, and resulting in the reduction of SOC content (Gebrehiwot, 2021). Similar findings were reported in studies conducted in the southern part of Ethiopia by Hailu et al. (2000) and Temesgen et al. (2014). These authors found that the SOC content of forest soils was significantly higher than that of open crop fields.
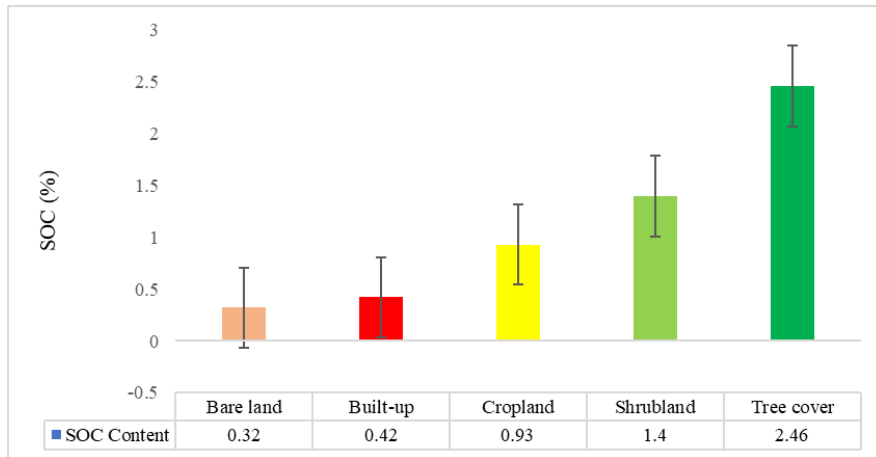
77

Figure 21. Variation of SOC in different LCLU types in the study area

This result, therefore, indicated that soil under tree cover and shrubland were good sequesters of carbon in Greater Gaborone. The spatial distribution of SOC content in Greater Gaborone is depicted in Figure 22, with the mean SOC content being 0.84%.
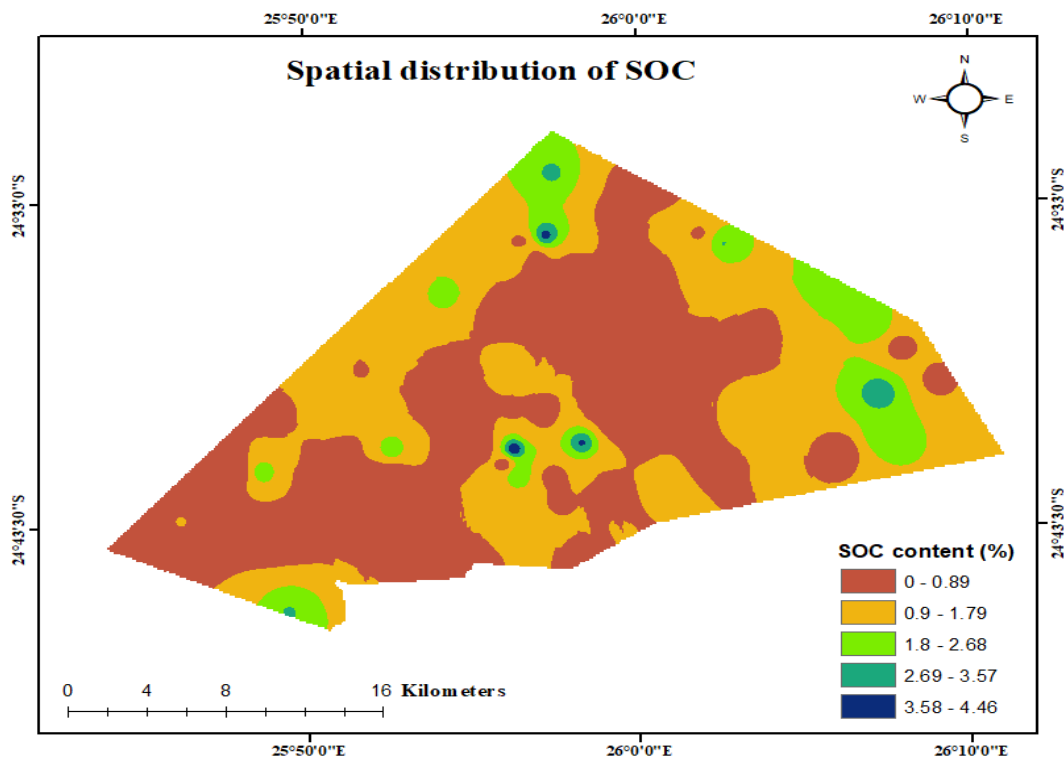

Figure 22. Spatial distribution of SOC in Greater Gaborone

In comparison to other Sub-Saharan regions with similar ecosystem characteristics, the mean SOC content in Greater Gaborone was found to be lower than that of Johannesburg (South Africa) and the Birr watershed (Ethiopia). It was, however, slightly higher than in Central Zimbabwe and Central Namibia. (Table 20).

Table 20. SOC content in Greater Gaborone compared to similar ecosystems around the Sub-Saharan African regions

Region	SOC (%)	Reference
Birr (Ethiopia)	2.55	Amanuel et al., 2018
Johannesburg	1.33	Seboko et al., 2021
Central Zimbabwe	0.68	Nyamadzawo et al., 2008
Central Namibia	0.39	Nghalipo et al., 2019
Greater Gaborone	0.84	This study

4.5.2. Relationship of SOC with Soil Parameters

4.5.2.1. SOC and Bulk Density

Many soil factors influence bulk density, one of which is SOC content (Chaudhari et al., 2013). Soils with a higher organic carbon content have a lower bulk density (Ali et al., 2017), indicating that the soil is less compacted. This study found a negative relationship between soil bulk density and SOC content ($R^2 = 0.995$) (Figure 23). For instance, the soil under tree cover with a bulk density of 1.35 ± 0.11 g/cm^3 had SOC content of $2.46 \pm 1.00\%$, whereas soil under bare land with a bulk density of 1.56 ± 0.14 g/cm^3 had a SOC content of 0.32 ± 0.26 %) (Table 19). The negative relationship between bulk density and SOC content found in this study was consistent with the findings of several studies conducted globally (for example, Dhakal et al., 2010; Chaudhari et al., 2013; Ali et al., 2017). This could be explained by the fact that SOC contains a food source for soil organisms, which aids in the breakdown of large and heavy soil aggregates into smaller, more nutritious, and lighter aggregates that are more stable. Also, soil compaction can inhibit SOC accumulation because it negatively affects soil aggregates by limiting enzyme access to the materials within the soil aggregates and physically maintaining soil organic matter (Kasper et al., 2009; Chia et al., 2020).
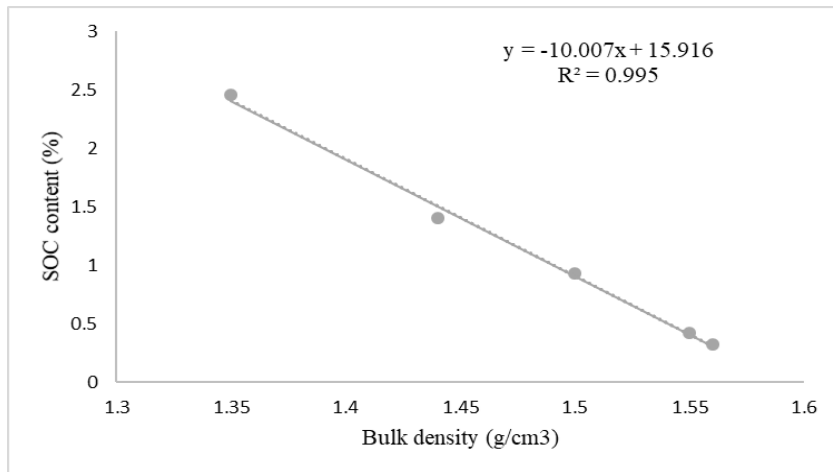
Figure 23. Relationship between SOC content and soil bulk density

4.5.2.2. SOC Content and pH

This study found a negative relationship between soil pH and SOC content ($R^2 = 0.8699$) (Figure 24). Several studies have found that oxidation of organic matter (for example, leaf litter) produces organic acids in the soil solution, causing a decrease in soil pH (Ali et al., 2017; Wainkwa Chia et al., 2017). Higher acidity generally inhibits microbial activity and reduces mineralization, resulting in a higher accumulation of SOC (Kemmitt et al., 2006).
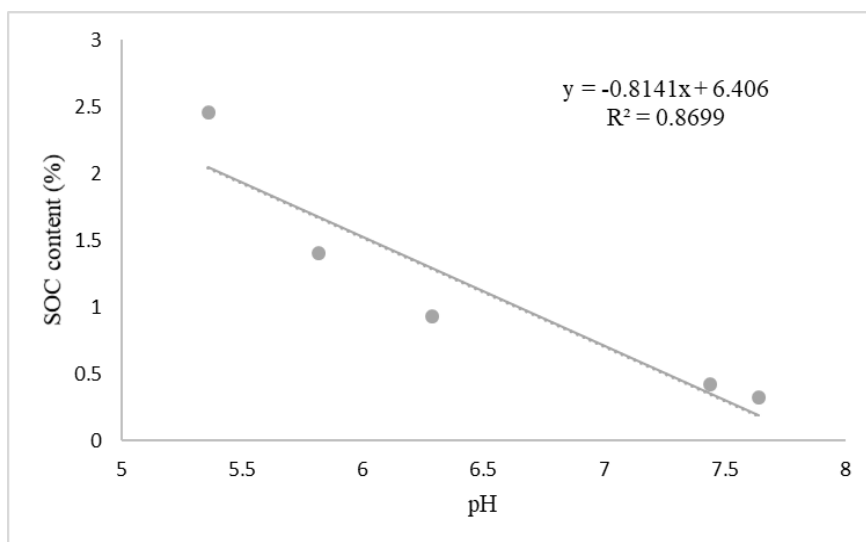
Figure 24. Relationship between SOC content and soil pH

Low pH favours SOC accumulation because the bacteria or organisms most responsible for breaking down the organic matter experience a sharp drop in activity once the pH falls below

6.0 (Zhou et al., 2019). This explains the significantly higher SOC content in tree cover (2.46 ± 1.00%) and shrubland (1.40 ± 0.68%) with pH of 5.36 ± 0.13 and 5.82 ± 0.54, respectively, compared to the low SOC content in bare land (0.32 ± 0.26) with high a pH (7.64 ± 0.90). Furthermore, Low pH (acidic) has the tendency to mechanically weather soil particles (Wainkwa Chia et al., 2017), thus, explaining the higher clay content in soils of tree cover and shrubland LCLU types than in bare land and built-up LCLU types (Table 19).

4.5.2.3. SOC and Soil Texture

The soil particle size fractions except sand showed a positive relationship with SOC content in the study area (Figure 25).
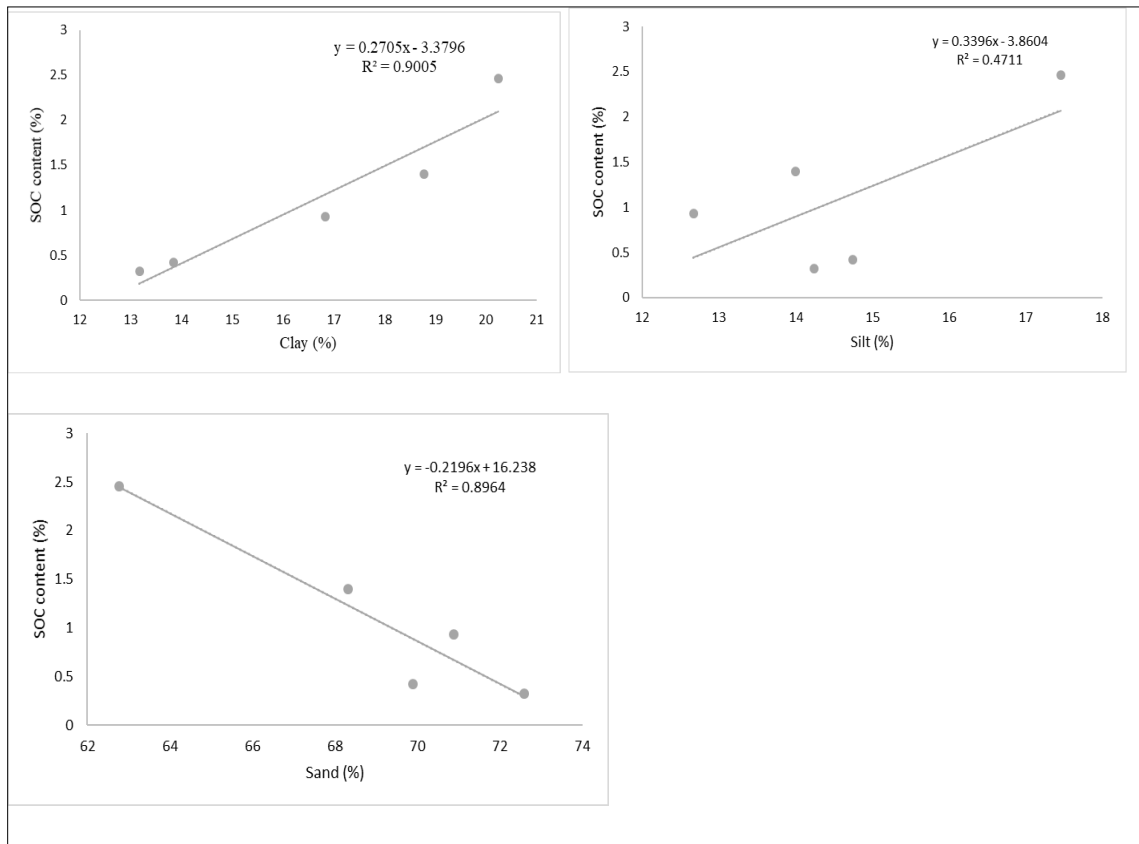
Figure 25. Relationship between SOC content and soil texture

This result was consistent with the findings of several studies conducted globally (for example, Kasper et al., 2009; Razafirmbelo et al., 2013; Dikinya et al., 2016; Ali et al., 2017; Zhou et al., 2019).

Clay and silt positively correlate with SOC content because they help to stabilize soil organic matter (Razafirmbelo et al., 2013; Zhou et al., 2019). The relationship between SOC content and soil texture has been linked to the chemical stabilization of SOC through the physicochemical adsorption of SOC on clay soil/mineral surfaces (Feller & Beare, 1997). This relationship demonstrated that clayey soils have a greater potential for SOC storage than sandy soils (Neto et al., 2010). This explains why the soil under tree cover had a significantly higher SOC content than the other LCLU types.

4.5.3. SOC Stock in Stable and Changed LCLU Types

4.5.3.1. SOC stock in areas without LCLU change

The total SOC stock in areas that did not experience LCLU change between 1988 and 2022 was estimated to be 1,861,477.2 tC (tonnes of carbon) or 1.86 MtC (megatonnes of carbon). The shrubland LCLU type with a total cover area of 304.87 km2 stored 1,600,572.88 tC or 1.6MtC (85.98% of the total SOC stock in the area), whereas bare land (BL) with a total cover area of 0.32 km^2 stored 252.43 tC (0.01% of the total SOC stock in the area). Even though the SOC stock per unit area was higher in tree cover (11.69 kgC/m^2) than in shrubland (5.25 kgC/m^2), shrubland stored 85.89% of the total SOC stock in the area due to its large area coverage (Table 21). The mean SOC content of cropland was estimated to be 0.29%. This result fell within the range of SOC values (0.1 to 0.3%) determined by Huesken et al. (1989) in cropland in the South East District of Botswana in 1989 (Table 2).

Table 21. Mean soil bulk density, SOC content and total SOC Stock in different LCLUs in Greater Gaborone between 1988 and 2022.

LCLU Type	Area (km^2)	BD (g/cm^3)	SOC (%)	SOC Stock (kgC/m^2)	Total SOC stock (tC) in LCLU type	% total SOC in LCLU type
Bare land	0.32	1.67 ± 0.14	0.16 ± 0.13	0.80 ± 0.65	252.43	0.01
Built-up	27.05	1.53 ± 0.09	0.27 ± 0.06	1.21 ± 0.24	32 727.30	1.76
Cropland	5.01	1.49 ± 0.02	0.29 ± 0.08	1.31 ± 0.38	6 560.41	0.35
Shrubland	304.87	1.43 ± 0.05	1.23 ± 0.44	5.25 ± 1.93	1 600 572.88	85.98
Tree cover	18.94	1.27 ± 0.07	3.09 ± 0.76	11.69 ± 2.48	221 364.18	11.89
Total	**356.18**				**1 861 477.20**	**100.**

Note: BD and SOC are expressed in mean and standard deviation

4.5.3.2. SOC Stock in areas with LCLU Change

The total SOC stock in areas affected by the LCLU change was estimated to be 777,479.34 tC or 0.78 MtC. TC – SL, with a total area of 57.87 km^2 stored 440,397.08 tC (56.64% of the total SOC stock in the area), while SL – BL, with an area of 15.4 km^2, stored 36,190.34 km^2 (4.65% of the total SOC stock in the area) (Table 22). Furthermore, SL – BU, with an area coverage of 66.13 km^2, stored 170,606.91 tC (21.94% of the total SOC stock in the area), while SL – CP, with an area coverage of 24.4 km^2, stored 130,285.01 tC (16.76% of the total SOC stock in the area).

Table 22. Mean SOC Stock and total stock for different LCLUs in areas affected by LCLU change during the study period.

LCLU type	Changed Area (km^2)	BD (g/cm^3)	SOC (%)	Mean SOC Stock (kgC/m^2)	Total SOC stock (tC) in LCLU type	% total SOC in LCLU type
SL - BL	15.40	1.54 ± 0.08	0.51 ± 0.29	2.35 ± 1.36	36 190.34	4.65
SL-BU	66.13	1.54 ± 0.12	0.57 ± 0.36	2.58 ± 1.54	170 606.91	21.94
SL-CP	24.40	1.45 ± 0.09	1.18 ± 1.14	3.14 ± 5.04	130 285.01	16.76
TC-SL	57.87	1.38 ± 0.06	1.85 ± 0.80	7.61 ± 3.17	440 397.08	56.64
Total	**163.80**				**777 479.34**	**100.00**

Note: SL – BL = shrubland to bare land, SL – BU = shrubland to built-up, SL – CP = shrubland to cropland and TC – SL = tree cover to shrubland.

The SOC stock in the study area was estimated to be 4.36 MtC, with tree cover accounting for 1.13 MtC (25.87%), shrubland 2.83 MtC (64.86%), cropland 0.14 MtC (3.24%), built-up 0.22 MtC (5.11%), and bare land 0.04 MtC (0.92%) as shown in Table 23.

Table 23. Total SOC stock in the different LCLUs in the study area

LCLU type	Area (km^2)	SOC stock (kgC/m^2)	Total SOC Stock (MtC) in LCLU type	% total SOC stock in LCLU type
Bare land	21.63	1.86	0.04	0.92
Built-up	99.41	2.24	0.22	5.11
Cropland	33.47	4.22	0.14	3.24
Shrubland	402.57	7.02	2.83	64.86
Tree cover	96.42	11.69	1.13	25.87
	653.50		4.36	100.00

4.5.4. Effects of LCLU change on SOC Stock

The effect of LCLU change on SOC stock was examined by assessing the change in SOC stock following LCLU conversion. It was assumed that the current SOC stock in the area with no LCLU change was the same stock that existed in 1988. The most significant LCLU conversions observed during the study period were the conversion of tree cover to shrubland and the conversion of shrubland to cropland, built-up, and bare land (Table 24).

Table 24. Change in SOC stock following LCLU conversion between 1988 and 2022

1988		2022		Change in SOC Stock	
LCLU type	**SOC stock (kgC/m^2)**	**LCLU type**	**SOC Stock (kgC/m^2)**	**kgC/m^2**	**%**
Shrubland	5.25	Bare land	2.35	-2.9	-55.24
Shrubland	5.25	Built-up	2.58	-2.67	-50.86
Shrubland	5.25	Cropland	3.14	-2.11	-40.19
Tree cover	11.69	Shrub land	7.61	-4.08	-34.90

It was found that converting from tree cover to shrubland resulted in a 34.9% (4.08 kg C/m^2) loss of SOC stock. This result was consistent with the findings of previous studies conducted globally, which found that 20 to 50 % of SOC stock is lost when a natural forest is converted to another type of cover or use (Don et al., 2010; Guo & Gifford, 2002; Murty et al., 2002; Wei et al., 2014). Similarly, the conversion of shrubland to bare land, built-up, and cropland resulted in 55.24% (2.9 kg C/m^2), 50.86% (2.67 kgC/m^2), and 40.19% (2.11 kgC/m^2) loss of SOC stock, respectively. The change in SOC stock following LCLU conversion supports the hypothesis that changes in LCLU bring about changes in SOC stock. The 55.24% loss in SOC stock when shrubland is converted to cropland is slightly lower than the result (-59%) reported in the global meta-analysis by Guo and Gifford (2002). From the results, it can be deduced that the conversion of tree covers or shrubland to other uses reduces SOC stock in the study area. The loss of SOC from an ecosystem is one of the primary contributors to rising levels of greenhouse gas concentrations (such as CO_2) and climate change (IPCC, 2014). Furthermore, the reduction in SOC stock has a negative impact on soil fertility, which in turn negatively impacts biomass productivity and food security. However, the conversion of bare land, built-up or cropland to shrubland or tree cover can enhance SOC accumulation.

CHAPTER 5: CONCLUSIONS AND RECOMMENDATIONS

5.1. Conclusions

This study focused on assessing the LCLU change effects on the SOC stocks in Greater Gaborone between 1988 and 2022. The supervised classification method based on a Maximum Likelihood classifier was used to classify Landsat images of 1988 and 2002 and Sentinel-2 images of 2022, downloaded from the USGS website (www.usgs.gov). Six major LCLU types (water body, tree cover, cropland, shrubland, bare land, and built-up) were identified in the study area. The overall classification accuracies for the 1988, 2002 and 2022 images were 85.8%, 86.1% and 94.0%, with Kappa coefficients of 0.83, 0.83 and 0.93, respectively. The Post Classification Comparison (PCC) approach was used to detect the LCLU changes that had happened during the study period (1988 – 2022). Overall, a significant gain in area coverage was observed for the built-up class, 75.12 km^2 (310.16%), while significant losses were observed for the shrub land class, 24.16 km^2 (5.67%) and the tree cover class, 33.32 km^2 (25.69%). The results of the predicted LCLU for 2040 using MOLUSCE revealed that tree cover and cropland classes will shrink while shrubland, bare land and built-up classes will increase, indicating the need for proper land use management strategy to be put in place to avoid land degradation and possible loss of biodiversity.

It was also found that LCLU type has a significant influence on SOC content, soil bulk density, pH, and texture. The SOC content was found to have a negative correlation with soil bulk density, pH and sand fraction. However, LCLU correlates positively with clay and silt content. Soil organic carbon content was found to be higher in the tree cover class than in the other LCLU types. The total SOC stock in the study area was estimated to be 4.36 MtC, with the shrubland LCLU type accounting for 64.86% (2.83 MtC), mostly due to the spatial extent of this class. Furthermore, it was also found that the LCLU conversion had a significant impact on the SOC stock in the study area between 1988 and 2022. The conversion of tree cover to shrubland resulted in a 34.9% (4.08 kg C/m2) loss of SOC stock from the study area. Also, the conversion of shrubland to cropland, built-up or bare land resulted in 55.24% (2.9 kgC/m^2), 50.86% (2.67 kgC/m^2), or 40.19% (2.11 kgC/m^2) loss of SOC stock, respectively. The predicted future LCLU change between 2022 and 2040 shows that tree cover will shrink by 17.8 km^2, indicating that more SOC will be lost from the study area in the future.

5.2. Recommendations

It is recommended that:

1. Appropriate land management strategies, such as conservation agricultural operations, should be encouraged; overgrazing and the conversion of natural vegetation to other land uses should be discouraged.

2. Stakeholders should make greater efforts to raise public awareness about the importance of environmental protection in order to mitigate the threat of natural vegetation loss, SOC stock depletion, and greenhouse gas increases.

5.3. Suggestions for future study

It is suggested that:

1. A similar study should be conducted in the future (for example, after 10 years) using the current study results as a reference in order to obtain more accurate results for changes in SOC content following LCLU changes.

2. Research on SOC loss due to soil erosion, mineralization, and decomposition should be conducted in the study area to improve our understanding of the mechanisms of SOC stock changes, as this study did not determine how much SOC was lost in each of the LCLU types due to these factors.

3. Other methods, such as the Bare Soil Index (BSI) or Normalized Difference Vegetation Index (NDVI), should be used to estimate the SOC in the study area in order to compare the results and determine which method produces the most reliable results. In an attempt to estimate SOC content using the NDVI method, the study found a positive correlation between estimated SOC and NDVI ($R^2 = 0.9123$) and thus suggested the following equation for estimating SOC stock:

$$SOC = -0.0082 + 0.1846 * NDVI \qquad (19)$$

Where SOC is the Soil Organic Carbon content (%) and NDVI is the Normalized Difference Vegetation Index of a given pixel.

REFERENCES

Aguirre-Gutiérrez, J., Seijmonsbergen, A. C., & Duivenvoorden, J. F. (2012). *Optimizing land cover classification accuracy for change detection, a combined pixel-based and object-based approach in a mountainous area in Mexico*. Applied Geography, *34*, 29–37.

Ahmed, S., Diffenbaugh, N., Hertel, T., Lobel, D., Ramankutty, N., Rios, A., & Rowhani, P. (2011). *Climate volatility and poverty vulnerability in Tanzania. Global Environmental Change*, *2*(1), 46-55.

Akinyemi, F. O. (2017). *Climate change and variability in semiarid Palapye, Eastern Botswana: An assessment from smallholder farmers' perspective*. Retrieved June 9, 2022, from https://doi.org/10.1175/WCAS-D-16-0040.s1

Ali, S., Begum, F., Hayat, R., & Bohannan, B. J. M. (2017). *Variation in soil organic carbon stock in different land uses and altitudes in Bagrot Valley, Northern Karakoram. Acta Agriculturae Scandinavica Section B: Soil and Plant Science*, *67*(6), 551–561. Retrieved June 9, 2022, from https://doi.org/10.1080/09064710.2017.1317829

Alphan, H., Doygun, H., & Unlukaplan, Y. I. (2009). *Post-classification comparison of land cover using multitemporal Landsat and ASTER imagery: the case of Kahramanmaraş, Turkey*. Environ Monit Assess, 151, 327–336.

Alqurashi, A. F., & Kumar, L. (2013). *Investigating the Use of Remote Sensing and GIS Techniques to Detect Land Use and Land Cover Change: A Review*. Advances in Remote Sensing, *02*(02), 193–204. Retrieved July 13, 2022, from https://doi.org/10.4236/ars.2013.22022

Amanuel, W., Yimer, F., & Karltun, E. (2018). *Soil organic carbon variation in relation to land use changes. The case of Birr watershed, upper Blue Nile River Basin, Ethiopia*. Journal of Ecology and Environment, 42(1). Retrieved June 21, 2022, from https://doi.org/10.1186/s41610-018-0076-1

Andualem, T. G., Belay, G., & Guadie, A. (2018). *Land Use Change Detection Using Remote Sensing Technology*. Journal of Earth Science & Climatic Change, *9*(10). Retrieved August 19, 2022, from https://doi.org/10.4172/2157-7617.1000496

Anokye, J., Logah, V., & Opoku, A. (2021). *Soil carbon stock and emission: estimates from three land-use systems in Ghana.* Ecological Processes, 10(1). Retrieved June 6, 2022, from https://doi.org/10.1186/s13717-020-00279-w

Arp, P. A., & Krause, H. H. (1984). *The Forest Floor: Lateral Variability as Revealed by Systematic Sampling*. Can. J. Soil Sci., 1984, 423–437

Assefa, D., Rewald, B., Sandén, H., Rosinger, C., Abiyu, A., Yitaferu, B., & Godbold, D. L. (2017). *Deforestation and land use effects on soil organic carbon and nitrogen stock in Northwest Ethiopia*. Catena, *153*, 89–99. Retrieved September 15, 2022, from https://doi.org/10.1016/j.catena.2017.02.003

Badgery, W. B., Simmons, A. T., Murphy, B. W., Rawson, A., Andersson, K. O., & Lonergan, V. E. (2014). *The influence of land use and management on soil carbon levels for crop-pasture systems in Central New South Wales, Australia*. Agriculture, Ecosystems and Environment, *196*, 147–157. Retrieved July 18, 2022, from https://doi.org/10.1016/j.agee.2014.06.026

Baldock, J. A., & Skjemstad, J. O. (2000). *Role of the soil matrix and minerals in protecting natural organic materials against biological attack*. Retrieved May 3, 2022, from www.elsevier.nl/locate/orggeochem

Batjes, N. H. (1996). *Total carbon and nitrogen in the soils of the world*. European Journal of Soil Science, *47*(2), 151–163. Retrieved June 9, 2022, from https://doi.org/10.1111/j.1365-2389.1996.tb01386.x

Bayer, C., Martin-Neto, L., Mielniczuk, J., Pavinato, A., & Dieckow, J. (2006). *Carbon sequestration in two Brazilian Cerrado soils under no-till*. Soil and Tillage Research, 86(2), 237–245. Retrieved August 16, 2022, from https://doi.org/10.1016/j.still.2005.02.023

Bekalo, M. T. (2009). *Spatial Metrics and Landsat Data for Urban Land use Change Detection in Addis Ababa, Ethiopia* [MSc]. University of Jaume I.

Benzer, N. (2010). *Using the Geographical Information System and Remote Sensing Techniques for Soil Erosion Assessment*. Polish J. of Environ, *19*(2010), 881–886.

Bessah, E., Bala, A., Agodzo, S. K., Okhimamhe, A., Boakye, E. A., & Ibrahim, S. U. (2019). *The impact of crop farmers' decisions on future land use, and land cover changes in Kintampo North Municipality of Ghana*. International Journal of Climate Change Strategies and Management, 11(1), 72–87. Retrieved June 29, 2022, from https://doi.org/10.1108/IJCCSM-05-2017-0114

Bhattacharjee, S., & Ghosh, S. K. (2015). *Spatio-Temporal Change Modeling of LULC: A Semantic Kriging Approach.* ISPRS Annals of the Photogrammetry, Remote Sensing and Spatial Information Sciences, *2*(42), 177–184. Retrieved September 14, 2022, from https://doi.org/10.5194/isprsannals-II-4-W2-177-2015

Biazen Molla, M., Ikporukpo, C. O., & Olatubara, C. O. (2018). *The Spatio-Temporal Pattern of Urban Green Spaces in Southern Ethiopia*. American Journal of Geographic Information System, 2018(1), 1–14. Retrieved June 22, 2022, from https://doi.org/10.5923/j.ajgis.20180701.01

Blair, D., Shackleton, C. M., & Mograbi, P. J. (2018). *Cropland Abandonment in South African Smallholder Communal Lands: Land Cover Change (1950-2010) and Farmer Perceptions of Contributing Factors*. *7*(121). Retrieved June 3, 2022, from https://doi.org/10.3390/land7040121.

Blake, G. R., & Hartge, K. H. (1986). *Bulk density. In: Klute, A., Ed., Methods of Soil Analysis, Part 1—Physical and Mineralogical Methods* (A. Klute, Ed.; 2nd Edition, Vol. 9). American Society of Agronomy—Soil Science Society of America.

Blaschke, T., Lang, S., Lorup, E., Strobl, J., & Zeil, P. (2000). *Object-Oriented Image Processing in an Integrated GIS / Remote Sensing Environment and Perspectives for Environmental Applications*. Environmental Information for Planning, Politics and the Public, (1995), 555-570.

Bone, C., & Dragicevic, S. (2009). *Defining Transition Rules with Reinforcement Learning for Modeling Land Cover Change*. 85(5), 291–305.

Briassoulis, H. (2003). Factors Influencing Land-Use and Land-Cover Change. Vol.1. University of the Aegean, Greece.

Brink, A. B., & Eva, H. D. (2009). *Monitoring 25 years of land cover change dynamics in Africa: A sample-based remote sensing approach*. ArticlesJournal Article, 29(4), 501-512.

Brown, D., & Duh, J. D. (2004). *Spatial Simulation for Translating Between Land Use and Land Cover*. International Journal of Geographical Information Science, 1(18), 35–60.

Byakatonda, J., Parida, B. P., Moalafhi, D. B., & Kenabatho, P. K. (2018). *Analysis of long-term drought severity characteristics and trends across semiarid Botswana using two drought indices*. Atmospheric Research, 213, 492–508. Retrieved June 23, 2022, from https://doi.org/10.1016/J.ATMOSRES.2018.07.002

Campbell, J. B., & Wynne, R. H. (2011). *Introduction to Remote Sensing*. Edition 5, Vol. 5). The Guilford Press.

Cavrić, B., & Keiner, M. (2006). *Managing Development of a Rapidly Growing African City: A Case of Gaborone, Botswana*. In Keiner Geoadria.11(1).

Chaikaew, P. (2019). *Land Use Change Monitoring and Modelling using GIS and Remote Sensing Data for Watershed Scale in Thailand*. 165–181.

Chander, G., Markham, B. L., & Helder, D. L. (2009). *Summary of current radiometric calibration coefficients for Landsat MSS, TM, ETM+, and EO-1 ALI sensors*. Remote Sensing of Environment, 113(5), 893–903. Retrieved July 3, 2022, from https://doi.org/10.1016/J.RSE.2009.01.007

Chan, K. Y., Oates, A., Li, G. D., Conyers, M. K., Prangnell, R. J., Poile, G., Liu, D. L., & Barchia, I. M. (2010). *Soil carbon stocks under different pastures and pasture management in the higher rainfall areas of south-eastern Australia*. Australian Journal of Soil Research, *48*(1), 7–15. Retrieved May 13, 2022, from https://doi.org/10.1071/SR09092

Chaturvedi, P. (2004). Biomass: *The Fuel of the Rural Poor in Developing Countries in Sims, REH (ed), Bioenergy Options for a Cleaner Environment, in Developed and Developing Countries*. Elsevier Science & Technology.

Chaudhari, P. R., Ahire, D. v, Ahire, V. D., Chkravarty, M., & Maity, S. (2013). *Soil Bulk Density as related to Soil Texture, Organic Matter Content and available total Nutrients of Coimbatore Soil*. International Journal of Scientific and Research Publications, *3*(2). Retrieved July 13, 2022, from www.ijsrp.org

Chia, R. W., Son, Y., Cho, W., Lee, Y. G., Tsetsegmaa, G., & Kang, H. (2020). *Do different land use changes in a deciduous forest ecosystem result in alterations in soil organic C and total N stocks?*

Plant and Soil, *457*(1–2), 153–165. Retrieved October 10, 2022, from https://doi.org/10.1007/s11104-020-04724-9

Chingombe, W., Pedzisai, E., Gondo, R., & Mangizvo, R. (2021). *Land Use and Land Cover Changes at Hova Farm in Bindura District, Zimbabwe*. Journal of Sustainable Development, 14. Retrieved September 3, 2022, from https://doi.org/10.5539/jsd.v14n4p42

Cochran, R. L., Collins, H. P., Kennedy, A., & Bezdicek, D. F. (2007). *Soil carbon pools and fluxes after land conversion in a semiarid shrub-steppe ecosystem.* Biology and Fertility of Soils, 43(4), 479–489. Retrieved July 18, 2022, from https://doi.org/10.1007/s00374-006-0126-1

Dar, J. A., & Sundarapandian, S. (2015). *Variation of biomass and carbon pools with forest type in temperate forests of Kashmir Himalaya, India*. Environmental Monitoring and Assessment, 187(2). Retrieved September 25, 2022, from https://doi.org/10.1007/s10661-015-4299-7

Dejun, L., Niu, S., & Luo, Y. (2012). *Global patterns of the dynamics of soil carbon and nitrogen stocks following afforestation: a meta-analysis*. New Phytologist, *195*, 172–181. Retrieved June 3, 2022, from https://doi.org/10.1111/j.1469-8137.2012.04150.x

Dhakal, S., Koirala, M., Sharma, E., & Subedi, N. (2010). *Effects of Land Use Change on Soil Organic Carbon Stock in Balkhu Khola Watershed Southwestern Part of Kathmandu Valley, Central Nepal*. Journal of World Academy of Science, 66.

Dietzel, C., Herold, M., Hemphill, J. J., & Clarke, K. C. (2005). *Spatio-temporal dynamics in California's Central Valley: Empirical links to urban theory*. International Journal of Geographical Information Science, 19(2), 175–195. Retrieved July 3, 2022, from https://doi.org/10.1080/13658810410001713407

Dikinya, O., Atlhopheng, J., & Manyiwa, T. (2016a). *Variations on soil carbon dioxide flux with land-use type and selected soil properties in the hardveld of Botswana.* South African Journal of Plant and Soil, 33(4), 309–316. Retrieved July 17, 2022, from https://doi.org/10.1080/02571862.2016.116109.

Dikinya, O., Atlhopheng, J., & Manyiwa, T. (2016b). *Variations on soil carbon dioxide flux with land-use type and selected soil properties in the hardveld of Botswana*. South African Journal of Plant

and Soil, *33*(4), 309–316. Retrieved April 3, 2022, from https://doi.org/10.1080/02571862.2016.1161091

Dlamini, P., Chivenge, P., Manson, A., & Chaplot, V. (2014). *Land degradation impact on soil organic carbon and nitrogen stocks of sub-tropical humid grasslands in South Africa*. Geoderma, 235–236, 372–381. Retrieved June 13, 2022, from https://doi.org/10.1016/j.geoderma.2014.07.016

Don, A., Schumacher, J., & Freibauer, A. (2010). *Impact of tropical land use change on soil organic carbon stocks-a meta-analysis*. Global Change Biology, *17*(4). https://doi.org/10.1111/j.1365

Donovan, P. (2013). *Measuring soil carbon change: A Flexible, Practical, Local Method*. Retrieved June 27, 2022, from http://soilcarboncoalition.org/taxonomy/term/2.

Dougill, A. J., Akanyang, L., Perkins, J. S., Eckardt, F. D., Stringer, L. C., Favretto, N., Atlhopheng, J., & Mulale, K. (2016). *Land use, rangeland degradation and ecological changes in the southern Kalahari, Botswana.* Afr. J. Ecol., *54*(59–67).

Drayton Chandler, R. (2016). *TigerPrints Soil Organic Carbon Distribution with Depth: Implications for Ecosystem Services.* Retrieved June 5, 2022, from https://tigerprints.clemson.edu/all_theses

Du, Y., Teillet, P. M., & Cihlar, J. (2002). *Radiometric normalization of multitemporal high-resolution satellite images with quality control for land cover change detection*. Remote Sensing of Environment, *82*(1), 123–134. Retrieved September 13, 2022, from https://doi.org/10.1016/S0034-4257(02)00029-9.

Eastman, J. R. (2009). *IDRISI Taiga Guide to GIS and Image Processing*. Clark Labs for Cartographic Technology and Geographic Analysis, Clark University, Worcester.

Edmondson, J. L., Davies, Z. G., McCormack, S. A., Gaston, K. J., & Leake, J. R. (2014). *Land-cover effects on soil organic carbon stocks in a European city*. Science of the Total Environment, 472, 444–453. Retrieved September 10, 2022, from https://doi.org/10.1016/j.scitotenv.2013.11.025

Erasu, D. (2017). *Remote Sensing-Based Urban Land Use/Land Cover Change Detection and Monitoring*. Journal of Remote Sensing & GIS, 06(02). Retrieved June 17, 2022, from https://doi.org/10.4172/2469-4134.1000196

Fan, S., Guan, F., Xu, X., Forrester, D. I., Ma, W., & Tang, X. (2016). *Ecosystem Carbon Stock Loss after Land Use Change in Subtropical Forests in China*. Retrieved September 6, 2022, from https://doi.org/10.3390/f7070142

FAO. (2006). *World reference base for soil resources 2006*. Retrieved March 29, 2022, from http://www.fao.org

FAO. (2019*). Measuring and modelling soil carbon stocks and stock changes in livestock production systems Guidelines for assessment*. Retrieved may 13, 2022, from http://www.fao.org/partnerships/leap/publications/en/

Feldmann, L., & Marlis, K. (2011). *The roles of donor organisations in promoting energy efficient cook stoves*. Energy Policy, *39*(12).

Feller, C., & Beare, M. H. (1997). *Physical control of soil organic matter dynamics in the tropics*. Geoderma, 79(1–4), 69–116. Retrieved September 15, 2022, from https://doi.org/10.1016/S0016-7061(97)00039-6

Fentie, S. F., Jembere, K., Fekadu, E., & Wasie, D. (2020). *Land Use and Land Cover Dynamics and Properties of Soils under Different Land Uses in the Tejibara Watershed, Ethiopia*. Scientific World Journal, 2020. Retrieved May 2, 2022, from https://doi.org/10.1155/2020/1479460

Foody, G. M. (2002). *Status of land cover classification accuracy assessment*. Remote Sensing of Environment, *80*(1), 185–201. Retrieved September 13, 2022, from https://doi.org/10.1016/S0034-4257(01)00295-4

Foody, G. M. (2008). *Harshness in image classification accuracy assessment*. International Journal of Remote Sensing, *29*(11), 3137–3158. Retrieved June 19, 2022, from https://doi.org/10.1080/01431160701442120

Fox, J. T., Vandewalle, M. E., & Alexander, K. A. (2017). *Land cover change in Northern Botswana: The influence of climate, fire, and elephants on Semi-Arid Savanna Woodlands*. Land, 6(4). Retrieved September 23, 2022, from https://doi.org/10.3390/land6040073

Gašparović, M. (2020). *Urban growth pattern detection and analysis*. Urban Ecology, 35–48. Retrieved September 18, 2022, from https://doi.org/10.1016/B978-0-12-820730-7.00003-3

Gebrehiwot, H. H. (2021). *Land Use Conversion Induced changes in Soil Organic Carbon Stock in Semi-Arid Areas of Africa.* Retrieved July 7, 2022, from https://doi.org/10.24163/ijart/2017/5(3):72-82

Geist, H. J., & Lambin, E. F. (2002). *Proximate Causes and Underlying Driving Forces of Tropical Deforestation.* BiosScience, *52*(2), 143–150.

Gelaw, A. M., Singh, B. R., & Lal, R. (2014). *Soil organic carbon and total nitrogen stocks under different land use in a semi-arid watershed in Tigray, Northern Ethiopia*. Agriculture, Ecosystems and Environment, *188*, 256–263. Retrieved September 13, 2022, from https://doi.org/10.1016/j.agee.2014.02.035

Ghimire, P., Bhatta, B., Pokhrel, B., Kafle, G., & Paudel, P. (2019). *Soil organic carbon stocks under different land use in the Chure region of Makawanpur district, Nepal.* SAARC Journal of Agriculture, 16(2), 13–23. Retrieved May 10, 2022, from https://doi.org/10.3329/sja.v16i2.40255

Gismondi, M. M. M., Kamusoko, C., Furuya, T., Tomimura, S., & Maya, M. (2014). *Module for Land Use Change Evaluation* (MOLUSCE). An open-source land use change analyst for QGIS.

GoB. (2013). *Guidelines for Integrated Support Programme for Arable Agriculture Development (ISPAAD).* Government of Botswana.

Grinblat, Y., Kidron, G. J., Kidron, G. J., Karnieli, A., & Benenson, I. (2015). *Simulating land-use degradation in West Africa with the ALADYN model*. Journal of Arid Environments, 112, 52–63.

Guillaume, K., Damris, M., & Kuzyakov, Y. (2015*). Losses of soil carbon by converting tropical forest to plantations: erosion and decomposition estimated by d 13 C*. Retrieved May 17, 2022, from https://doi.org/10.1111/gcb.12907

Guo, L. B., & Gifford, R. M. (2002). *Soil Carbon Stocks and Land Use Change: A Meta-Analysis.* Global Change Biology, 8, 345-360. Retrieved May 10, 2022, from https://doi.org/10.1046/j.1354-1013.2002.00486.x

Haile, G., Lemenhi, M., & Senbeta, F. (2014). *Impacts of Land Uses Changes on Soil Fertility, Carbon and Nitrogen Stock under Smallholder Farmers in Central Highlands of Ethiopia: Implication for*

Sustainable Agricultural Landscape Management Around Butajira Area. In New York Science Journal. *7*(2). Retrieved May 20, 2022, from http://www.sciencepub.net/newyork

Hailu, T., Negash, L., & Olsson, M. (2000). *Millettia ferruginea from southern Ethiopia: Impacts on soil fertility and growth of maize.* Agroforestry Systems, 48(1), 9–24. Retrieved April 17, 2022, from https://doi.org/10.1023/A:1006274912762

Haller, Tobias, Galvin, Marc, Meroka, Patrick, Alca, Jamil, Alvarez, & Alex. (2008). Who gains from community conservation? intended and unintended costs and benefits of participative approaches in Peru and Tanzania. Journal of Environment and Development, 17(2), 118–144.

Haque, M. I., & Basak, R. (2017). *Land cover change detection using GIS and remote sensing techniques: A Spatio-temporal study on Tanguar Haor, Sunamganj, Bangladesh*. The Egyptian Journal of Remote Sensing and Space Science, 20(2), 251–263. Retrieved July 20, 2022, from https://doi.org/10.1016/J.EJRS.2016.12.003

Hassan, M. M., Smith, A. C., Walker, K., Rahman, M. K., & Southworth, J. (2018). *Rohingya refugee crisis and forest cover change in Teknaf, Bangladesh*. Remote Sensing, 10(5). Retrieved September 10, 2022, from https://doi.org/10.3390/rs10050689

Hassen, E. E., & Assen, M. (2017). *Land use/cover dynamics and its drivers in Gelda catchment, Lake Tana watershed, Ethiopia.* Hassen and Assen Environ Syst Res, 6, 4. Retrieved June 10, 2022, from https://doi.org/10.1186/s40068-017-0081-x

Hossain, F., & Moniruzzaman, D. M. (2021). *Environmental change detection through remote sensing technique: A study of Rohingya refugee camp area (Ukhia and Teknaf sub-district), Cox's Bazar, Bangladesh.* In Environmental Challenges (Vol. 2). Elsevier B.V. Retrieved May 16, 2022, from https://doi.org/10.1016/j.envc.2021.100024

Huesken, J., van Waveren, E., & Nachtergaele, F. (1989). *Soil Mapping and Advisory Services Botswana. Soil and Land Suitability for Arable Farming of South-East district*. Retrieved June 25, 2022, from https://docslib.org/doc/8926486/soils-and-land-suitability-for-arable-farming-of-South-east-district

Husein, H. H., Mousa, M., Sahwan, W., Bäumler, R., & Lucke, B. (2019). *Spatial Distribution of Soil Organic Matter and Soil Organic Carbon Stocks in Semi-Arid Area of Northeastern Syria*. Natural Resources, 10(12), 415–432. Retrieved May 28, 2022, from https://doi.org/10.4236/nr.2019.1012028

IPCC. (2007). *Core Writing Team Extended Writing Team Climate Change 2007: Synthesis Report: An Assessment of the Intergovernmental Panel on Climate Change*. Retrieved May 3, 2022, from http://www.ipcc.ch/meetings/ar4-workshops-express-meetings/uncertainty-guidance-note.pdf

IPCC. (2013). *Annex II: ClimateSystem Scenario Tables* [Prather, M., G. Flato, P. Friedlingstein, C. Jones, J.-F. Lamarque, H. Liao and P. Rasch (eds.)]. In: Climate Change 2013: The Physical Science Basis. Contribution of Working Group I to the Fifth Assessment Report of the Intergovernmental Panel on Climate Change [Stocker, T.F., D. Qin, G.-K. Plattner, M. Tignor, S.K. Allen, J. Boschung, A. Nauels, Y. Xia, V. Bex and P.M. Midgley (eds.)]. Cambridge University Press, Cambridge, United Kingdom, NY, USA.

IPCC. (2014). *Summary for Policymakers. In: Climate Change 2014: Mitigation of Climate Change*. Contribution of Working Group III to the Fifth Assessment Report of the Intergovernmental Panel on Climate Change [Edenhofer, O., R. Pichs-Madruga, Y. Sokona, E. Farahani, S. Kadner, K. Seyboth, A. Adler, I. Baum, S. Brunner, P. Eickemeier, B. Kriemann, J. Savolainen, S. Schlömer, C. von Stechow, T. Zwickel and J.C Minx (eds.)].

Jabbar, M. T., & Zhou, X. (2011). *Eco-environmental change detection by using remote sensing and GIS techniques: A case study Basrah province, south part of Iraq*. Environmental Earth Sciences, 64(5), 1397–1407. Retrieved May 19, 2022, from https://doi.org/10.1007/s12665-011-0964-5

Jansen, L. J. M., & Gregorio, A. di. (2000). *Land Cover Classification System (LCCS): Classification Concepts and User Manual Land Cover View Project Global programme to support the implementation of the "Voluntary Guidelines on the Responsible Governance of Tenure of Land, Fisheries and Forests in the Context of National Food Security" (VGGT) View project*. Retrieved May July, 2022, from https://www.researchgate.net/publication/229839605

Jensen, J. R. (2005). *Introductory Digital Image Processing: A Remote Sensing Perspective*. (3rd Edition). Prentice Hall.

Jensen, J. R., & Cowen, D. C. (1999). R*emote Sensing of Urban/Suburban Infrastructure and Socio-Economic Attributes*. Photogrammetric Engineering and Remote Sensing, 5, 611–622.

Kalaba, F. K. (2014). *A conceptual framework for understanding forest socio-ecological systems*. Biodiversity and Conservation, *23*(14), 3391–3403. Retrieved September 7, 2022, from https://doi.org/10.1007/s10531-014-0792-5

Kamaraj, manikandan, Rangarajan, S., & Kamaraj, M. (2022). *Predicting the Future Land Use and Land Cover Changes for Bhavani Basin, Tamil Nadu, India Using QGIS MOLUSCE Plugin Predicting the Future Land Use and Land Cover Changes for Bhavani basin, Tamil Nadu, India Using QGIS MOLUSCE Plugin 2 3 4 6 7*. Environ Sci Pollut Res Int., *603*(203), 17904–17906. Retrieved May 14, 2022, from https://doi.org/10.21203/rs.3.rs-616393/v1

Kamwi, J. M., Cho, M. A., Kaetsch, C., Manda, S. O., Graz, F. P., & Chirwa, P. W. (2018). *Assessing the Spatial Drivers of Land Use and Land Cover Change in the Protected and Communal Areas of the Zambezi Region, Namibia*. *7*(131). Retrieved June 17, 2022, from https://doi.org/10.3390/land7040131

Kangalawe, R., & Lyimo, J. (2010). *Population dynamics, rural livelihoods and environmental degradation: some experiences from Tanzania. 12*(6), 985–997.

Kasper, M., Buchan, G. D., Mentler, A., & Blum, W. E. H. (2009). *Influence of soil tillage systems on aggregate stability and the distribution of C and N in different aggregate fractions*. Soil and Tillage Research, 105(2), 192–199. Retrieved July 26, 2022, from https://doi.org/10.1016/J.STILL.2009.08.002

Kassa, H., Dondeyne, S., Poesen, J., Frankl, A., & Nyssen, J. (2017). *Impact of deforestation on soil fertility, soil carbon and nitrogen stocks: the case of the Gacheb catchment in the White Nile Basin, Ethiopia*. Agriculture, Ecosystems and Environment, 247, 273–282. Retrieved May 27, 2022, from https://doi.org/10.1016/j.agee.2017.06.034

Kemmitt, S. J., Wright, D., Goulding, K. W. T., & Jones, D. L. (2006). *pH regulation of carbon and nitrogen dynamics in two agricultural soils.* Soil Biology and Biochemistry, 38(5), 898–911. Retrieved June 23, 2022, from https://doi.org/10.1016/j.soilbio.2005.08.006

Kindu, M., Schneider, T., Teketay, D., & Knoke, T. (2013). *Land use/land cover change analysis using an object-based classification approach in the Munessa-Shashemene landscape of the Ethiopian highlands*. Remote Sensing, *5*(5), 2411–2435. Retrieved May 12, 2022, from https://doi.org/10.3390/rs5052411

Knops, J. M. H., & Bradley, K. L. (2009). *Soil Carbon and Nitrogen Accumulation and Vertical Distribution across a 74-Year Chronosequence*. Soil Science Society of America Journal, 73(6), 2096–2104. Retrieved May 21, 2022, from https://doi.org/10.2136/sssaj2009.0058

Kumar, P., Pandey, P. C., Singh, B. K., Katiyar, S., Mandal, V. P., Rani, M., Tomar, V., & Patairiya, S. (2016). *Estimation of accumulated soil organic carbon stock in the tropical forest using geospatial strategy*. Egyptian Journal of Remote Sensing and Space Science, 19(1), 109–123. Retrieved June 10, 2022, from https://doi.org/10.1016/j.ejrs.2015.12.003

Lal, R., Safriel, U., & Boer, B. (2012). *Zero Net Land Degradation: A New Sustainable Development Goal for Rio+20. A report prepared for the Secretariat of the United Nations Convention to Combat Desertification*. Retrieved May 03, 2022, from http://www.unccd.int/Lists/SiteDocumentLibrary/secretariat/2012/Zero%20Net%20Land%20Degradation%20Report%20UNCCD%20May%202012%20background.pdf.

Lal, R., Smith, P., Jungkunst, H. F., Mitsch, W. J., Lehmann, J., Ramachandran Nair, P. K., McBratney, A. B., de Moraes Sá, J. C., Schneider, J., Zinn, Y. L., Skorupa, A. L. A., Zhang, H. L., Minasny, B., Srinivasrao, C., & Ravindranath, N. H. (2018). *The carbon sequestration potential of terrestrial ecosystems.* Journal of Soil and Water Conservation, 73(6), 145A-152A. Retrieved June 18, 2022, from https://doi.org/10.2489/jswc.73.6.145A

Lambin, E. F., Geist, H. J., & Lepers, E. (2003). *Dynamics of land-use and land-cover change in tropical regions. Annual Review of Environment and Resources*. 28, 205–241. Retrieved June 15, 2022, from https://doi.org/10.1146/annurev.energy.28.050302.105459.

Lefèvre, C., Rekik, F., Alcantara, V., & Wiese-Rozanov, L. (2017). *Soil organic carbon: the hidden potential Burial of organic matter for carbon sequestration: Potentials, processes and long-term effects View project.* Retrieved May 23, 2022, from https://www.researchgate.net/publication/328345849.

le Houerou, H. N., Bingham, R. L., & Skerbek, W. (1988). *Relationship between the variability of primary production and the variability of annual precipitation in world arid lands*. Journal of Arid Environments, 15(1), 1–18. Retrieved June 2, 2022, from https://doi.org/10.1016/S0140-1963(18)31001-2.

Lillesand, T. M., Kiefer, R. W., & Chipman, J. (2008). *Remote Sensing and Image Interpretation*. (6th ed.). John Wiley and Sons: Hoboken.

Li, M., Verburg, P. H., & van Vliet, J. (2022). *Global trends and local variations in land take per person. Landscape and Urban Planning.* 218. Retrieved September 6, 2022, from https://doi.org/10.1016/j.landurbplan.2021.104308.

Liping, C., Yujun, S., & Saeed, S. (2018*). Monitoring and predicting land use and land cover changes using remote sensing and GIS techniques: A case study of a hilly area, Jiangle, China*. PLoS ONE, 13(7). Retrieved June 7, 2022, from https://doi.org/10.1371/journal.pone.0200493.

Lubowski, R. N., Bucholtz, S., Claassen, R., Roberts, M. J., Cooper, J. C., Gueorguieva, A., & Johansson, R. (2006). Environmental Effects of Agricultural Land-Use Change United States Department of Agriculture the Role of Economics and Policy. www.ers.usda.gov.

Lu, D., Mausel, P., Brondízio, E., & Moran, E. (2004). *Change detection techniques*. International Journal of Remote Sensing, 25(12), 2365–2401. Retrieved May 16, 2022, from https://doi.org/10.1080/0143116031000139863

Macleod, R. D., & Congalton, R. G. (1988). *A Quantitative Comparison of Change-Detection Algorithms for Monitoring Eelgrass from Remotely Sensed Data*. Photogrammetric Engineering and Remote Sensing, 64, 207-216.

Madisa, M. E., Assefa, Y., Kelemoge, O. D., Mathowa, T., & Segwagwe, A. T. (2017). *Incidence and Level of Mistletoe Infestation in Tree Species at Botswana University of Agriculture and Natural Resources' Sebele Content Farm Campus, Botswana*. International Journal of Environmental and Agriculture Research, *3*(11), 53–58. Retrieved May 28, 2022, from https://doi.org/10.25125/agriculture-journal-ijoear-nov-2017-9.

Magidi, J. T. (2010). *Spatio-Temporal Dynamics in Land Use and Habitat Fragmentation in the Sandveld, South Africa*. MSc Thesis. University of the Western Cape.

Mather, P. M. (1999). *Land Cover Classification Revisited.* In Advances in Remote Sensing and GIS (P. M. Atkinson & N. J. Tate, Eds.). John Wiley & Sons. New York. pp. 7–16.

Mather, P. M. (2004). *Computer Processing of Remotely-Sensed Images: An Introduction*. (3rd Edition). John Wiley & Sons.

Mather, P., & Tso, B. (2009). *Classification Methods for Remotely Sensed Data*. In Engineering & Technology, Environment & Agriculture. 2nd Edition. CRC Press. Retrieved May 9, 2022, from https://doi.org/10.1201/9781420090741

Matlhodi, B., Kenabatho, P. K., Parida, B. P., & Maphanyane, J. G. (2019). *Evaluating land use and land cover change in the Gaborone dam catchment, Botswana, from 1984-2015 using GIS and remote sensing*. Sustainability (Switzerland), *11*(19). Retrieved June 28, 2022, from https://doi.org/10.3390/su11195174.

Matlhodi, B., Kenabatho, P. K., Parida, B. P., & Maphanyane, J. G. (2021). *Analysis of the future land use land cover changes in the Gaborone dam catchment using CA-Markov model: Implications on water resources*. Remote Sensing, *13*(13). Retrieved July 17, 2022, from https://doi.org/10.3390/rs13132427.

Mnyali, E. T., & Materu, S. F. (2021). *Analysis of the Current and Future Land Use/Land Cover Changes in Peri-Urban Areas of Dar es Salaam City, Tanzania using Remote Sensing and GIS Techniques.* Tanzania Journal of Science, *47*(5), 1622–1636. Retrieved June 8, 2022, from https://doi.org/10.4314/tjs.v47i5.12.

Moleele, M., Ringrose, S., Matheson, W., & Vanderpost, C. (2002). More Woody Plants? The status of bush encroachment in Botswana's grazing areas. Journal of Environmental Management, Volume 64(0301–4797), 3–11. Retrieved June 23, 2022, from https://doi.org/10.1006/jema.2001.0486.

Mosier, A. R., Pendall, E., & Morgan, J. A. (2003). Atmospheric Chemistry and Physics Effect of water addition and nitrogen fertilization on the fluxes of CH_4, CO_2, NO_x, and N_2O following five years

of elevated CO 2 in the Colorado Shortgrass Steppe. In Atmos. Chem. Phys (Vol. 3). Retrieved May 8, 2022, from www.atmos-chem-phys.org/acp/3/1703.

Muhammad, R., Zhang, W., Abbas, Z., Guo, F., & Gwiazdzinski, L. (2022). *Spatiotemporal Change Analysis and Prediction of Future Land Use and Land Cover Changes Using QGIS MOLUSCE Plugin and Remote Sensing Big Data: A Case Study of Linyi, China*. Land, 11(3). Retrieved May 8, 2022, from https://doi.org/10.3390/land11030419.

Mukete, B., Bakla, M.-A., Baninia, Y., & Saeed, S. (2017). *Perspectives of Remote Sensing and GIS Applications in Tropical Forest Management*. American Journal of Agriculture and Forestry, 5(3), 33. Retrieved May 16, 2022, from https://doi.org/10.11648/j.ajaf.20170503.11.

Muktar, M., Bobe, B., Kibebew, K., & Yared, M. (2018). *Soil organic carbon stock under different land use types in Kersa Sub Watershed, Eastern Ethiopia*. African Journal of Agricultural Research, 13(24), 1248–1256. Retrieved June 7, 2022, from https://doi.org/10.5897/ajar2018.13190

Munthali, M. G. (2020). *Analysis of Land Use and Land Cover Change Dynamics and its Implications on Natural Resources in Dedza District, Malawi*.

Murty, D., Kirschbaum, M. U. F., Mcmurtrie, R. E., & Mcgilvray, H. (2002). *Does conversion of forest to agricultural land change soil carbon and nitrogen? A review of the literature*. Global Change Biology, 8(13541013), 105–123.

Nghalipo, E., Joubert, D., Throop, H., & Groengroeft, A. (2019). *The effect of fire history on soil nutrients and soil organic carbon in a semi-arid savanna woodland, central Namibia*. African Journal of Range and Forage Science, *36*(1), 9–16. Retrieved May 16, 2022, from https://doi.org/10.2989/10220119.2018.1526825.

Nhamo, L., van Dijk, R., Magidi, J., Wiberg, D., & Tshikolomo, K. (2018). *Improving the accuracy of remotely sensed irrigated areas using post-classification enhancement through UAV capability*. Remote Sensing, *10*(5). Retrieved June 1, 2022, from https://doi.org/10.3390/rs10050712.

Nkambwe, M., & Totolo, O. (2005). *Customary land tenure saves the best arable agricultural land in the peri-urban zones of an African city: Gaborone, Botswana*. Applied Geography, *25*(1), 29–46. Retrieved June 16, 2022, from https://doi.org/10.1016/J.APGEOG.2004.07.002.

Noor, N. M., Abdullah, A., Nasrul, M., & Manzahari, H. (2013). *Land Cover Change Detection Analysis on Urban Green Area Loss Using GIS and Remote Sensing Techniques*. In Journal of the Malaysian Institute of Planners: Vol. XI.

Nordt, L.C., Hallmark, C.T., Wilding, L.P., Boutton, T.W. (1998). *Quantifying pedogenic carbonate accumulations using stable carbon isotopes*. Geoderma 82, 115–136.

Nyamadzawo, G., Chikowo, R., Nyamugafata, P., Nyamangara, J., & Giller, K. E. (2008). *Soil organic carbon dynamics of improved fallow-maize rotation systems under conventional and no-tillage in Central Zimbabwe.* Nutrient Cycling in Agroecosystems. *81*(1), 85–93. Retrieved June 4, 2022, from https://doi.org/10.1007/s10705-007-9154-y.

Ogle, S. M., Breidt, F. J., & Paustian, K. (2005). *Agricultural management impacts on soil organic carbon storage under moist and dry climatic conditions in temperate and tropical regions*. Biogeochemistry. *72*(1), 87–121. Retrieved May 19, 2022, from https://doi.org/10.1007/s10533-004-0360-2

Okalebo, J. Robert., Gathua, K. W., & Woomer, P. L. (2002). *Laboratory Methods of Soil and Plant Analysis: A Working Manual.* Second Edition. The Sustainable Agriculture Centre For Research Extension and Development in Africa. (J. R. Okalebo, K. W. Gathua, & P. L. Woomer, Eds.; Second).

Pandian M, Sakthivel G, & Amrutha D. (2014). Land Use and Land Cover Change Detection Using Remote Sensing and GIS in Parts of Coimbatore and Tiruppur Districts, Tamil Nadu, India. International Journal of Remote Sensing & Geoscience (IJRSG). Retrieved July 19, 2022, from www.ijrsg.com.

Parker, D. C., Manson, S. M., Janssen, M. A., Hoffmann, M. J., & Deadman, P. (2003). *Multi-agent systems for the simulation of land-use and land-cover change: A review.* In Annals of the Association of American Geographers (Vol. 93, Issue 2, pp. 314–337). Retrieved May 8, 2022, from https://doi.org/10.1111/1467-8306.9302004

Pattarawan, W. (2016). *Factors Influencing Greenhouse Gas Emissions from Land Use, Land-Use Change, And Forest Activities*. Retrieved April 16, 2022, from https://trace.tennessee.edu/utk_graddiss.

Peng, Y., Xiong, X., Adhikari, K., Knadel, M., Grunwald, S., & Greve, M. H. (2015). *Modelling soil organic carbon at a regional scale by combining multi-spectral images with laboratory spectra*. PLoS ONE, 10(11). Retrieved May 28, 2022, from https://doi.org/10.1371/JOURNAL.PONE.0142295.

Permatasari, R. J., Damayanti, A., Indra, T. L., & Dimyati, M. (2021). *Prediction of land cover changes in Penajam Paser Utara Regency using Cellular Automata and Markov model*. IOP Conference Series: Earth and Environmental Science, 623(1). Retrieved September 16, 2022, from https://doi.org/10.1088/1755-1315/623/1/012005

Peters, A., Walter-Shea, E., Hayes, M. J., & Svoboda, M. (2002). *Drought monitoring with NDVI-based Standardized Vegetation IndexClimatic Extremes in the Greater Horn of Africa View project Climate change impact assessment on the hydrological cycle in Europe.* View project. Retrieved May 26, 2022, from https://www.researchgate.net/publication/284778912

Petrenko, L. R., & Berezhnyak, Y. M. (2008). *Soil Science*: Practical Methods Manual Methodological Instruction Book for the Undergraduate Students of Agronomy and Ecology.

Phuntsho. (2016). Soil Carbon Stock Under Different Land Use Types: *A Case Study from Phobjikha Valley, Wangduephodrang Dzongkhag.* [Master, Royal University of Bhutan]. Retrieved May 28, 2022, from https://www.academia.edu/32740690.

Pinto, C. T., Jing, X., & Leigh, L. (2020). *Remote Sensing Evaluation Analysis of Landsat Level-1 and Level-2 Data Products Using In Situ Measurements*. Retrieved May 8, 2022, from https://doi.org/10.3390/rs12162597

Podeh, S. S., Oladi, J., Pormajidian, M. R., & Zadeh, M. M. (2009). *Forest Change Detection in the North of Iran using TM/ETM+Imagery.* Asian Journal of Applied Science, 2 (1996–3343), 464–474.

Priano, M. E., Fusé, V. S., Mestelan, S., Berkovic, A. M., Guzmán, S. A., Gratton, R., & Juliarena, M. P. (2018). *Afforested sites in a temperate grassland region: influence on soil properties and methane uptake*. Agroforestry Systems, 92(2), 311–320. Retrieved May 3, 2022, from https://doi.org/10.1007/s10457-017-0104-7

Pule-Meulenberg, F., Moganane, B., & Dikinya, O. (2005). *Physicochemical Properties of Soil from Five Villages in Botswana with Respect to Soil Degradation*. Caspian Journal of Environmental Sciences Caspian 3(1). pp. 29-34. Retrieved May 8, 2022, from www.cjes.net.

Ramachandra, T. v., & Kumar, U. (2004). *Geographic Resources Decision Support System for land use, land cover dynamics analysis*. FOSS/GRASS Users Conference. Retrieved May 3, 2022, from https://www.researchgate.net/publication/256838566

Razafirmbelo, F., Chevallier, T., Albrecht, A., CHapuis-Lardy, L., Rakotondrasollo, F. N., Michellon, R., Rabeharisoa, L., & Bernoux, M. (2013). *Texture and organic carbon content do not impact the amount of carbon protected in Malagasy soils*. Sci. Agric., 70(3), 204–208.

Ringrose, S., Vanderpost, C., & Matheson, W. (1996). *The use of integrated remotely sensed and GIS data to determine causes of vegetation cover change in southern Botswana*. In Applied Geography (Vol. 16, Issue 3).

Rutherford, M. C. (1980). *Annual Plant Production Precipitation Relations in Arid and Semi-Arid Regions Vegetation of Africa View project*. S. Afr. J. Sci., *76*(53–57.). Retrieved May 3, 2022, from https://www.researchgate.net/publication/202000552

Santisteban, J. I., Mediavilla, R., López-Pamo, E., Dabrio, C. J., Zapata, M. B. R., García, M. J. G., Castaño, S., & Martínez-Alfaro, P. E. (2004). *Loss on ignition: A qualitative or quantitative method for organic matter and carbonate mineral content in sediments?* Journal of Paleolimnology, *32*(3), 287–299. Retrieved June 3, 2022, from https://doi.org/10.1023/B:JOPL.0000042999.30131.5b

Saputra, M. H., & Lee, H. S. (2019a). *Prediction of land use and land cover changes for North Sumatra, Indonesia, using an artificial-neural-network-based cellular automaton*. Sustainability (Switzerland), 11(11). Retrieved July 13, 2022, from https://doi.org/10.3390/su11113024

Saputra, M. H., & Lee, H. S. (2019). *Prediction of land use and land cover changes for North Sumatra, Indonesia, using an artificial-neural-network-based cellular automaton*. Sustainability (Switzerland), *11*(11). Retrieved May 3, 2022, from https://doi.org/10.3390/su11113024

Schaldach, R., Alcamo, J., Koch, J., Koelking, C., Lapola, D., Schuengel, J., & Priess, J. (2011). *An integrated approach to modelling land-use change on continental and global scales.* Environmental Modelling and Software, *26*(8), 1041–1051.

Sebego, R. (2014). *Historical Vegetation changes in the Greater Gaborone area*. Retrieved June 20, 2022, from https://www.researchgate.net/publication/237644346

Sebego, R. J., & Gwebu, T. D. (2013). *Patterns, determinants, impacts and policy implications of the spatial expansion of an African capital city: The Greater Gaborone example. International Journal of Sustainable Built Environment. 2*(2), 193–208. Retrieved June 11, 2022, from https://doi.org/10.1016/j.ijsbe.2013.12.002

Seboko, K. R., Kotze, E., van Tol, J., & van Zijl, G. (2021). *Characterization of soil carbon stocks in the city of Johannesburg. Land. 10*(1), 1–12. Retrieved May 24, 2022, from https://doi.org/10.3390/land10010083

Senwo, Z. (2021). *What is Soil Organic Carbon (SOC)? Highlights how Soil organic carbon (SOC) interlinks with soil health, agriculture, climate change, and food security*. Retrieved June 24, 2022, from https://www.openaccessgovernment.org/what-is-soil-organic-carbon-soc/120702/

Seto, K. C., Güneralp, B., & Hutyra, L. R. (2012). *Global forecasts of urban expansion to 2030 and direct impacts on biodiversity and carbon pools.* Proceedings of the National Academy of Sciences of the United States of America, 109(40), 16083–16088. Retrieved May 22, 2022, from https://doi.org/10.1073/pnas.1211658109

Seto, K. C., Woodcock, C. E., Song, C., Huang, X., Lu, J., & Kaufmann, R. K. (2002). *Monitoring land-use change in the Pearl River Delta using Landsat TM*. International Journal of Remote Sensing, 23(10), 1985–2004. Retrieved May 28, 2022, from https://doi.org/10.1080/01431160110075532

Shackleton, R., Shackleton, C., Shackleton, S., & Gambiza, J. (2013). *Deagrarianisation and Forest Revegetation in a. Biodiversity Hotspot on the Wild Coast, South Africa*. PLoS ONE, 8(10), 76939. Retrieved July 24, 2022, from https://doi.org/10.1371/journal.pone.0076939

Shaoqing, Z., & Lu, X. (2008). *The Comparative Study of Three Methods of Remote Sensing Image Change Detection*. Remote Sensing and Spatial Information Sciences, 37, 1–4.

Sharma, G., Sharma, L. K., & Sharma, K. C. (2019). *Assessment of land use change and its effect on soil carbon stock using multitemporal satellite data in the semiarid region of Rajasthan, India*. Ecological Processes, *8*(1). https://doi.org/10.1186/s13717-019-0193-5

Shi, S., Zhang, W., Zhang, P., Yu, Y., & Ding, F. (2013). *A synthesis of change in deep soil organic carbon stores with afforestation of agricultural soils*. Forest Ecology and Management, 296, 53–63. Retrieved May 2, 2022, from https://doi.org/10.1016/j.foreco.2013.01.026

Shrestha, B. M., Sitaula, B. K., Singh, B. R., & Bajracharya, R. M. (2004). *Soil organic carbon stocks in soil aggregates under different land use systems in Nepal*. Nutrient Cycling in Agroecosystems, 70(2), 201–213. Retrieved May 4, 2022, from https://doi.org/10.1023/B:FRES.0000048472.25373.7e

Solomon, D., Fritzsche, F., Lehmann, J., Tekalign, M., & Zech, W. (2002). *Soil organic matter dynamics in the subhumid agroecosystems of the Ethiopian highlands: Evidence from natural C-13 abundance and particle-size fractionation*. Soil Science Society of America Journal, *66*(66), 969–978.

Statistics Botswana (2014). *Population and housing census 2011*. Retrieved June 4, 2022, from https://unstats.un.org/unsd/demographic/sources/census/wphc/Botswana/census%20project.pdf

Statistics Botswana (2022). *Population and Housing Census 2022 Population of Cities, Towns and Villages (Vol. 2)*. Retrieved October, 2022, from www.statsbots.org.bw

Stockmann, U., Adams, M. A., Crawford, J. W., Field, D. J., Henakaarchchi, N., Jenkins, M., Minasny, B., McBratney, A. B., Courcelles, V. de R. de, Singh, K., Wheeler, I., Abbott, L., Angers, D. A., Baldock, J., Bird, M., Brookes, P. C., Chenu, C., Jastrow, J. D., Lal, R., Zimmermann, M. (2013). *The knowns, known unknowns and unknowns of sequestration of soil organic carbon*. In

Agriculture, Ecosystems and Environment (Vol. 164, pp. 80–99). Elsevier B.V. Retrieved June 14, 2022, from https://doi.org/10.1016/j.agee.2012.10.001

Szatmári, G., Pirkó, B., Koós, S., Laborczi, A., Bakacsi, Z., Szabó, J., & Pásztor, L. (2019). *Spatio-temporal assessment of topsoil organic carbon stock change in Hungary*. Soil and Tillage Research, 195. Retrieved May 24, 2022, from https://doi.org/10.1016/j.still.2019.104410

Temesgen, H., Worku, G., & Bantider, A. (2014). *Effects of land use/land cover change on some soil physical and chemical properties in Ameleke micro-watershed, Gedeo and Borena Zones, South Ethiopia.* 4(11). Retrieved May 9, 2022, from www.iiste.org

Tempfli, K., Huurneman, G. C., Bakker, W. H., Janssen, L. L. F., Feringa, W. F., Gieske, A. S. M., Grabmaier, K. A., Hecker, C. A., & Horn, J. A. van der. (2009*). Principles of remote sensing:* An introductory textbook*.* ITC.

Theau, J. (2012). *Change detection. springer of geographic information* (W. Kresse & D. M. Danko, Eds.; 2nd ed., Vol. 1). Springer-Verlag Berlin Heidelberg.

Tsao, C.-H. (2017). *Carbon Sequestration Under Different Land Uses and Soils in The State of Quintana Roo, Mexico* [Master, UNIVERSIDAD AUTÓ NOMA DE SAN LUIS POTOSI]. Retrieved June 2, 2022, from https://repositorioinstitucional.uaslp.mx/xmlui/handle/i/4513

Tsheko, R. (2021*). Land Cover Land Use (LCLU) Classification Methods in Semi-Arid Botswana. Journal of Remote Sensing &GIS*. 10(1000), 497. Retrieved August 12, 2022, from https://www.walshmedicalmedia.com/open-access/land-cover-land-use-lclu-classification-methods-in-semiarid-botswana.pdf.

Tsheko, R. (2022*). Non-seasonal Landsat-based bare area gain detection in Botswana from 2002 to 2020 Period using the Maximum Likelihood Classifier (MLC*). South African Journal of Geomatics, 11(1). Retrieved October 2, 2022, from https://doi.org/10.4314/sajg.v11i1.7

Turner, B. L., & Meyer, W. (1994*). Changes in Land Use and Land Cover: A Global Perspective*. Vol. 4, Cambridge University Press, Cambridge.

Turner, B. L., Skole, D. L., Sanderson, S., Fischer, G., & et al. (1995). *Land-use and land-cover change. Science/research plan* (Vol. 7). IGBP Secretariat.

Turner, M. G. (2005). *Landscape Ecology in North America: Past, Present, and Future. In Special Feature Ecology* (Vol. 86, Issue 8).

United Nations Framework Convention on Climate Change (UNFCCC, 2004). *Report Of The Conference Of The Parties on Its Ninth Session, Held At Milan From 1 To 12 December 2003*. Retrieved October 2, 2022, from https://unfccc.int/resource/docs/cop9/06a01.pdf#page=31

Vågen, T. G., & Winowiecki, L. A. (2013). *Mapping of soil organic carbon stocks for spatially explicit assessments of climate change mitigation potential*. Environmental Research Letters, 8(1). Retrieved June 24, 2022, from https://doi.org/10.1088/1748-9326/8/1/015011

van Reeuwijk, L. P. (2002). *Procedures for soil analysis*. Technical Paper No. 9, 6th Edition, 2002, FAO/ISRIC, Wageningen, the Netherlands. 120pp.

Verburg, P. H., Schot, P. P., Dijst, M. J., & Veldkamp, A. (2004). *Land use change modelling: Current practice and research priorities*. In GeoJournal (Vol. 61, Issue 4, pp. 309–324). Springer Netherlands. Retrieved June 2, 2022, from https://doi.org/10.1007/s10708-004-4946-y.

Vicente-Serrano, S. M., Pérez-Cabello, F., & Lasanta, T. (2008). *Assessment of Radiometric Correction Techniques in Analyzing Vegetation Variability and Change Using Time Series of Landsat Images*. Remote Sensing of Environment, 7(112), 3916–3934.

Wainkwa Chia, R., Kim, D. G., & Yimer, F. (2017). *Can afforestation with Cupressus lusitanica restore soil C and N stocks depleted by crop cultivation to levels observed under native systems? Agriculture, Ecosystems and Environment*. 242, 67–75. Retrieved April 30, 2022, from https://doi.org/10.1016/j.agee.2017.03.023

Walkley, A., & Black, A. I. (1934). *An examination of Degtjareff method for determining soil organic matter and a proposed modification of the chromic acid titration method. Soil Sci.*, *37*, 29–38.

Wei, X., Shao, M., Gale, W., & Li, L. (2014). *Global pattern of soil carbon losses due to the conversion of forests to agricultural land.* Retrieved June 3, 2022, from https://doi.org/10.1038/srep04062

Weng, Q. (2002). *Land use change analysis in the Zhujiang Delta of China using satellite remote sensing, GIS and stochastic modelling*. Journal of Environmental Management, 64(3), 273–284. Retrieved June 5, 2022, from https://doi.org/10.1006/JEMA.2001.0509

Williams, D. L., Goward, S., & Arvidson, T. (2006). *Landsat: Yesterday, Today, and Tomorrow*. Photogrammetric Engineering & Remote Sensing, *72*, 1171–1178.

Yang, Sheng, D., Adamowski, J., Gong, Y., Zhang, J., & Cao, J. (2018). *Effect of land use change on soil carbon storage over the last 40 years in the Shi Yang River Basin, China*. *7*(1). Retrieved June 2, 2022, from https://doi.org/10.3390/land7010011

Yan, Y., Tian, J., Fan, M., Zhang, F., Li, X., Christie, P., Chen, H., Lee, J., Kuzyakov, Y., & Six, J. (2012). *Soil organic carbon and total nitrogen in intensively managed arable soils*. Agriculture, Ecosystems and Environment, 150, 102–110. Retrieved May 26, 2022, from https://doi.org/10.1016/j.agee.2012.01.024

Yao, X., Yu, K., Deng, Y., Liu, J., & Lai, Z. (2020). *Spatial variability of soil organic carbon and total nitrogen in the hilly red soil region of Southern China*. Journal of Forestry Research, 31(6), 2385–2394. Retrieved June 7, 2022, from https://doi.org/10.1007/S11676-019-01014-8

Yihenew, G. S., & Getachew, A. (2013). *Effects of Different Land Use Systems on Selected Physico-Chemical Properties of Soils in Northwestern Ethiopia*. Journal of Agricultural Science, 5(4). Retrieved June 7, 2022, from https://doi.org/10.5539/jas.v5n4p112

Yimer, F., Ledin, S., & Abdelkadir, A. (2007). *Changes in soil organic carbon and total nitrogen contents in three adjacent land use types in the Bale Mountains, south-eastern highlands of Ethiopia*. Forest Ecology and Management, 242(2–3), 337–342. Retrieved June 3, 2022, from https://doi.org/10.1016/j.foreco.2007.01.087

Zhou, Han, G., Liu, M., & Li, X. (2019). *Effects of soil pH and texture on soil carbon and nitrogen in soil profiles under different land use in Mun River Basin, Northeast Thailand*. Retrieved July 26, 2022, from https://doi.org/10.7717/peerj.7880

Zimmermann, J. (2013). *Soil carbon sequestration during the establishment phase of Miscanthus x giganteus. A study on three spatial scales*. [PhD, University of Dublin]. Retrieved April 2, 2022, from https://www.tcd.ie/research/simbiosys/images/JZ_PhD.pdf